U.S. DEPARTMENT OF ENERGY | Energy Efficiency & Renewable Energy

BUILDING TECHNOLOGIES PROGRAM

Cost Analysis of Simple Phase Change Material-Enhanced Building Envelopes in Southern U.S. Climates

Jan Kosny, Nitin Shukla, and Ali Fallahi
Fraunhofer CSE

January 2013

Building AMERICA SM
U.S. Department of Energy

NOTICE

This report was prepared as an account of work sponsored by an agency of the United States government. Neither the United States government nor any agency thereof, nor any of their employees, subcontractors, or affiliated partners makes any warranty, express or implied, or assumes any legal liability or responsibility for the accuracy, completeness, or usefulness of any information, apparatus, product, or process disclosed, or represents that its use would not infringe privately owned rights. Reference herein to any specific commercial product, process, or service by trade name, trademark, manufacturer, or otherwise does not necessarily constitute or imply its endorsement, recommendation, or favoring by the United States government or any agency thereof. The views and opinions of authors expressed herein do not necessarily state or reflect those of the United States government or any agency thereof.

Available electronically at http://www.osti.gov/bridge

Available for a processing fee to U.S. Department of Energy
and its contractors, in paper, from:
U.S. Department of Energy
Office of Scientific and Technical Information
P.O. Box 62
Oak Ridge, TN 37831-0062
phone: 865.576.8401
fax: 865.576.5728
email: mailto:reports@adonis.osti.gov

Available for sale to the public, in paper, from:
U.S. Department of Commerce
National Technical Information Service
5285 Port Royal Road
Springfield, VA 22161
phone: 800.553.6847
fax: 703.605.6900
email: orders@ntis.fedworld.gov
online ordering: http://www.ntis.gov/ordering.htm

Printed on paper containing at least 50% wastepaper, including 20% postconsumer waste

Cost Analysis of Simple Phase Change Material-Enhanced Building Envelopes in Southern U.S. Climates

Prepared for:

The National Renewable Energy Laboratory

On behalf of the U.S. Department of Energy's Building America Program

Office of Energy Efficiency and Renewable Energy

15013 Denver West Parkway

Golden, CO 80401

NREL Contract No. DE-AC36-08GO28308

Prepared by:

Jan Kośny, Nitin Shukla, and Ali Fallahi

Fraunhofer CSE

25 First Street

Cambridge, MA 02141

NREL Technical Monitor: Chuck Booten

Performed Under Subcontract No. KNDJ-0-40345-00

January 2013

Contents

List of Figures ..... **v**
List of Tables ..... **vii**
Definitions ..... **viii**
Executive Summary ..... **ix**
Acknowledgments ..... **x**
1 Introduction **1**
1.1 Phase Change Materials for Building Applications 1
1.2 Overview of U.S. Performance Data for Concentrated Phase Change Material Building Envelope Systems 3
1.3 Research Studies Focused on Concentrated Phase Change Material Applications in Walls and Roofs 4
2 Phase Change Material Price Challenges **8**
2.1 Phase Change Material Cost Components 8
2.2 Material Cost 8
2.2.1 Organic Phase Change Materials 8
2.2.2 Inorganic Phase Change Materials 9
2.2.3 Material Cost of Phase Change Materials 9
2.3 Alternatives to Paraffin 10
2.3.1 Salt Hydrates 11
2.3.2 Biobased Phase Change Materials 13
2.3.3 Shape-Stabilized Phase Change Material 14
2.4 Expected Future Cost Reductions 14
3 Whole-Building Energy Simulations—Theoretical Performance Limits for Building Envelopes Using Conventional Thermal Insulations **16**
3.1 Theoretical Performance Limits for Dynamic Insulations Using Dispersed Phase Change Material Applications 20
3.2 Estimation of the Competitive Price Level for Phase Change Material Attic and Wall Applications 30
3.3 Payback Period Analysis for Attic Applications of Dispersed Phase Change Materials 31
3.4 Additional Benefits of Thick Applications of the Phase Change Material-Enhanced Attic Floor Insulation 38
3.5 Potential Cost Savings Associated With Phase Change Material Load Reductions in Phase Change Material-Enhanced Attic Floor Insulations 42
3.6 Payback Period Analysis for Wall Applications of Dispersed Phase Change Materials 44
3.7 Payback Period Analysis for Wall Applications of Phase Change Material-Enhanced Gypsum Boards 49
3.8 Performance Comparisons Between Conventional Insulations and Phase Change Material-Enhanced Insulations 53
4 Discussion of Results **56**
4.1 Selection of Climatic Locations 56
4.2 Phase Change Material Load Levels in Blends With Thermal Insulations 56
4.3 Phase Change Material Cost Limits 56
4.4 Payback Periods 57
5 Conclusions **59**
References **60**

List of Figures

Figure 1. Layout of the single-story ranch house used for the energy modeling 16
Figure 2. Annual energy savings as a function of wall R-value increase in increments of R-4 17
Figure 3. Annual energy savings as a function of attic R-value increasing in increments of R-4 ... 18
Figure 4. Scanning electron microscope (SEM) images of microencapsulated PCM mixed with (a) cellulose fiber insulation, (b) blown fiberglass matrix and fiberglass, and (c) polyurethane foam 20
Figure 5. Temperature versus effective heat capacity data for PCM used in thermal simulations .. 23
Figure 6. Diurnal external temperature profiles T_{es} used in numerical analysis with assumption of T_i = 68°F (20°C) and T_i = 77°F (25°C) 24
Figure 7. Comparison of the daily heat flux profiles at the internal surface of the wall containing 5.5-in. (0.14-m) thick insulation layer with 0% PCM and 30% PCM for internal temperature T_i = 68°F (20°C) and temperature swing schedules with thermal peaks of 113°F (45°C) in schedule "a" 149°F (65°C) in schedule "b," and 185°F (85°C) in schedule "c" 25
Figure 8. Comparison of the daily heat flux profiles at the internal surface of the wall containing 5.5-in. (0.14-m) thick insulation layer with 0% PCM and 30% PCM for internal temperature *Ti* = 77°F (25°C) and temperature swing schedules with thermal peaks of 45°C (113°F) in schedule "a," 149°F (65°C) in schedule "b," and 185°F (85°C) in schedule "c" 26
Figure 9. Comparison of the daily heat flux profiles at the internal surface of the attic floor containing 11.8-in. (0.3-m) thick insulation layer with 0% PCM and 30% PCM for internal temperature T_i = 68°F (20°C) and temperature swing schedules with thermal peaks of 113°F (45°C) in schedule "a," 149°F (65°C) in schedule "b," and 185°F (85°C) in schedule "c"..... 27
Figure 10. Comparison of the daily heat flux profiles at the internal surface of the attic floor containing 12-in. (30-cm) thick insulation layer with 0% PCM and 30% PCM for internal temperature T_i = 77°F (25°C) and temperature swing schedules with thermal peaks of 113°F (45°C) in schedule "a," 149°F (65°C) in schedule "b," and 185°F (85°C) in schedule "c"..... 28
Figure 11. Reductions of heat gains calculated for the two thicknesses of the building envelope assemblies. For each material configuration and at internal temperatures T_i, heat gains represent heat fluxes integrated over the time period. 29
Figure 12. Payback periods for the PCM-enhanced R-30 cellulose insulation configuration installed on the attic floor as a function of the PCM price for a single-story ranch house in Atlanta. The external temperature profiles have been defined as "a" and "b."..... 33
Figure 13. Payback periods for the PCM-enhanced R-30 cellulose insulation configuration installed on the attic floor as a function of the PCM price for a single-story ranch house in Bakersfield. The external temperature profiles have been defined as "a" and "b." 34
Figure 14. Payback periods for the PCM-enhanced R-30 cellulose insulation configuration installed on the attic floor as a function of the PCM price for a single-story ranch house in Fort Worth. The external temperature profiles have been defined as "a" and "b." 35
Figure 15. Payback periods for the PCM-enhanced R-30 cellulose insulation configuration installed on the attic floor as a function of the PCM price for a single-story ranch house in Miami. Two external temperature profiles have been defined as "a" and "b."..... 36
Figure 16. Payback periods for the PCM-enhanced R-30 cellulose insulation configuration installed on the attic floor as a function of the PCM price for a single-story ranch house in Phoenix. The external temperature profiles have been defined as "a" and "b."..... 37
Figure 17. Percent peak-hour cooling load reductions for 11.8-in. (0.3-m) thick PCM-enhanced attic floor insulation 39
Figure 18. Peak-hour cooling load time-shifting for 11.8 in. (0.3-m) thick PCM-enhanced attic floor insulation..... 39
Figure 19. Payback periods calculated using cooling cost reductions for 11.8-in. (0.3-m) thick PCM-enhanced attic floor insulation computed using the off-peak-hour electricity tariff for Phoenix. The external temperature schedules have been defined as "a" and "b." 40
Figure 20. Reverse heat flow effect generated by significant time shifting of thermal loads in 11.8-in. (0.3-m) thick PCM-enhanced attic floor insulation in Phoenix. The external temperature schedule has been defined as "a" 41

Figure 21. Photograph of the test attic with blown PCM-enhanced fiberglass insulation 42
Figure 22. Modified levels of payback periods for attic PCM applications in Miami and Phoenix, considering a 25% reduction in PCM loading 43
Figure 23. Payback period for PCM-enhanced cavity wall insulation as a function of the PCM price for a single-story ranch house in Atlanta. Wall assemblies are assumed to experience the external temperature schedule defined as "a." 45
Figure 24. Payback period for PCM-enhanced cavity wall insulation as a function of the PCM price for a single-story ranch house in Bakersfield. Wall assemblies are assumed to experience the external temperature schedule defined as "a." 46
Figure 25. Payback period for PCM-enhanced cavity wall insulation as a function of the PCM price for a single-story ranch house in Fort Worth. Wall assemblies are assumed to experience the external temperature schedule defined as "a." 46
Figure 26. Payback period for PCM-enhanced cavity wall insulation as a function of the PCM price for a single-story ranch house in Miami. Wall assemblies are assumed to experience the external temperature schedule defined as "a." 47
Figure 27. Payback period for PCM-enhanced cavity wall insulation as a function of the PCM price for a single-story ranch house in Phoenix. Wall assemblies are assumed to experience the external temperature schedule defined as "a." 47
Figure 28. Payback period for PCM-enhanced cavity wall insulation as a function of the PCM price for a single-story ranch house in Phoenix. Wall assemblies are assumed to experience the external temperature schedule defined as "a" and an off-peak tariff is included. 48
Figure 29. Payback period for PCM-enhanced gypsum boards that are used for wall application as a function of the PCM price for a single-story ranch house in Atlanta. Wall assemblies are assumed to experience the external temperature schedule defined as "a." 50
Figure 30. Payback period for PCM-enhanced gypsum boards that are used for wall application as a function of the PCM price for a single-story ranch house in Bakersfield. Wall assemblies are assumed to experience the external temperature schedule defined as "a." 50
Figure 31. Payback period for PCM-enhanced gypsum boards that are used for wall application as a function of the PCM price for a single-story ranch house in Fort Worth. Wall assemblies are assumed to experience the external temperature schedule defined as "a." 51
Figure 32. Payback period for PCM-enhanced gypsum boards that are used for wall application as a function of the PCM price for a single-story ranch house in Miami. Wall assemblies are assumed to experience the external temperature schedule defined as "a." 51
Figure 33: Payback period for PCM-enhanced gypsum boards that are used for wall application as a function of the PCM price for a single-story ranch house in Phoenix. Wall assemblies are assumed to experience the external temperature schedule defined as "a." 52
Figure 34. Payback period for PCM-enhanced gypsum boards that are used for wall application as a function of the PCM price for a single-story ranch house in Phoenix. Wall assemblies are assumed to experience the external temperature schedule defined as "a" and an off-peak tariff is used. 52
Figure 35: Payback period for 3/8-in. thick PCM-enhanced gypsum boards that are used for wall application as a function of the PCM price for a single-story ranch house in Phoenix. Wall assemblies are assumed to experience the external temperature schedule defined as "a" and an off-peak tariff is used. 53

Unless otherwise noted, all figures were created by Fraunhofer.

List of Tables

Table 1. Summary of U.S. Test Results for Concentrated PCM Applications 7
Table 2. Five Southern U.S. Climates Used in Whole-Building Energy Modeling 19
Table 3. Energy Load Contributions From Walls and Attic Calculated for a Single-Story Ranch House for Five Southern U.S. Climates 19
Table 4. Cooling Energy Contributions From Walls and Attic Calculated for the Floor Area of the 1,540-ft^2 (143-m^2) Single-Story Ranch House 19
Table 5. Thermophysical Properties Used in Numerical Modeling 23
Table 6. Residential Electric Energy Prices for Five Southern U.S. Climates Used in Whole-Building Energy Analysis 30
Table 7. Annual Costs of Cooling Electric Energy Generated by the Attic Calculated for a Single-Story Ranch House for Five Southern U.S. Climates 32
Table 8. Calculated Annual Cooling Electricity Cost Savings Generated by the Attic for a Single-Story Ranch House for Five Southern U.S. Climates 32
Table 9. Annual Costs of Cooling Electric Energy Generated by 2 × 6 Walls, Calculated for a Single-Story Ranch House for Five Southern U.S. climates 44
Table 10. Annual Cooling Electricity Cost Savings Generated by the Attic Calculated for a Single-Story Ranch House for Five Southern U.S. Climates 45
Table 11. Potential Savings in Annual Costs of Cooling Electric Energy Generated by the Attic Calculated for a Single-Story Ranch House and for Five Southern U.S. Climates 54
Table 12. Comparisons of Energy Cost Savings and Material Costs Calculated for a Single-Story Ranch House for Five Southern U.S. Climates 55

Unless otherwise noted, all tables were created by Fraunhofer.

Definitions

ACH	air changes per hour
ANSI	American National Standards Institute
APS	Arizona Public Service
ARRA	American Recovery and Reinvestment Act
ASHRAE	American Society of Heating, Refrigerating and Air-Conditioning Engineers
ASTM International	formerly known as the American Society for Testing and Materials
CDD	cooling degree-days
CMC	carboxymethyl cellulose
CO_2	Carbon dioxide
DOE	U.S. Department of Energy
DSC	Differential scanning calorimetry
GJ	Gigajoules
h	Hour
HDD	Heating degree-days
HDPE	High-density polyethylene
IEA	International Energy Agency
in.	Inch
K	Kelvin
L	Liter
LA	Lauric acid
LBNL	Lawrence Berkeley National Laboratory
m	Meter
MF	Melamineformaldehyde
OSB	Oriented strand board
PCES	Phase Change Energy Solutions Inc.
PCM	Phase change material
PV	Photovoltaic
SAP	Super-absorbent polymer
SEM	Scanning electron microscope
ss-PCM	Shape-stabilized PCM
W	Watt

Executive Summary

Traditionally, the thermal design of building envelope assemblies is based on steady-state energy flows. In practice, however, building envelopes are subject to varying environmental conditions. Design work to support the development of very low-energy homes shows that the conventional insulations may not always be the most cost-effective energy solution for improving the thermal performance of the building envelope. This report focuses on building envelopes that have been enhanced with phase change materials (PCMs), which can simultaneously reduce total cooling loads and shift peak-hour loads.

Researchers at the Fraunhofer Center for Sustainable Energy Systems performed an economic analysis to evaluate the cost effectiveness of simple PCM-enhanced building envelopes and determined the target cost levels at which PCMs can be cost competitive with conventional building thermal insulations. The study team selected two basic PCM applications for analysis: dispersed PCM applications and simple building board products using concentrated PCMs. In addition to describing Fraunhofer's work, this report summarizes the results of previous experimental and theoretical studies that have been conducted in North America to understand the performance of PCM-enhanced building envelopes. The study team used these results as performance benchmarks for different PCM configurations that were tested in the United States for different building applications. This work did not, however, seek to optimize the configurations of PCMs.

The investigators performed numerical parametric analyses exclusively for insulation blends. Specifically, the study team used a series of one-dimensional dynamic simulations with sinusoidal exterior temperature profiles to generate transient heat flux data for different configurations of building insulation containing PCM. The thermal performance characteristics obtained for blends of thermal insulations and organic PCMs show significant energy storage potential in such mixtures. The study team evaluated two thicknesses of the PCM-enhanced insulations in a simulation study: a typical 5.5-in. (0.14-m) thick wall assembly and 11.8-in. (0.3-m) thick attic floor configuration. From an energy savings perspective, the thinner wall assembly containing PCM–insulation blends (5.5-in. thick) achieved a lower reduction in cooling loads (by three to five times) than the thicker attic floor assembly (11.8 in. [0.3-m]). Comparing the heat flux values indicated that PCM-enhanced insulation in the thinner assembly exposed to cyclic external temperatures reduces the heat fluxes during peak cooling hours and delays the peak heat flux to a later time. The study team noted the same effects in the thicker assembly representing attic floor insulation; however, this assembly also resulted in significant reductions of the total load. Moreover, the thicker assembly showed a notably larger shift in the time of the peak heat flux (reaching 11 hours) and an approximate four-fold reduction in the peak-hour cooling load relative to the thinner assembly.

The simulation results also demonstrated that thicker layers of PCM-enhanced insulation, exposed to periodic thermal excitations, have the potential to generate a reverse heat flux, a phenomenon in which heat starts flowing in the opposite direction, compared to a similar assembly without PCM. For an 11.8-in. (0.3-m) assembly with PCM, analysts found that reverse heat fluxes can occur up to 70% of the time (~17 hours a day). This effect can result in "passive" cooling of internal spaces, reducing air-conditioning energy consumption. For a PCM-enhanced

attic insulation, the simulations suggest that during the summer months, such passive cooling has the potential to reduce attic-generated cooling loads by up to 25%.

The study team's simulations also revealed that the thicker assembly lowers the amplitude of exterior thermal excitations. In another interesting observation, investigators found that the potential cooling load reductions are greater when the internal set-point temperature is very close to the PCM melting point (in this modeling, a 3.6°F - 2°C) difference). Numerical analysis demonstrated that these reductions can be at least four times larger than those seen in the case with 12.6°F (7°C) difference between internal set-point temperature and the PCM melting point. Because PCM-enhanced materials usually perform well only during a part of the cooling season, the study team recommends a follow-on study to evaluate the long-term performance using annual weather data to assess the dynamic thermal performance of the PCM building applications in different climates.

Applications of building systems in which PCM-enhanced materials face the interior of the building depend on HVAC systems or overnight pre-cooling to remove heat absorbed by PCM during the day. For applications of the PCM-enhanced gypsum boards in walls, cooling energy savings ranging between 7% and 20% were previously reported by several research groups in different U.S. locations. Following this historical experimental data, in this work, 15% cooling energy savings was considered for the PCM-enhanced gypsum board applications. For PCM-enhanced gypsum board applications in Phoenix, Arizona, the study team estimated a payback period of 7 years for PCMs of enthalpies between 82 and 95 Btu/lb (190 and 220 kJ/kg) with a price limit of $3.00/lb, taking into account the reduced off-peak electricity rates. Similarly, a 10-year payback period was determined for a PCM price level not exceeding $3.50/lb. Another finding of the work was that application of a thinner 3/8-in. (1-cm) thick board that contains PCM in conjunction with carbon or graphite fillers (to enhance thermal conductivity) may be considered as an alternative for improving performance and reducing costs.

Finally, the study team analyzed several potential methods for future cost reductions for PCM-enhanced building applications. In particular, from a materials perspective, development of the following technologies could play a key role in reducing PCM prices in the future: (1) cheaper microencapsulation or micropackaging methods for organic PCMs, (2) microencapsulation of inorganic PCMs, and (3) less costly inorganic and biobased PCMs with higher enthalpies.

Acknowledgments

The authors acknowledge the U.S. Department of Energy, particularly Marc LaFrance, for funding the U.S. PCM research program. This project was made possible by direct cofunding from the Fraunhofer Center for Sustainable Energy Systems.

1 Introduction

Phase change process involves transforming a material from one phase (solid, liquid, or gas) into another. For example, melting of ice into liquid water or boiling of liquid water into water vapor is classified as a phase change process. During a phase change, molecules rearrange themselves, causing an entropy change of the material system. Thermodynamics necessitates that the material absorb or release thermal energy or heat because of this entropy change, and this heat associated with the unit mass of the material is defined as the latent heat of the material. The latent heat is released by a material during melting and evaporation; it is absorbed during freezing and condensation phase change processes. The amount of latent heat is significantly larger than the sensible heat gain/loss for temperature changes of ~10 K. The difference could be one to two orders of magnitude. For example, the latent heat of melting ice to water at 32°F (0°C) is 142 Btu/lb (330 kJ/kg). Compare this with 18 Btu/lb (42 kJ/kg) of sensible heat, which is required to change the water temperature by 10 K. During a phase change, the temperature of the material remains constant. In short, a phase change process involves a large amount of heat transfer at a constant temperature, and both are attractive features for heating, cooling, and temperature stabilization applications. A material that uses its phase-changing ability for the purpose of heating, cooling, or temperature stabilization is defined as a phase change material (PCM). PCMs have found applications in a wide array of areas such as in thermal energy storage, building energy efficiency, food product cooling, spacecraft thermal systems, solar power plants, microelectronics thermal protection, and waste heat recovery.

1.1 Phase Change Materials for Building Applications

Continuing improvements in building envelope technologies suggest that residences will soon be routinely constructed with low heating and cooling loads. The use of novel building materials containing active thermal components (e.g., PCMs, subventing, radiant barriers, and integrated hydronic systems) would be an ultimate step in achieving significant heating and cooling energy savings from technological building envelope improvements. PCMs have been tested as a thermal mass component in buildings for the past 40 years, and most studies have found that PCMs enhance building energy performance. Some problems, though, such as high initial cost, loss of phase change capability, corrosiveness (in cases of some inorganic PCMs), and PCM leaking have hampered widespread adoption. Paraffinic hydrocarbon PCMs generally perform well, but they increase the flammability of the building envelope (Kissock et al. 1998; Tomlinson et al. 1992; Salyer and Sircar 1989). For these reasons, more attention is now paid to PCMs based on fatty acids or inorganic salt hydrates. Traditionally, PCMs were used to stabilize interior building temperature. In older applications, then, preferable locations for PCM were interior building surfaces such as walls, ceilings, and floors. In the more recent research projects performed in the United States, PCMs are often used as an integral part of the building thermal envelope.

Microencapsulated PCMs are positioned in the wall cavity or installed as a part of the attic insulation system. The development of PCM integrated with thermal insulations was a critical step (Kośny et al. 2006). PCM-enhanced cellulose was one of the first successful developments of this kind of product in the building arena (Kośny et al. 2007). Subsequently, researchers developed PCMs blended with blown fiberglass (Kośny et al. 2010) and plastic foams (Kośny et al. 2008; Mehling and Cabeza 2008). The major advantage of PCM-enhanced insulations is their

capability of significantly lessening and shifting peak-hour thermal loads generated by building envelopes.

As described in this report, Fraunhofer Center for Sustainable Energy Systems (Fraunhofer) performed an economic analysis to evaluate whether simple PCM-enhanced building envelope products can be cost effective. Another goal of the work was determining the cost levels at which PCMs can be cost competitive with conventional building thermal insulations. The study team considered two basic PCM applications in this analysis: (1) dispersed PCMs, and (2) simple building systems using concentrated PCMs. A third group of advanced PCM applications uses different forms of PCM containers or PCM-enhanced boards in conjunction with thermal breaks, reflective insulations, or ventilation channels. Most current experiments show that the thermal performance of advanced integrated PCM technologies can be significantly higher than the simpler dispersed PCM applications. Because these systems are complex, though, they are difficult to analyze using existing whole-building energy simulation tools. As a result, field test results are particularly valuable for energy performance and cost analyses before sufficient computer tools are developed and validated for these technologies.

Dispersed PCM systems are less complex, easier to analyze, and more forgiving from the perspective of potential errors in numerical analysis. Usually, a wide selection of PCMs with slightly different PCM functional temperatures can be used for the same climatic conditions and for the same location within the building envelope. At the same time, concentrated PCM applications require more precise selection of the PCM's functional temperature range, location, and heat storage density.

In addition to the limited theoretical analysis, this report summarizes the results of experimental and theoretical analyses previously performed in North America. These results are subsequently used as performance benchmarks for different PCM configurations that were tested in the United States for building applications. This work was not intended to optimize the configurations of PCMs. Theoretical parametric analysis was used only for the dispersed PCM applications. Thermal and building energy simulations are used here for PCM performance comparisons as a function of different insulation configurations and thermal conditions.

To reiterate, a wide variety of PCMs with different temperature profiles, hysteresis, and heat storage capacities are available today for building envelope applications. Earlier research demonstrated that to accurately analyze the thermal performance of specific PCMs, computer models need to use detailed enthalpy/temperature profiles developed during either very slow (heating rate about 0.2°F or 0.1°C/minute) differential scanning calorimetry (DSC) (Günther et al. 2009; Mehling and Cabeza 2008), or other dynamic testing methods using step function procedures (Kośny et al. 2009). Because dynamic testing was not an objective of this project and to simplify analysis and minimize the number of necessary simulations, "ideal" PCM thermal characteristics with very small hysteresis were used for the parametric thermal simulations. A series of these simulations helped to estimate the performance limits for two of the most common thicknesses representing the wall and attic PCM-enhanced insulation applications and for different intensities of exterior thermal excitations. Earlier experiments demonstrated that selecting a PCM with a proper functional temperature range is critical for the thermal performance of PCM-enhanced building envelope systems (Dincer and Rosen 2011; Kośny 2008). Therefore, in this work, the study team also analyzed the effect of selecting a proper PCM

melting point against the internal space temperature. Thermal performance limits developed during this parametric analysis were later used in the whole-building energy consumption analysis, which facilitated an estimation of the potential cooling energy savings for each of the selected climates.

In this work, only one concentrated PCM system was used for energy and cost performance analyses. This system— PCM-enhanced gypsum board—is one of the earliest and the most popular PCM applications. In the United States, this application has been tested for at least 40 years. In cases with this PCM system, theoretical thermal analysis was not conducted because of a very strong performance dependence on individual properties of PCMs (microencapsulation, shape stabilization, impregnation, and heat storage density); PCM loads; internal space temperature profiles; and locations, among others. A large number of similar concentrated PCM-building products are currently available as well. The study team believes that only the computer models developed for these specific systems and validated with the experimental data should be used to analyze the performance of each of these individual systems. Fortunately, a substantial amount of theoretical and experimental research has been carried out on these technologies during the past several decades. In this report, then, the basic performance levels of PCM-enhanced gypsum board applications are assessed using either the available experimental data or the predictions generated by the validated computer models.

As mentioned before, the economic analysis presented in this report is almost exclusively for dispersed PCM systems with fiber insulations and PCM-enhanced gypsum boards. For each of the PCM applications analyzed and for five southern U.S. climates, the study team estimated the potential cooling energy savings. The cost of the saved energy was estimated based on the unit electricity costs in each of the selected locations. Four typical PCM enthalpies used by the industry—52 Btu/lb (120 kJ/kg), 65 Btu/lb (150 kJ/kg), 82 Btu/lb (190 kJ/kg), and 95 Btu/lb (220 kJ/kg)—were assumed in the cost analysis. The amount of PCM was normalized against the heat storage capacity of the basic wall and roof systems using 52 Btu/lb (120 kJ/kg) as a baseline. Next, the cost of the PCM was analyzed for the PCM price range between $1.50/lb and $7.50/lb. Subsequently, a payback period was computed for each PCM-enhanced envelope configuration that the study team considered.

The final part of this report is the cost performance analysis of conventional insulation applications. Similar energy savings as in cases with PCM applications were used as targets for the comparisons. Whole-building energy analyses were performed for different levels of wall and attic insulation. Economic effectiveness of conventional attic insulation was estimated based on 2011 RSMeans national cost data (http://www.rsmeans.com/chgnotice/index.asp). Next, payback periods were computed for all considered climates and compared with similar applications containing PCM.

1.2 Overview of U.S. Performance Data for Concentrated Phase Change Material Building Envelope Systems

Different technologies utilizing phase transition were investigated for energy performance improvement of building envelopes. They included concentrated PCM applications in building board products in which PCMs were integrated with thermal insulations or stored in arrays of containers. Experimental results were reported for both laboratory-scale and field-scale full-size building elements. Some PCM-enhanced building materials, like PCM-enhanced gypsum boards,

PCM-impregnated concretes, or PCM-enhanced fiber insulations have already found limited applications in countries outside the United States. To be fully effective, however, concentrated PCM systems need to be well engineered, taking into account the amount of PCM, its optimum functional temperature, and its location.

Many potential PCMs have been tested for building applications, including inorganic salt hydrates, organic fatty acids, eutectic mixtures, fatty alcohols, neopentyl glycol, and paraffinic hydrocarbons. There were several moderately successful attempts in the 1970s and 1980s to use different types of organic and inorganic PCMs to reduce peak loads and heating and cooling energy consumption (Kissock et al. 1998; Tomlinson et al. 1992; Salyer and Sircar 1989; Balcomb et al. 1982). Historically, performance investigations focused on impregnating concrete, gypsum, or ceramic masonry with salt hydrates or paraffinic hydrocarbons. Most of these studies found that PCMs improved the building energy performance by shifting the peak demands, thus reducing the peak hour cooling loads.

During early testing, paraffinic hydrocarbon PCMs generally performed well, but they compromised the flammability resistance of the building envelope. Salyer and Sircar (1989) reported that during the testing of 4 ft × 8 ft (1.22 m × 2.44 m) wallboard with PCM, no statistically significant loss of PCM or "pooling" occurred, even after 3 months of exposure to continuously cycled 100°F (37°C) air. In addition, Kissock and coworkers (1998) reported that wallboard containing a paraffin mixture made up mostly of n-octadecane, which had a mean melting temperature of 75°F (24°C) and a latent heat of fusion of 65 Btu/lb (143 kJ/kg), "was easy to handle and did not possess a waxy or slick surface. It scored and fractured in a manner similar to regular wallboard. Its unpainted color changed from white to gray. The drywall with PCM required no special surface preparation for painting."

1.3 Research Studies Focused on Concentrated Phase Change Material Applications in Walls and Roofs

Initial concentrated PCM testing in whole-building conditions took place about 60 years ago. One of the first documented applications of a PCM used for passive solar heating of a home was in 1948 in a house designed by Maria Telkes (Dincer and Rosen 2011). This house in Dover, Massachusetts, contained a Glauber's salt PCM, placed in drums housed in spaces between the main rooms that were ventilated with fans to move the warm air into the living space in winter. In summer the same system delivered cool air to the rooms. This system alone could keep the house warm for approximately 11 sunless days.

At the University of Kansas, Zhang and colleagues (2005) developed a thermally enhanced R-11 frame wall that integrated a paraffinic PCM via macroencapsulating. Results from the field testing showed that the PCM wall reduced wall peak heat fluxes by as much as 38%. For walls that faced in different directions, over a period of several days, the average wall peak heat flux reduction was approximately 15% for a 10% concentration of PCM. When a 20% PCM concentration was used, the flux reduction was approximately 9%. The average space-cooling load was reduced by approximately 8.6% when 10% PCM was applied and by 10.8% when 20% PCM was used.

In 2006, Kissock and Limas of the University of Dayton investigated paraffinic PCM that can be added to the building envelope components, such as the walls or roofs, to reduce the peak diurnal

cooling and heating loads transmitted through the envelope (Kissock and Limas 2006). This work was a combined numerical-experimental study to quantify the effectiveness of PCM in reducing thermal loads through the building envelope components and to develop a design strategy for the placement of PCM within the massive walls. The PCM studied was paraffin octadecane with an average melting temperature of 78.1°F (25.6°C). For the climate of Dayton, Ohio, thermal loads through the PCM-enhanced wood frame wall were simulated using an explicit finite-difference procedure with the indoor air temperature held constant. Compared to the conventional wall, cooling load savings were close to 16%. The simulation technique has been validated against the experimental work.

During the Greenbuild 2009 conference, National Gypsum introduced its ThermalCORE gypsum panels, which contain microencapsulated PCM and can store approximately 22 Btu of thermal energy per square foot (250 kJ/m^2).[1] Dynamic testing was performed on ½-in. thick samples of the PCM-enhanced gypsum board using an ASTM C-518 heat flow meter apparatus (ASTM International 2006a). PCM with a melting point close to 79°F (26°C) was used in these experiments. Preliminary thermal performance evaluation that incorporated 300-minute temperature ramps showed about a 13.5% reduction in cooling load.

Murugananthama and coworkers (2010) performed a series of field test measurements on two test huts in Arizona. One of the test attics contained conventional R-30 fiberglass insulation. The other one had arrays of plastic containers with a biobased PCM installed within all building envelope components. The structures had enclosed attic spaces with R-30 fiberglass batt between 61-cm (24-in.) on. center. ceiling framing. Half-inch oriented strand board (OSB) roof sheathing was covered with 15 lb roofing felt and standard three tab fiberglass desert tan shingles. Walls were constructed with 2 × 4 studs 16-in. o.c. with R-13 fiberglass insulation, T-111 siding, and ½-in. finished gypsum board. Arrays of plastic containers holding a PCM with a density of 0.56 lb/ft^3 (9 kg/m^3) inside were installed in all walls between the fiberglass insulation and sheetrock of one of the test huts. In addition, PCM with a density of 1 lb/ft^3 (16 kg/m^3) was installed in both the ceiling and the floor. Experimental work was carried out by Arizona Public Service (APS) in collaboration with Phase Change Energy Solutions Inc. (PCES) with a new class of organic-based PCM. The experimental setup showed maximum energy savings of about 30%, a maximum peak load shift of ~60 minutes, and a maximum cost savings of about 30%. During the entire cooling season (March through October) average energy savings for the PCM test hut reached about 16%, ranging between 12% and 14% during the June–July time period and reaching 25% during the shoulder months.

In 2006, Kissock and Limas investigated paraffinic PCMs that can be added to steel roofs to reduce the peak diurnal cooling and heating loads (Kissock and Limas 2006). This work was a combined numerical-experimental study where the simulation technique was validated against the experimental data. The PCM studied was the paraffin octadecane, which has an average melting temperature of 78.1°F (25.6°C). Analyzed metal roof had two 1-in. thick layers of the polyisocyanurate foam. The bottom layer of the foam was enhanced with the paraffinic PCM. For the climate of Dayton, Ohio, thermal loads through the PCM-enhanced polyisocyanurate board were simulated using an explicit finite-difference procedure with the indoor air

[1] See http://www.thermalcore.info/product-info.htm for more information.

temperature held constant. When compared to the conventional roof (no PCM), cooling load savings were close to 14%.

A prototype residential roof with a cool-roof surface, natural subventing, and PCM heat sink was designed and field tested (Miller and Kośny 2008; Kośny et al. 2007). A multilayer configuration of PCM-enhanced polyurethane foams, PCM-impregnated fabrics, and highly reflective aluminum foil were used. Loading of PCM was about 0.08 lb/ft^2 (0.39 kg/m^2) of the surface area. Two types of PCMs were used. Their melting temperatures were around 78° and 90°F (26° and 32°C). The total storage capacity of the PCM heat sink was about 4.8 Btu/ ft^2 (54 kJ/m^2) of the roof area. The results show that for the metal roof assembly using cool-roof pigments, reflective insulation, and subventing air channels, the summertime peak heat flow crossing the roof deck was reduced by about 70% compared with the heat flow penetrating the conventional shingle roof. Installation of the PCM heat sink generated an additional 20% reduction in the peak-hour heat flow, bringing the total reduction to 90%. A similar configuration of a roof containing metal roof panels with photovoltaic (PV) laminates and PCM heat sink was field tested during 2009 and 2010 (Kośny et al. 2012) in eastern Tennessee. Under those climatic conditions, PCM-associated cooling energy savings were found to be about 25% compared to the conventional shingle roof.

The capability of PCMs to reduce the peak loads is relatively well documented. For example, Zhang and coworkers (2005) found peak cooling load reductions of 35% to 40% in side-by-side testing of conditioned small houses with and without paraffinic PCM inside the walls. Similarly, Kissock and colleagues (1998) measured peak temperature reductions of up to 18°F (10°C) in side-by-side testing of unconditioned experimental houses with and without paraffinic PCM wall board. Kośny and coinvestigators (2006) reported that PCM-enhanced foam insulation can reduce wall-generated peak-hour cooling loads by about 40%. Miller and Kośny (2008) reported over 90% of cooling peak-hour load reductions for a prototype metal roof using a cool-roof surface, natural subventing, and PCM heat sink installed over the roof deck.

RADCOOL, a thermal building simulation program based on the finite difference approach, was used by Lawrence Berkeley National Laboratory (LBNL; Feustel and Steti 1997; Feustel 1995) to numerically evaluate the latent storage performance of treated wallboard. Simulation results for a living room with high internal loads and weather data in Sunnyvale, California, showed significant reduction of room air temperature when heat was stored in PCM-treated wallboards. In the case of the prototype International Energy Agency (IEA) building located in California climate zone 4, it was estimated that PCM wallboard would reduce the peak cooling load by 28%.

Table 1 summarizes experimental thermal performance results from different studies presented above.

Table 1. Summary of U.S. Test Results for Concentrated PCM Applications

Reference	PCM Location	PCM Enthalpy, Btu/lb (kJ/kg)	PCM Loading, Btu/ft^2 (lb/ft^2; percentage PCM load, if available)	Approximate Cooling Load Savings (%) and city/application
Zhang et al. (2005)	Wall core, containers	52 (123.7)	~10 (0.2; 10%)	9 Lawrence, Kansas
Zhang et al. (2005)	Wall core, pipes	52 (123.7)	~21 (0.4; 20%)	11 Lawrence, Kansas
Kissock and Limas (2006)	Wall, gypsum board	65 (143)	~32 (0.5; 30%	16 Dayton, Ohio
Willson (2009)	Wall, gypsum board	50 (110)	22 ~0.4	13.5 Dynamic Heat Flow Meter Aapparatus testing
Murugananthama et al. (2010)	Wall, ceiling, floor, PCM containers	81 (178)	Walls; 45 ~0.56	16 Whole building, Tempe, Arizona
Kissock (2006)	Metal roof, polyisocyanurate board	65 (143)	30 0.5	14 Dayton, Ohio
Kośny et al. (2012)	Roof deck, PCM containers	81 (178)	27 ~0.3	25 PCM participation, Oak Ridge, Tennessee

2 Phase Change Material Price Challenges

2.1 Phase Change Material Cost Components

PCM prices are driven by market demand and supply relationships. Today's U.S. market for PCMs is not yet fully developed, resulting in limited demand that is largely responsible for their relatively higher prices. The market potential for PCMs in wide-ranging applications including building energy improvements, however, is significant. Because manufacturers base their prices on future market expectations, prices are likely to drop in the future. The current energy performance studies that the U.S. research community is conducting on PCMs are expected to play a crucial role in shaping their prospects for building applications. Encouraging field energy performance data developed during the last decade by different laboratories and universities will help fuel market demand for PCMs, most likely enabling reductions in the cost of these products.

PCM product cost is primarily governed by the cost of the raw PCM material and the cost of encapsulation. Encapsulation, or enclosing the material with an inert coating, is required to prevent the external environment from contaminating the PCM. At the same time, encapsulation allows for easy handling of the PCM for most building-related applications. Two main approaches are used to encapsulate PCMs: (1) macroencapsulation or packaging, where PCMs are encapsulated in large pouches, tubes, rectangular panels, or spherical capsules; and (2) microencapsulation, where microscopic amounts of PCMs are coated with a protective shell material. Microencapsulation provides improved heat transfer between the PCM and its surroundings because of increased surface area but usually adds cost because it involves several chemical synthesis steps. The final PCM product cost varies greatly depending on the approach adopted to encapsulate the PCM.

2.2 Material Cost

PCMs considered for building applications rely on a solid-liquid transition and can be classified into the two categories: organic PCMs and inorganic PCMs.

2.2.1 Organic Phase Change Materials

Organic PCMs are most often composed of organic materials such as paraffins, fatty acids, and sugar alcohols. For building applications, paraffinic PCMs are the most commonly used for several reasons. First, paraffinic PCMs are straight chain n-alkane hydrocarbon compounds such as n-Heptadecane and n-Eicosane. Their melting temperature and phase change enthalpy increase with the length of the carbon chain. When the number of carbon atoms in the paraffin molecule is between 13 and 28, the melting temperature falls within a range of approximately 23° to 140°F (–5° to 60°C) (Mehling and Cabeza 2008), a temperature range that covers building applications in most climates around the world. In addition, paraffinic PCMs are chemically inert, nontoxic, reliable, and biocompatible. They also show a negligible subcooling effect (Boh and Sumiga 2008). Fatty acids are represented by the chemical formula $CH_3(CH_2)_{2n}COOH$ (e.g., capric acid, lauric acid, and palmitic acid). Fatty acids have storage densities very similar to paraffins, and like paraffins their melting temperatures increase with the length of the molecule. Although chemically stable upon cycling, they tend to react with the environment because they are acidic by nature.

Sugar alcohols are a hydrogenated form of a carbohydrate such as D-sorbitol or xylitol, among others. They generally have higher latent heat and density than paraffins and fatty acids. Because they melt at temperatures between 194° to 392°F (90° and 200°C), though, they are unsuitable for building applications.

2.2.2 Inorganic Phase Change Materials

Inorganic PCMs cover a wide range of temperatures. Although inorganic PCMs have similar latent heat per unit mass as organic PCMs, their latent heat per unit volume is generally higher because of their higher density. Salt hydrates are one type of inorganic salts containing one or multiple water molecules such that the resulting crystalline solid has a chemical formula of $AB.nH_2O$. Some of the examples are $CaCl_2.6H_2O$, $LiNO_3.3H_2O$, and $KF.3H_2O$. Salt hydrates are nontoxic, nonflammable and less corrosive, with higher thermal conductivity than organic PCMs. Salt hydrates have melting temperatures in the range of 41° to 266°F (5° to 130°C), a suitable range for building applications.

2.2.3 Material Cost of Phase Change Materials

The material cost depends significantly on the classification of the PCM (i.e., organic, inorganic, or biomaterial). Commercial paraffinic PCMs are byproducts from the oil refineries; therefore, they are available in abundant supply at a relatively cheaper price. The price of paraffins increases with the purity. Pure paraffin wax (>99%) is more expensive than technical grade p-wax (90%−95%) (Mulligan and Gould 2002). The current cost of paraffin wax is $0.85−$0.91/lb ($1.88−$2.00/kg).[2] As a reference, pure laboratory-grade eicosane is $24.50/lb ($53.90/kg); the technical grade is $3.20/lb ($7.04/kg). The estimated cost of microencapsulation for a similar paraffin octacosane is ~45%−65% of the total cost of the paraffin PCM.[3] Another low-cost paraffin alternative available is Baker Petrolite's POLYWAX, which costs $2.00/gal ($0.53/L).

The cost of fatty acid PCMs such as stearic acid, palmitic acid, and oleic acid are $0.65−$0.71/lb ($1.43−$1.56/kg); $0.73−$0.78/lb ($1.61−$1.72/kg); and $0.76−$0.80/lb ($1.67−$1.76/kg), respectively. Biodiesel crude glycerine (biocrude) is $0.10−$0.13/lb ($0.22−$0.29/kg) CIF China Mainland.[4]

Entropy Solutions Inc. quotes $0.75−$2.50/lb ($1.65−$5.50/kg) for its commercial volume organic PCM products. Chemical components for Entropy's products are derived from agricultural sources and their melting temperature ranges between -40° to 302°F (−40°C and 150°C). PCES sells biobased PCMs with melting temperatures of 77°, 81°, and 84°F (25°, 27°, and 29°C). The cost of the PCES products varies with M-values. For example, M-27, M-51, M-91, and M-182 products have wholesale prices of $1.94/ft^2, $2.83/ft^2, $4.59/ft^2, and $8.79/ft^2 ($20.88/m^2, $30.46/m^2, $49.40/m^2, and $94.61/m^2), respectively. The prices for M-27, M-51, M-91, and M-182 products are $6.47/lb, $5.05/lb, $4.59/lb, and $4.40/lb ($14.26/kg, $11.13/kg, $10.12/kg, and $9.70/kg), respectively.[5]

[2] See www.icispricing.com/ for more information.
[3] Private communication with Tim Riazzi, Microtek Labs
[4] CIF = cost + domestic fee + overseas freight + overseas insurance + net profit
[5] Private communication with Peter Horwath - PCES

In 2010, Syntroleum Corporation received a U.S. Department of Energy (DOE) American Recovery and Reinvestment Act (ARRA) award (DE-EE0003924) for development of low-cost, biobased PCMs for building envelope applications.[6] Syntroleum's plant was built to compete with a commodity product—diesel fuel—it can manufacture the octadecane-rich paraffin intermediate at the price of biodiesel (which sells in the $4.50−$5.50/gal ($1.19−$1.45/L) or $0.69−$0.85/lb ($1.52−$1.87/kg) range. The cost of converting the paraffin into form-stable composites is not yet well defined. But because Syntroleum's plant uses a low priced commodity plastic (high-density polyethylene; HDPE) in a continuous process using "workhorse" polymers industry equipment (extruders/pelletizers), the costs are expected to be significantly lower than those for microencapsulation. Prices for these new PCM pellets that have 60% to 70% paraffin in HDPE are expected to range between $3.00/lb and $4.00/lb ($6.60/kg and $8.80/kg) with a target enthalpy of approximately 43 Btu/lb (100 kJ/kg).

The average cost of inorganic PCM calcium chloride is $0.059−$0.091/lb ($0.13−$0.20/kg); the cost of a small quantity of 1 lb (1 kg) is $0.35 ($0.77).[7] Calcium chloride is a salt of calcium and chloride, and is a colorless, odorless, and nontoxic solution. PCMEnergy India produces salt hydrate PCMs with a melting temperature range of 64° to 118°F (18°−48°C). The PCM is prepared in house and contains no impurities. The cost of the raw material used is $0.90−$1.80/lb ($1.98−$3.96/kg). The PCM products are in the packaged form instead of microencapsulated. The price of the final product is $1.40−$2.25/lb ($3.08−$4.95/kg) with the packaging step contributing ~20%−35% of the total cost.

Alderman Research produces inorganic PCMs composed of $CaCl_2.6H_2O$ as the main compound. Viscosity modifiers, nucleating agents, and other stabilizers make up less than 20% of the total weight. The PCMs are prepared in house and the melting temperature is kept around 174° to 176°F (79°−80°F). The product cost breakdown includes $0.21/lb ($0.46/kg) for formula and $0.18/ft^2 ($1.94/m^2) for packaging the film (raw materials only; no labor, overhead, or profit). An ordinary food-packaging machine, similar to the ones that package condiments for national fast food chains, is used to package the PCM. The packaging procedure involves cutting the individual packets at a desired length rather than slitting them. The final cost of the product is $1.00−$2.00/ft^2 ($10.76−$21.52/m^2) with the packaging process accounting for 9%−18% of the total cost. This product is available in one-pallet size quantities.

2.3 Alternatives to Paraffin

Cost and volumetric latent heat are two key parameters that will decide the market adoption of PCMs as a building energy efficiency material. Today, paraffins are the most widely used PCMs in building applications because they are nontoxic, abundant in supply, and easy to microencapsulate. Other attractive features include small subcooling, chemical inertness, and good recyclability. Although the technology is ready for the incorporation of paraffinic PCMs in the building materials, the high cost of paraffin chemicals along with low phase change enthalpies (4,027−5,369 Btu/ft^3;150−200 MJ/m^3) and high fire loads are proving to be major

[6] See http://www.recovery.gov/Transparency/RecipientReportedData/pages/RecipientProjectSummary508.aspx?AwardIdSur=117469 for more information.

[7] See http://www.kaycircle.com/What-Is-the-Average-Cost-of-Calcium-Chloride-per-ton-lb-Average-Calcium-Chloride-Price for more information.

barriers to their widespread acceptance. Because paraffins are derived from crude oil, their prices are sensitive to the season and to geopolitical scenarios. In fact, crude oil prices have been on the rise in recent years. All these factors underline the need to shift the focus away from paraffinic PCM to another class of PCM. Salt hydrates and biobased PCMs are two alternative materials with great potential to substitute for paraffin in the future, as well as to compete with the existing energy efficient building materials and technologies.

2.3.1 Salt Hydrates

Inorganic salt hydrates with low chemical cost, higher enthalpies (6,711−9,397 Btu/ft^3; 250−350 MJ/m^3), better thermal conductivity (0.29 Btu/h/ft/°F; 0.5 W/m/K), and suitable melting temperatures of 41°–248°F (5°−120°C) show great promise to become a primary PCM for building applications. In fact, inorganic salts such as Glauber's salt were the first PCM ever to be applied in building applications (Telkes 1952). So far inorganic PCMs have found very limited application in buildings because of their undesirable properties. They have poor nucleating properties, meaning that their subcooling effect, corrosive nature, incongruent melting, and phase segregation during transition are problematic. With the advances made over the last few decades in the field of salt hydrates, however, it is now possible to control these adverse properties to a large extent.

2.3.1.1 Approaches to Improve Phase Change Properties

Garg and colleagues (1985) showed that adding a nucleating agent with a crystal structure similar to the energy storage material reduces the amount of subcooling. And because most salt hydrates suffer from a low rate of crystallization, uniformly distributing the nucleating seed agent throughout the phase change media helps increase the rate of crystallization.

Inorganic salts experience incongruent melting. This happens when the solubility of the salt is not high enough to dissolve all the anhydrous salt in the water of crystallization that is released. This effect reduces the PCM product's efficiency because undissolved salt settles down at the bottom of the container and does not contribute to the heat storage process. The extra water principle is used to avoid incongruent melting. The method involves using extra water to dissolve the entire anhydrous salt during melting. This thickens the material to gel form as suggested by Telkes (1952).

Thickening materials are used to minimize the phase separation in solid and liquid phases and also to prevent nucleating agents from settling down because of their density. Super-absorbent polymer (SAP) synthesized from an acrylic acid copolymer has been used as an effective thickener to prevent phase separation of the high-hydrate inorganic salts ($Na_2SO_4.10H_2O$ $Na_2HPO_4.12H_2O$, and $Na_2CO_3.10H_2O$) (Ryu et al.1992). SAP included in the amount of 3–5 wt % was found to be an effective thickener for most of these salt hydrates. For the low hydrate inorganic salts ($CH_3COONa.3H_2O$ and $Na_2S_2O_a.5H_2O$), adding small amounts of 2−4 wt % of carboxymethyl cellulose (CMC) stabilized the salt hydrate. Three different powders of carbon (1.5−6.7 µm), copper (1.5−2.5 µm) and titanium oxide (2−200 µm) are found to reduce the subcooling of thickened $Na_2HPO_4.12H_2O$. Also, the subcooling of thickened $CH_aCOONa.3H_2O$ is reduced from 36°F (20°C) to 3°–5°F (2°−3°C) by adding 2 wt % potassium sulfate. Thixotropic thickening agents are another low-cost option.

To improve thermal/mechanical properties, foreign materials such as graphite fiber or metal can be embedded into the PCM to form a composite. Alternatively, PCM can be incorporated into the matrix of other materials such as graphite, metallic, or polymer matrix. Matrix network holds the PCM inside the pores even when it has melted. Li and coworkers (2009) developed novel microencapsulation method where organic PCMs were coated with HDPE/wood floor compound. They introduced micromist graphite during the microencapsulation of organic PCMs to increase thermal conductivity. The shell and matrix prevented the leakage when PCM was melted, forming a shape-stabilized PCM. Thermal conductivity was enhanced by 17.7% by adding 8% weight of graphite. The inclusion of graphite was shown to have no adverse effect on the mechanical and thermal stability of the composite PCM.

2.3.1.2 Glauber's Salt

It is worthwhile to describe here the significant technological progress that has been made to improve the adverse properties of Glauber's salt, because it is one of the most inexpensive heat storage materials that can be used in building applications. It is composed of 44% Na_2SO_4 and 56% H_2O by weight and has a high latent heat of 254 kJ/kg (377 MJ/m^3). Its melting temperature is about 90°F (32°C), which is well-suited to building applications. Glauber's salt shows a very large subcooling of ~27°F (15°C). Borax has been successfully used as a nucleating agent to reduce subcooling of this salt to 5°–6°F (3– 4°C). Adding borax to the salt improves thermal cycling of the mixture as well. The extra water principle has been employed to prevent incongruent melting and to improve thermal cycling (Farid et al. 2004). To avoid phase segregation, thickening agents, such as bentonite clay, have been used. Bentonite-enhanced salt has an additional advantage in that its application reduces the heat transfer to the salt that results from the lower thermal conductivity of the mixture, a desirable feature for peak-hour load shifting in building applications.

2.3.1.3 Calcium Chloride Hydrate

Calcium chloride hydrate ($CaCl_2.6H_2O$) is another popular salt hydrate that has received a lot of attention in the scientific community because of its high latent heat and its ability to melt congruently. $SrCl_2$, $BaCO_3$, $SrCO_3$, and BaF_2 have been proposed as nucleating agents to reduce subcooling and incongruent melting of $CaCl_2.6H_2O$. These were chosen for testing based on either their similar crystal structure or using intuition. For example, $SrCl_2$ and $CaCl_2.6H_2O$ both have hexagonal structures. $SrCl_2$ acts as a site for crystals to grow, allowing $CaCl_2.6H_2O$ to solidify without as much subcooling. $BaCO_3$ was also found to be an effective nucleating agent, although it is currently unclear why. In certain quantities, both of these additives can eliminate subcooling (Lane 1992). These nucleating agents also help prevent phase segregation of high-hydrate $CaCl_2.6H_2O$ into low-hydrate $CaCl_2.4H_2O$.

2.3.1.4 Microencapsulation of Salt Hydrates

Heterogeneous polymerization techniques such as emulsion polymerization, dispersion polymerization, microemulsion polymerization, and miniemulsion polymerization have typically been used to encapsulate inorganic materials (Jing et al. 2011). The resulting encapsulated product suffers from low solid content inside the capsule and poor encapsulation yield. Microencapsulation of salt hydrates becomes even more challenging because salt hydrates are hydrophilic in nature and contain a well-defined water fraction. To be useful in building applications, shell material needs to act as a water/vapor barrier and to be hydrophobic. Both characteristics prevent the salt hydrate from evaporating. Organic polymers are typically used as

shell material in the encapsulation process; however, they are chemically incompatible with salt hydrates.

Recently, efforts to microencapsulate salt hydrates have been successful.[8,9] Fraunhofer ISC has developed a method in which a salt hydrate melt is encapsulated by an inorganic–organic hybrid polymer known as ORMOCER. The process involves injecting salt hydrate melt drops into the ORMOCER solution that solidifies locally as it comes in contact with the surface of the drop, forming a hard encapsulating layer around the salt hydrate drop. The encapsulated drops are removed from the coating solution via mechanical means and washed thoroughly, then allowed to dry in air under ambient condition. Salt hydrate drops subsequently crystallize as they cool down. Capsules produced in this way have diameters ranging from a few micrometers to a few millimeters. Although the final product has water permeability and stability issues, this is nonetheless an encouraging step.

Hessbrugge and Vaidya (1997) developed a novel technique for encapsulating of water-soluble salts. The method employs a simple process where additives such as emulsifiers and acid acceptors that are needed to stabilize the aqueous–organic interface and to remove the excess acid formed by hydrolysis are not required. This results in a cheaper microencapsulation process because the post-treatment required to remove additives and their byproducts is no longer required. In addition, there is less likelihood of contamination of encapsulated product because trace amounts of the reaction components and their byproducts are absent.

Brandt and colleagues (2006) encapsulated powdered Na_2CO_3 hydrate particles with an inorganic SiO_x layer via a sol-gel process in a TMOS solution (Rößner 1999).

2.3.2 Biobased Phase Change Materials

Biobased PCMs, which are obtained from animal fat such as beef tallow and lard and oils from plants such as palms, coconuts, and soybeans, are a renewable and green alternative to paraffinic PCMs. They are nontoxic and can be recycled through thousands of cycles without experiencing any material degradation. Because they are hydrogenated hydrocarbons with a saturated electronic configuration, they are chemically stable and can last for decades. In addition, fat- and oil-based PCMs offer similar or improved performance, a greater degree of fire resistance, and reduced costs.

2.3.2.1 Fatty Acids

Among all PCMs including biobased PCMs, fatty acids have superior advantages, such as congruent melting and cooling, high latent heat of fusion, low costs, fire resistance, nontoxicity, very small subcooling and volume change, and good chemical and thermal stability after a large number of thermal cycles (Sari et al. 2009; Sari 2003).[10,11] Another attractive feature is that the melting temperatures can be adjusted to the match the requirement by selecting a right combination of eutectic binary mixtures of fatty acids. The eutectic mixtures of fatty acids as

[8] See www.messib.eu/about_project/messib_innovative_elements/phase_change_materials/microencapsulation_of_salt_hydrates.php for more information.
[9] See www.freepatentsonline.com/y2011/0017944.html for more information.
[10] See www.renewablealternatives.com/pcm.htm for more information.
[11] See www.reeis.usda.gov/web/crisprojectpages/197095.html for more information.

PCMs also retain their good thermal stabilities as a single fatty acid after repeated thermal cycling (Sari 2005; Sari et al. 2004).

In fact, these biobased PCMs have the potential to replace petroleum-based PCMs and help reduce carbon dioxide (CO_2) greenhouse gas emissions. Because major properties of fat and oil derivatives are similar to those of paraffin, fat and oil derivatives can be used for similar applications. For example, wax products such as candles, pencils, and coatings that have been largely dominated by paraffins are now being manufactured using biobased and renewable feedstocks such as hydrogenated soybean oil.

2.3.2.2 Coconut Oil

Coconut is a diet staple for millions of people living in tropical regions of the world. Coconut oil (oil extracted from coconut fats) is a type of saturated fatty acid containing about 44%−51% of lauric acid ($CH_3(CH_2)_{10}COOH$). For building applications, it is critical that fatty acids are encapsulated well. Otherwise, they tend to flow everywhere when experiencing phase changes. Microcapsules using lauric acid (LA) as the core and melamineformaldehyde (MF) resin as the shell have been successfully prepared as a PCM for latent heat thermal storage by in situ polymerization (Bao et al. 2011; Su et al. 2006). Özonur and coworkers (2006) successfully prepared microcapsules of natural coco fatty acid mixture as core and gelatin-gum Arabic as shell material by a complex coacervation technique. Chai and colleagues (2007) microencapsulated stearic acid and palmitic acid with SiO_2 using a one-step, solid-state chemical reaction at low temperature.

2.3.3 Shape-Stabilized Phase Change Material

Recently, a novel PCM known as shape-stabilized (ss) PCM has been developed that can retain the shape of the solid structure during phase transition. ss-PCM is a composite of PCM with another material, such as an ss-paraffin composite consisting of paraffin incorporated on a microscopic level into a porous supporting structure such as HDPE. ss-PCMs offer several benefits including high apparent heat capacity, suitable thermal conductivity, and no need for a container because ss-PCMs do not tend to flow out of the porous structure during melting. Inaba and Hu (1997) observed no leakage of paraffin through an HDPE network for paraffin loading levels as high as 75% by weight. Yinping and coinvestigators (2006) prepared ss-paraffin with 80% by weight loading of paraffin and found that no containment was required (i.e., samples can be cut into pieces without any drainage). Keep in mind that even with all the benefits mentioned here, HDPE adds to the cost of the final PCM product.

2.4 Expected Future Cost Reductions

The price of the raw material and the encapsulation process determine the cost of PCM products. The cost to macroencapsulate a PCM is ~20% of the total cost. The microencapsulation process is even more expensive at ~50% of the final product cost. Currently, paraffins are the most popular choice for PCMs because they offer several attractive features (i.e., they are chemically inert, nontoxic, and easy to encapsulate).

For building applications, latent enthalpy per unit volume and flammability are the two main performance criteria used to decide on the type of PCM. Paraffins do not fare well on either of these criteria. Because of their higher latent heat per unit volume and nonflammability, salt hydrates have the potential not only to replace paraffins as a PCM of choice for building

applications, but also to outperform other competing technologies such as thermal insulations. There are, however, some technological challenges that need to be addressed before salt hydrates can become a commonplace PCM in building applications: the subcooling effect and the difficulty in microencapsulating the salt hydrates because of their water content (although there have been recent encouraging steps in this area as mentioned previously). Recently, prices of salt hydrates have fallen, but the real solution lies in developing low-cost, easy-to-manufacture, and chemically, physically, and thermally stable salt hydrate PCMs that will work for building applications.

Biobased PCMs are another renewable, cheap, and ecofriendly option to paraffins. With more advanced knowledge to control the transition properties and improvements in the process technology, it is possible that biobased PCMs will become commonplace in the near future.

3 Whole-Building Energy Simulations—Theoretical Performance Limits for Building Envelopes Using Conventional Thermal Insulations

Conventional thermal insulations (fiber insulations and plastic foams) are the most popular and widely accepted technical means to improve the thermal performance of building envelopes. It is also well known, however, that the thermal effectiveness of the conventional insulations is not always the same. In fact, a law of diminishing return applies to the energy savings with the level of thermal insulation for new and retrofitted projects (Kośny et al. 2010; Huang et al. 1999). Furthermore, for building retrofits, a diminishing return on energy savings is obtained with increased levels of pre-existing thermal insulation

In this part of the project, the team used a whole-building energy performance analysis to estimate energy consumption levels for a single-story ranch house in five southern U.S. climates. Figure 1 shows the layout of the house. In addition, a detailed thermal load distribution analysis was performed to estimate the cooling energy consumption by the attic and the walls. The study team used DOE-2.1E, EnergyPlus and AtticSim computer software[12] to simulate a single-family residence and to perform thermal performance modeling of the residential attic and walls used in parametric analysis. To find a relation between the wall R-value and the heating and cooling energies, a lightweight ranch-type building of about 1,540 ft^2 (143 m^2) floor area was simulated on 12 different wood-frame walls with R-values from 2.3 to 39.0 h-ft^2-°F/Btu (0.4 to 6.9 K-m^2 /W). Similarly, to find a relation between the attic floor insulation R-value and the heating and cooling energies, five different attic insulation assemblies with R-values from 12 to 50 h-ft^2-°F/Btu (2.12 to 8.80 K-m^2 /W) were simulated. The main goal of this work was to identify situations in which PCM-enhanced building envelopes would become more effective in terms of cost and performance compared with the conventional thermal insulations.

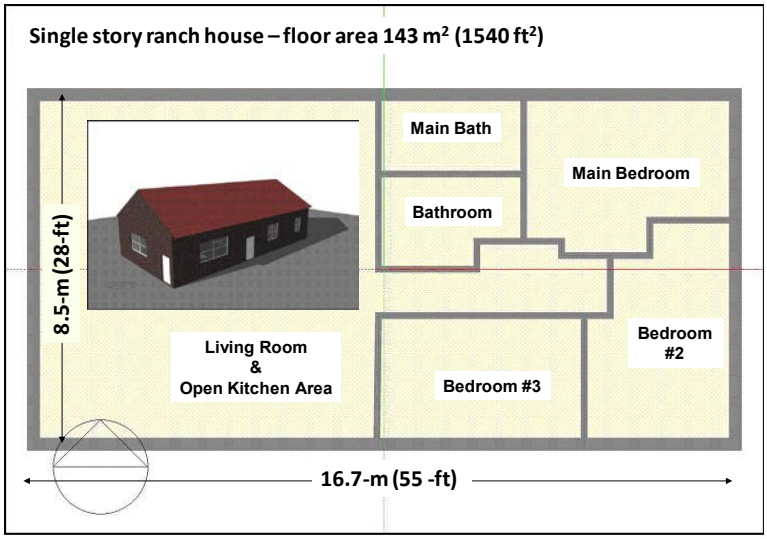

Figure 1. Layout of the single-story ranch house used for the energy modeling

[12] http://apps1.eere.energy.gov/buildings/tools_directory/

In DOE 2.1E simulations, the Sherman-Grimsrud Infiltration Method (Sherman and Grimsrud 1980) was used. For the analysis, the study team assumed an average total leakage area of 0.0005, expressed as a fraction of the floor area. This can be considered an average value for a vintage U.S. single-zone wood-framed residential structure (Huang et al. 1999; Christian and Kośny 1996; Huang et al. 1987). This number cannot be converted directly to average air changes per hour (ACH) because it is used in an equation driven by hourly wind speed and temperature differences between the inside and ambient,. For the 11 considered climatic locations, this represents an ACH range that will not fall below an annual average of 0.35 ACH. This annual average is an ASHRAE Standard 62−1999 requirement for outdoor ventilation of residential facilities (ASHRAE - 2001).

Using DOE-2.1E and EnergyPlus simulations, the study team analyzed the total space heating and cooling energies for 12 lightweight wood-frame walls and five attic configurations. Regression analysis was performed to analyze the relation between the steady-state R-values (for walls and attic floor insulation) and the whole-house annual energies for ten U.S. climates. To illustrate the effectiveness of the conventional insulations in reducing the wall- and attic-generated space conditioning loads, Figure 2 and Figure 3 show the potential annual energy consumption savings resulting from adding conventional insulation in R-4 intervals. For both cases, the results showed that, with the application of additional R-4 conventional insulation, the energy savings is significantly higher than for assemblies with lower R-values. As shown in these figures, an addition of R-16 to the low R-value wall or attic assembly is practically reducing effectiveness of the next R-4 insulation layer by a factor of about 10. This fact highlights the need to evaluate alternative energy saving options other than the conventional insulation for higher R-value walls and attics. PCM-enhanced building envelope components can be one such alternative in some climates dominated by cooling loads.

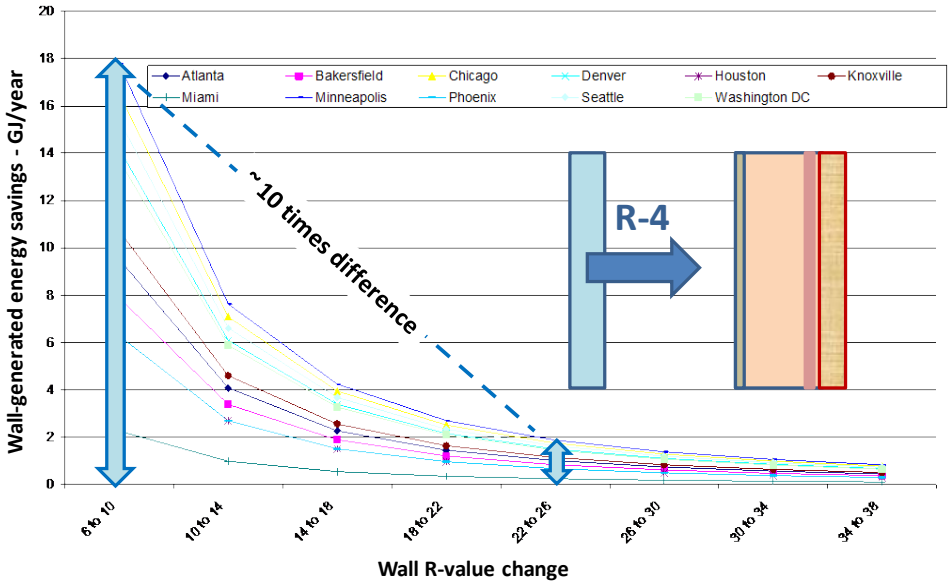

Figure 2. Annual energy savings as a function of wall R-value increase in increments of R-4

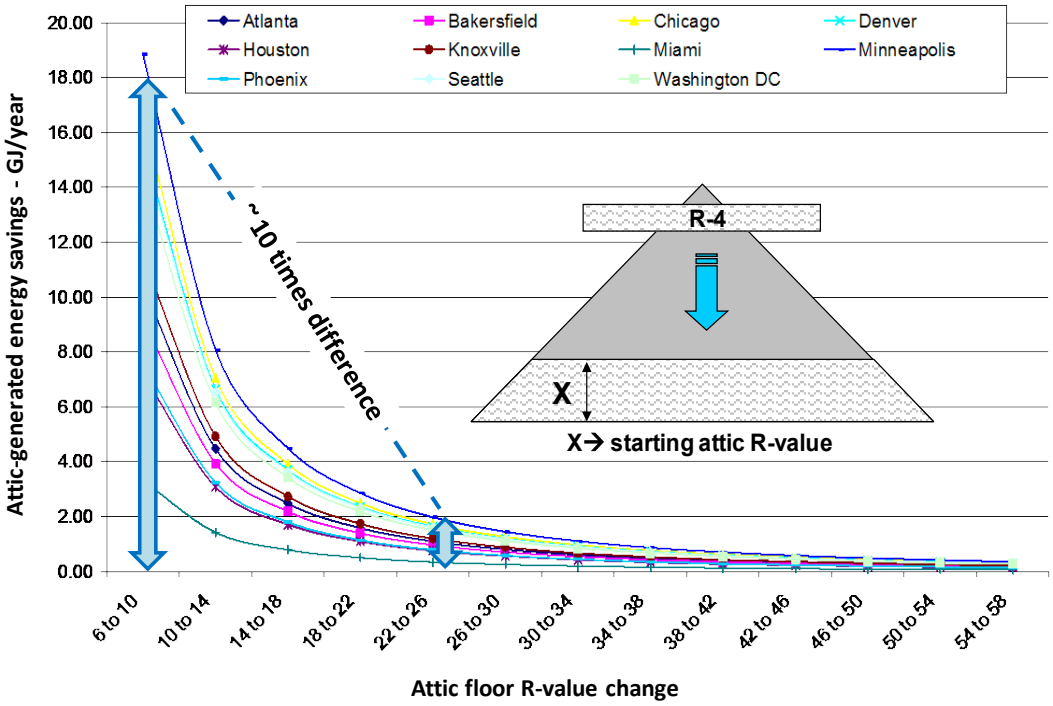

Figure 3. Annual energy savings as a function of attic R-value increasing in increments of R-4

In the next step, the study team performed similar DOE-2.1E and EnergyPlus whole-building energy simulations on five southern U.S. climates. The same 1,540-ft^2 (143-m^2) single-story ranch house shown in Figure 1 was used for modeling. This time, 2 × 6 wood stud walls insulated with an R-19 cavity insulation and conventional pitched R-30 attic insulation were assumed in computer simulations. Table 2 presents a list of cities and basic climate data.

In this analysis, the energy output data generated by these whole-building simulations were used to estimate the energy contributions from the walls and the attic for total whole-building cooling energy consumption. These contributions were computed based on comparisons of the detailed whole-building cooling loads against the local cooling loads generated by the above-grade opaque walls and the attic. Table 3 shows the computed energy contributions from walls and attic on the total whole-building cooling energy consumption of the single-story ranch house. Huang and coworkers (1999) reported that for U.S. single-family houses, walls and roofs generate an average 20% and 12% cooling energy contributions, respectively. Considering that the buildings analyzed by Huang and colleagues had significant configuration differences, the cooling energy contributions presented in Table 3 are within the above range, being 3%–6% lower for the walls and about 3%–4% higher for the attic.

Analyzed climates were then selected to demonstrate a variety of energy impacts in representative southern U.S. locations. The number of cooling degree-days (CDD) on which the temperature averages 74°F (23.3°C) are four times different between Atlanta, Georgia, and Phoenix. Following this relationship, the whole-house cooling energy consumption in simulated locations was found to range between 237 and 961 kWh/year. Table 4 shows the cooling energy

contributions from the walls and the attic calculated for the floor area of the analyzed house. In the simulated single-story ranch house, the combined area of all four walls was about 1,490 ft^2 (138 m^2). The area of windows and doors was about 328 ft^2 (30 m^2).

Table 2. Five Southern U.S. Climates Used in Whole-Building Energy Modeling

Cities	HDD[a] 65°F (18.3°C)	CDD 74°F (23.3°C)
Atlanta	1,705 (3,070)	8,475 (15,255)
Bakersfield[b]	1,182 (2,127)	16,641 (29,954)
Fort Worth	1,344 (2,420)	20,163 (36,294)
Miami	110 (198)	21,889 (39,401)
Phoenix	802 (1,444)	30,224 (54,404)

[a] HDD, heating degree-days
[b] Bakersfield, California

Table 3. Energy Load Contributions From Walls and Attic Calculated for a Single-Story Ranch House for Five Southern U.S. Climates

Cities	Wall Cooling Loads Contribution[a]	Attic Cooling Loads Contribution[b]	Total Cooling Energy Consumption (kWh)	Wall-Generated Cooling Energy Consumption (kWh)	Attic-Generated Cooling Energy Consumption (kWh)
Atlanta	0.14	0.16	1,683	236.8	269.3
Bakersfield	0.16	0.16	2,817	437.7	456.4
Fort Worth	0.15	0.15	3,082	455.6	458.0
Miami	0.14	0.15	6,076	856.7	911.4
Phoenix	0.17	0.15	5,805	960.7	870.8

[a] Fraction of the total building cooling loads generated by opaque walls
[b] Fraction of the total building cooling loads generated by attic

Table 4. Cooling Energy Contributions From Walls and Attic Calculated for the Floor Area of the 1,540-ft^2 (143-m^2) Single-Story Ranch House

Cities	Total Cooling Energy Consumption per Floor Area, kWh/ft^2 (kWh/m^2)	Wall-Generated Cooling Energy Consumption per Floor Area, kWh/ft^2 (kWh/m^2)	Attic-Generated Cooling Energy Consumption per Floor Area, kWh/ft^2 (kWh/m^2)
Atlanta	1.093 (11.76)	0.154 (1.66)	0.175 (1.88)
Bakersfield	1.829 (19.69)	0.284 (3.06)	0.296 (3.19)
Fort Worth	2.001 (21.54)	0.296 (3.19)	0.297 (3.20)
Miami	3.945 (42.46)	0.556 (5.98)	0.592 (6.37)
Phoenix	3.769 (40.57)	0.624 (6.72)	0.565 (6.08)

3.1 Theoretical Performance Limits for Dynamic Insulations Using Dispersed Phase Change Material Applications

Today, manufacturers around the world are developing a wide variety of different material configurations containing PCMs. In PCMs, energy is absorbed or released when the material changes from solid to liquid. During the past several decades, different technologies involving phase transition have been investigated to improve the energy performance of building envelopes. Some of these included concentrated PCM applications in which PCMs were installed using separate carriers. Two of the best-known applications are PCM-enhanced gypsum boards and arrays of plastic or aluminum foil containers containing PCMs. Another group of applications uses blends of microencapsulated PCMs with fiber insulations, or plastic foam boards containing microencapsulated PCMs. Figure 4 shows electron microscope images of the three most common insulation carriers for microencapsulated PCMs.

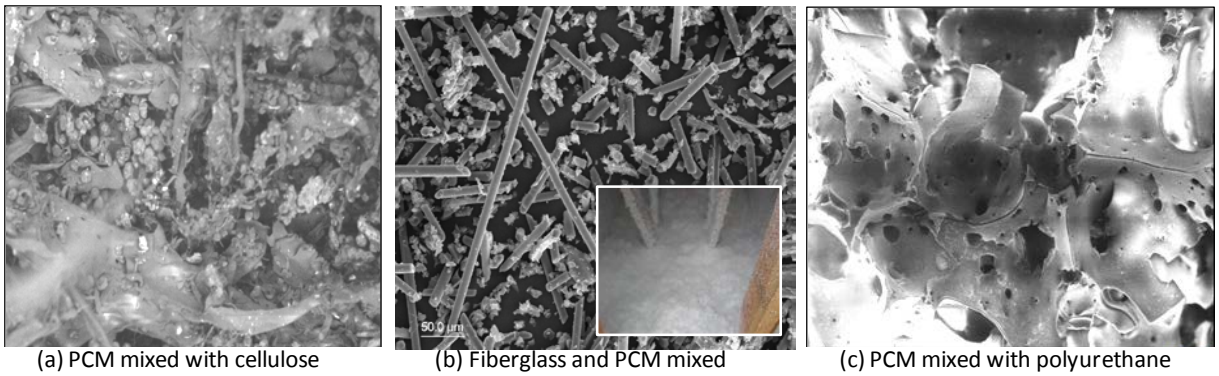

(a) PCM mixed with cellulose fiber insulation

(b) Fiberglass and PCM mixed with blown fiberglass

(c) PCM mixed with polyurethane foam

Figure 4. Scanning electron microscope (SEM) images of microencapsulated PCM mixed with (a) cellulose fiber insulation, (b) blown fiberglass matrix and fiberglass, and (c) polyurethane foam

This section of the report focuses exclusively on dispersed PCM applications that use a 30% by weight blend of the microencapsulated PCM with fiber insulation. In earlier research focused on PCM-enhanced cellulose and fiberglass insulations, different PCM concentrations were studied starting from 5% and reaching to 35%, which is close to the physical concentration limit for the cellulose insulation (Kośny et al. 2007). Therefore, the assumption of 30% PCM content will most likely yield the highest possible PCM cost in this kind of building envelope application. In light of the PCM study performed by Oak Ridge National Laboratory (ORNL 2012), for selected PCM blends, the PCM amount can be reduced by about 1/4 (from the 30% by weight level used in this study to 20% or 25%) without significant reductions in thermal performance. This means that "real" cost levels for PCM-enhanced insulations can be up to 25% lower than the predictions described in this section.

Remember, however, that in most building envelope applications PCMs are not always working in thermal conditions that allow full phase change processes. During the cooling season, the most common reason for the lack of phase transitions is too-high night air temperature, which keeps PCMs melted throughout the night. Historical field test data generated during the ORNL PCM-enhanced cellulose testing (Kośny et al. 2007) and the Metal Construction Association -ORNL metal roof experiment using a PCM heat sink (Kośny et al. 2012) demonstrated that, during the cooling season in eastern Tennessee's climate, PCM cycling was enabled by weather conditions during about 60%–70% of the total number of days. This means that below-computed maximum

thermal performance levels for specific PCM applications will need to be reduced by about 30% to include an impact of days not allowing phase change processes, if eastern Tennessee climatic conditions are taken into account. For other climates, additional field testing or detailed dynamic thermal simulations of a specific PCM application would be necessary.

Another important assumption for this part of the analysis is that the internal space temperature in the analyzed building remains constant. This means that the energy performance analysis presented in this report does not cover PCM application strategies that make use of variable internal space temperature profiles. Overnight pre-cooling of the conditioned space is a widely known strategy of this type.

The third assumption is about a perfect selection of the PCM for the specific climatic condition and for the specific application. Earlier field experiments have demonstrated that with a good knowledge of the temperature profile at the PCM location, it is possible to select PCM thermal characteristics that allow the number of days during the cooling season where complete phase transition takes place to be maximized (Kośny et al. 2012). The best way to investigate the local temperature profile within a building envelope assembly containing PCMs is to conduct full-scale laboratory/field testing or transient simulations using numerical algorithms that are validated against the test data.

In the past, several applications of PCM-enhanced fiber insulations have been tested in laboratory and field conditions (Kośny 2008; Kośny et al. 2007). In 2006 and 2007, ORNL performed two small-scale field tests on 2 × 6 in. (6 × 15.2 cm) wood frame walls with PCM-enhanced cellulose insulation (Kośny et al. 2008). Test walls were installed in Oak Ridge, Tennessee, and in Charleston, South Carolina. In both cases, the PCM walls were constructed next to identical wood stud walls containing cellulose insulation with no PCM. In these experiments, wall cavities were insulated with a cellulose–PCM blend of a density about 2.6 lb/ft^3 (42 kg/m^3) containing about 22% PCM by weight. As described by Kośny (2008), the PCM phase transition enthalpy was about 52 Btu/lb (115 kJ/kg).

After taking measurements during an entire summer, the cooling load reductions were found to average 42% at the Oak Ridge south-oriented site, with the peak-hour savings occasionally spiking to 80%. Results from the Charleston northwest-oriented site showed about a 5% reduction in the cooling load and a 30% reduction in the peak-hour cooling loads. Notable differences in the thermal performances recorded during these two field experiments were most likely caused by different geographic orientations and by significantly different internal space temperature profiles in the two locations. In the Oak Ridge experiment, the average interior air temperature was almost identical to the PCM melting point, which yielded perfect conditions for the PCM to work. In the Charleston experiment, the internal air temperature was about 10°F (~4°C) lower than the PCM melting point, which resulted in significantly lower overall energy performance.

To investigate the theoretical performance limits for the building envelope assemblies containing PCMs, the study team performed a series of transient simulations on several such building envelopes. Two thicknesses representing wall and attic applications were used in modeling: 5.5 in. (0.14 m), representing walls and vaulted ceiling applications, and 11.8 in. (0.3 m), representing attic floor insulations. The study team developed a numerical program for this

purpose using the control volume heat balance method, explicit scheme, with temperature-dependent effective heat capacity and experimentally determined thermal conductivity of the PCM carrier (Kossecka and Kośny 2010). The distance between nodes within the insulation was 0.39−0.79 in. (0.01−0.02 m), and the time step was set to 30 seconds. Table 5 lists the thermophysical properties of the materials used in these assemblies. For example, a 5.5-in. (0.14-m) thick assembly will offer a total thermal resistance of R_u = 23.5 h-ft^2-°F/Btu (4.14 m^2-K/W). This includes surface film resistances of R_{si} = 0.74 h-ft^2-°F/Btu (0.13 m^2-K/W) and of R_{se} = 0.22 h-ft^2-°F/Btu (0.04 m^2-K/W). Considering a 30% PCM content in the 5.5-in. (0.14-m) thick insulation layer and an insulation density of 2.1 lb/ft^3 (33.6 kg/m^3), the PCM load is close to 0.29 lb/ft^2 (1.4 kg/m^2). Next, simulations were repeated for the assemblies containing 11.8-in. (0.3-m) thick insulations.

To illustrate the effect of PCM melting temperature on the energy, the study team ran computer simulations for two different internal air temperatures, T_i, equal to either 68°F (20°C) or 77°F (25°C). Meanwhile, the melting point of the PCM material was 81°F (27°C). Earlier research on the PCM-enhanced envelope systems demonstrated that it is beneficial to have the PCM melting temperature as close as possible to the internal air set-point temperature (Kośny et al. 2008; Tomlinson et al. 1992). Figure 5 depicts the effective heat capacity data for the PCMs used in the modeling. In simulations, one-dimensional heat transfer was assumed and the effect of structural members was neglected. A major goal of this modeling exercise was to analyze the dynamic responses of a building envelope assembly containing PCM to different levels of external thermal excitations. Note that these thermal simulations were performed with the assumption of a constant interior space temperature.

As shown in Figure 6, T_{es} represents three diurnal surface temperature swing schedules with thermal peaks of 113°F (45°C) in schedule “a”; 149°F (65°C) in schedule “b”; and 185°F (85°C) in schedule “c.” These peaks result from solar radiation incident on the external surface during the day. According to the field experimental data developed by previous investigators (Biswas et al. 2011; Kośny et al. 2011; Murugananthama et al. 2010; Kośny 2008; Miller et al. 2007; Petrie et al. 2004), temperature schedule “a” with a temperature peak of 113°F (45°C) most likely represents a summer wall surface thermal excitation. Similarly, during the summer in southern U.S. locations, the attic floor insulation faces attic space temperature fluctuations falling closely between schedules “a” and “b.” Where vaulted ceilings and sandwiched roof assemblies exist, the exterior boundary conditions will most likely be close to the schedule “c” temperature profile with temperature peaks exceeding 167°F (75°C).

Table 5. Thermophysical Properties Used in Numerical Modeling

Material	Thickness (m)	Conductivity Btu-in/h·ft^{2}F (W/m·K)	Density lb/ft^3 (kg/m^3)	c_p Btu/lbF (kJ/kg·K)
Gypsum Bboard ½-in.	0.013	1.10 (0.16)	50 (800)	0.26 (1.088)
Insulation 5.5-in.	0.140	0.27 (0.039)	1.6 (25.6)	0.33 (1.381)
Insulation 11.8-in.	0.300	0.27 (0.039)	1.6 925.6)	0.33 (1.381)
Insulation 30% PCM		0.27 (0.039)	2.1 (33.6)	$C_p(T)$
Plywood ½-in.	0.013	0.83 (0.12)	34 (544)	0.29 (1.244)
Exterior Finish Layer ½-in.	0.013	0.48 (0.07)	34 (545)	0.29 (1.255)

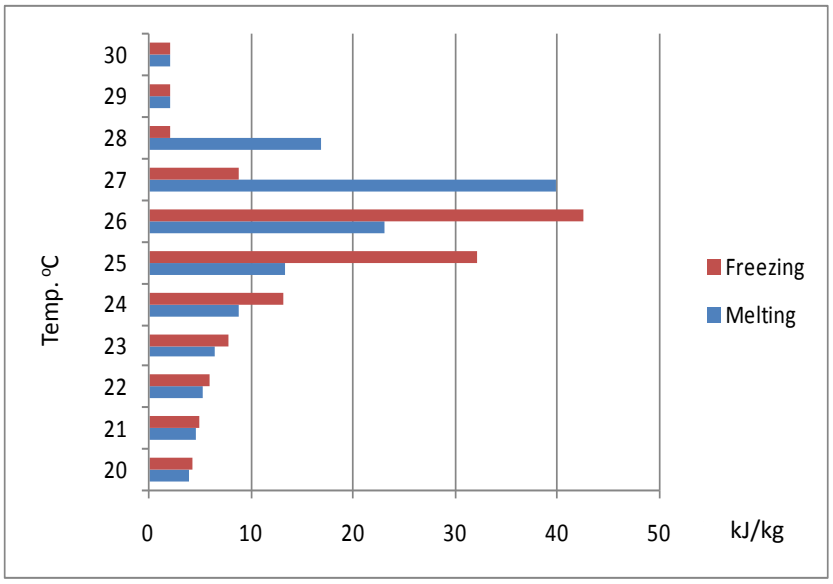

Figure 5. Temperature versus effective heat capacity data for PCM used in thermal simulations

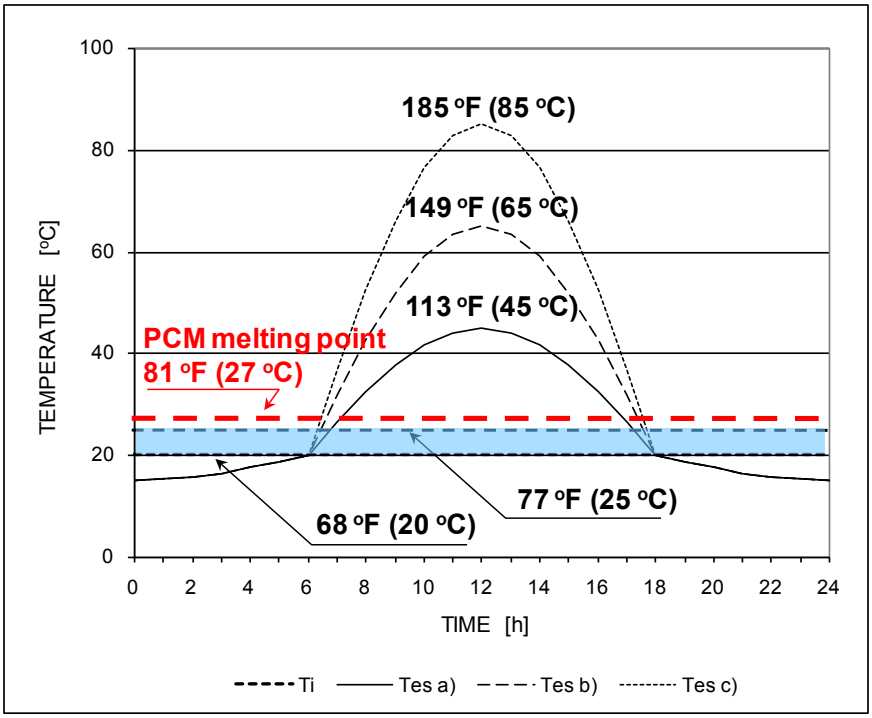

Figure 6. Diurnal external temperature profiles T_{es} used in numerical analysis with assumption of T_i = 68°F (20°C) and T_i = 77°F (25°C)

A theoretical model of the material with temperature-dependent specific heat can be used to predict the phase change processes in the most common PCM-enhanced materials. The one-dimensional heat transport equation for such a case is as follows:

$$\frac{\partial}{\partial t}(\rho h) = \frac{\partial}{\partial x}\left[\lambda \frac{\partial T}{\partial x}\right], \quad (1)$$

where ρ is the material density, λ is the thermal conductivity, T is temperature, and h is enthalpy per unit mass.

The enthalpy derivative over the temperature derivative (with consideration of constant pressure) represents the effective heat capacity, with the phase change energy as one of the components:

$$c_{eff} = \frac{\partial h}{\partial T}, \quad (2)$$

For most PCMs, variations of enthalpy associated with temperature depend to some extent on the direction of the process considered, and tend to differ for melting and solidification (Gunther et al. 2009). Transient characteristics of PCM-enhanced products depend on the PCM content and the quality of the PCM carrier. Usually, a smaller portion of the heat storage capacity (depending on the temperature difference) consists of sensible heat; a larger capacity portion represents heat of the phase transition. Effective heat capacity, c_{eff}, for a material consisting of a blend of the material carrier and PCM can be expressed as follows:

$$c_{eff} = (1 - \alpha)c_{carr} + \alpha\, c_{eff_PCM}, \quad (3)$$

where α denotes the percentage of PCM, c_{carr} is the specific heat of a carrier material without PCM, and c_{eff_PCM} is the effective heat capacity of the PCM.

To visualize the dynamic effects, the study team calculated the heat fluxes for steady state, which represent the "zero mass" wall. During these calculations, investigators took the dependence of insulation conductivity on the temperature into account. An accurate elementary solution to the nonlinear steady-state heat transfer problem, in case of a linear dependence of the conductivity on temperature, can be obtained using the Kirchoff transform method (Kossecka 1999). Figure 7 and Figure 8 represent a comparison of diurnal heat flux profiles at internal surfaces of the two walls—one containing a plain fibrous insulation layer, and the other containing 30% PCM-enhanced insulation. The steady-state heat flux profiles were added for comparison. In Figures 7 through 10, label "0% PCM" represents a case of plain fibrous insulation, label "30% PCM" represents the 30% blend of PCM and fibrous insulation, and label "steady state" represents the steady-state solution with no thermal mass effects taken into account.

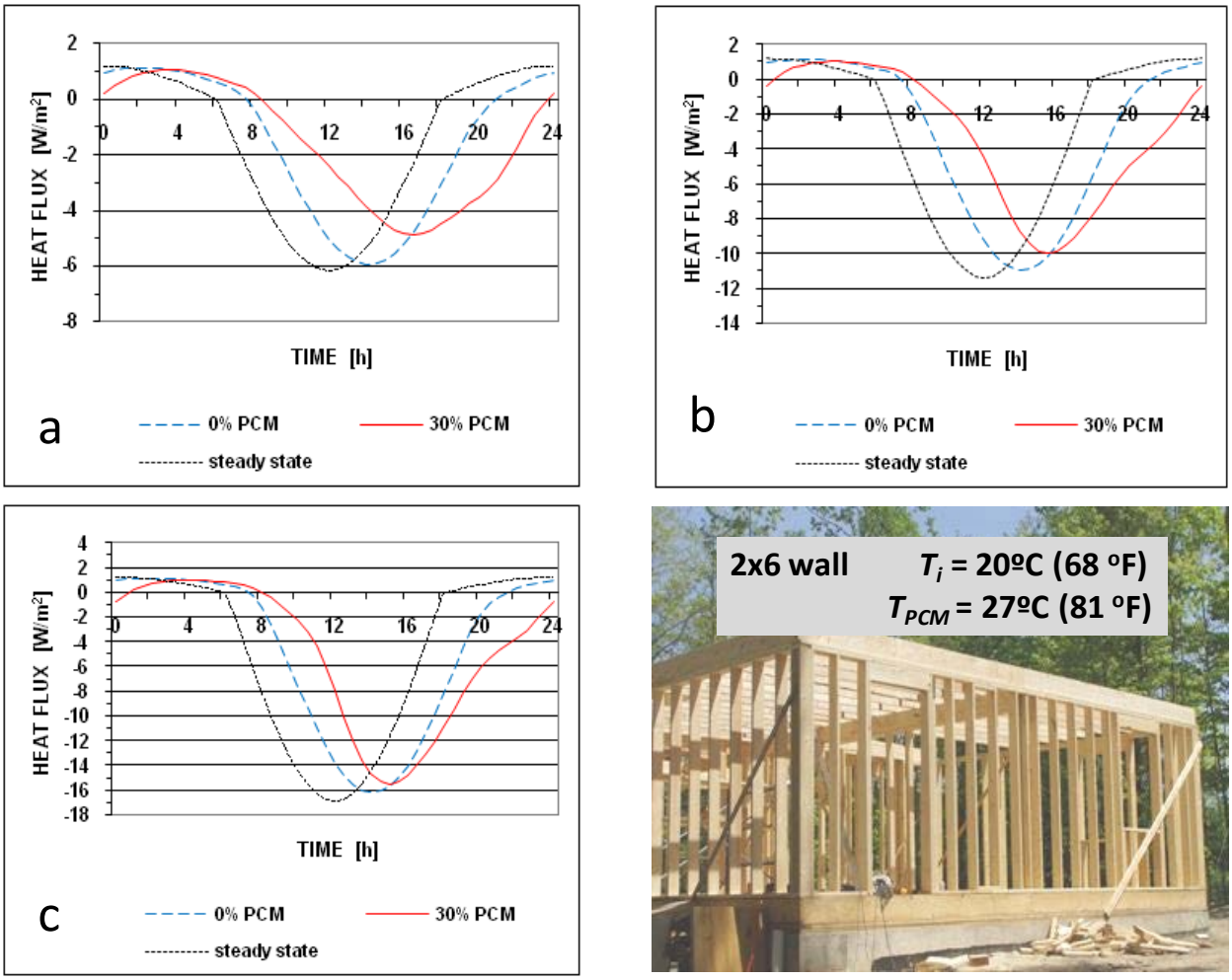

Figure 7. Comparison of the daily heat flux profiles at the internal surface of the wall containing 5.5-in. (0.14-m) thick insulation layer with 0% PCM and 30% PCM for internal temperature T_i = 68°F (20°C) and temperature swing schedules with thermal peaks of 113°F (45°C) in schedule "a" 149°F (65°C) in schedule "b," and 185°F (85°C) in schedule "c"

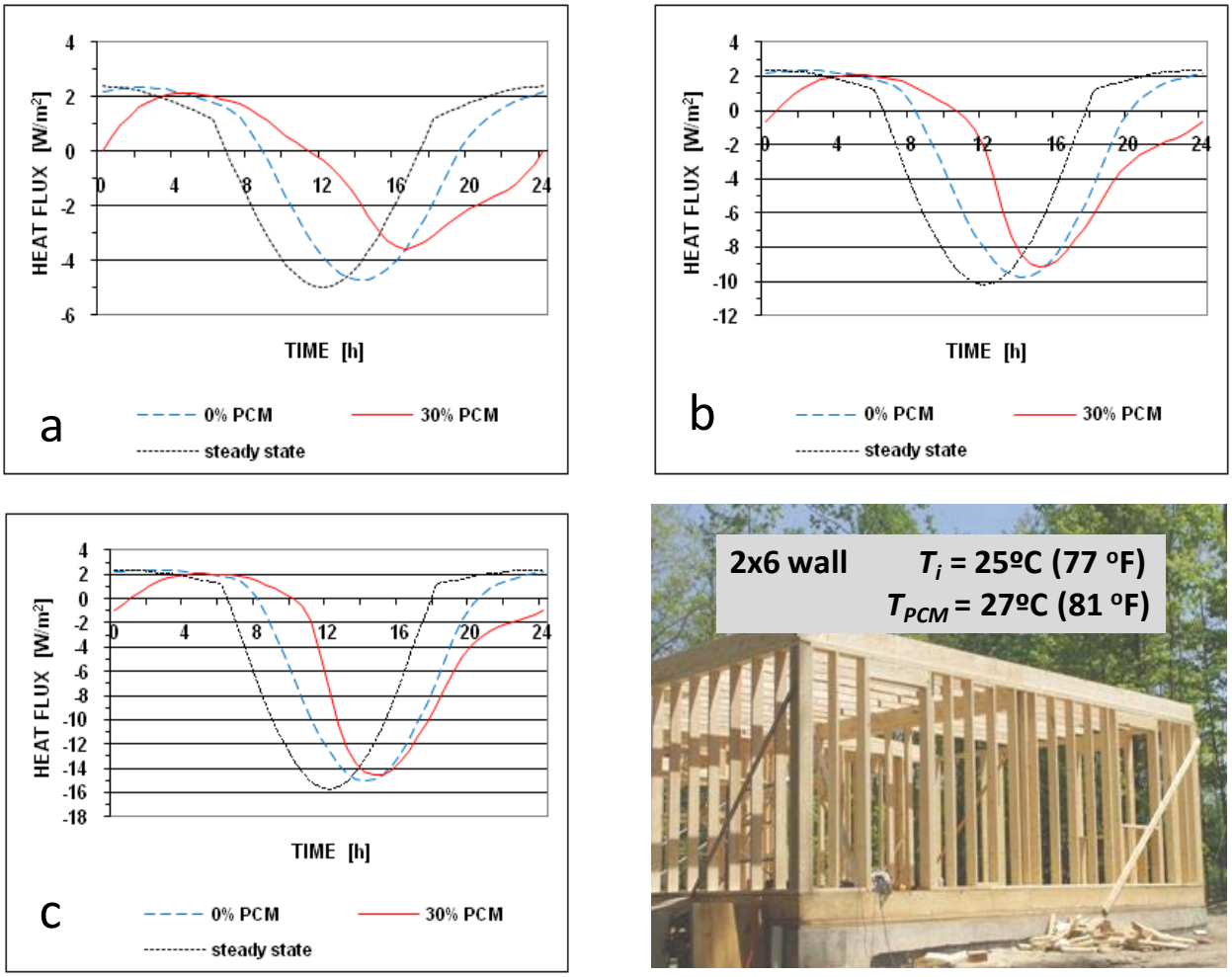

Figure 8. Comparison of the daily heat flux profiles at the internal surface of the wall containing 5.5-in. (0.14-m) thick insulation layer with 0% PCM and 30% PCM for internal temperature *Ti* = 77°F (25°C) and temperature swing schedules with thermal peaks of 45°C (113°F) in schedule "a," 149°F (65°C) in schedule "b," and 185°F (85°C) in schedule "c"

Comparison of the plots and calculated daily heat flow values indicates that for the 5.5-in. (0.14-m) thick assemblies and for cyclic processes, the effect of PCMs in an insulation layer results in notable time shifting of the heat flux maxima. Heat losses corresponding to minimum external temperatures at midnight are shifted to morning. At the same time, large heat gains from midday are shifted by about 2 hours to the afternoon. Overall, for the 5.5-in. (0.14-m) thick assemblies, the highest reductions of the total heat flow can be observed for temperature swing schedules "a" and "b" with thermal peaks of 113°F (45°C) and 149°F (65°C), respectively. For T_i = 68°F (20°C), the heat gain maxima are reduced by 18%, 8%, and 4% for schemes "a," 'b," and "c," respectively, as external sol-air temperature maxima increases from 113°F (45°C) to 185°F (85°C). For T_i = 77°F (25°C), the corresponding heat gains (heat fluxes integrated over the time) are reduced by 25%, 6%, and 3%. In the case of temperature swing schedule "c," the effect of the PCM in an insulation layer is positive, but perhaps not as strong as one would expect. A PCM of about 0.29 lb/ft^2 (1.4 kg/m^2) in the insulation layer cannot significantly reduce high negative heat fluxes, resulting in cooling loads on the room space for very high external sol-air temperatures.

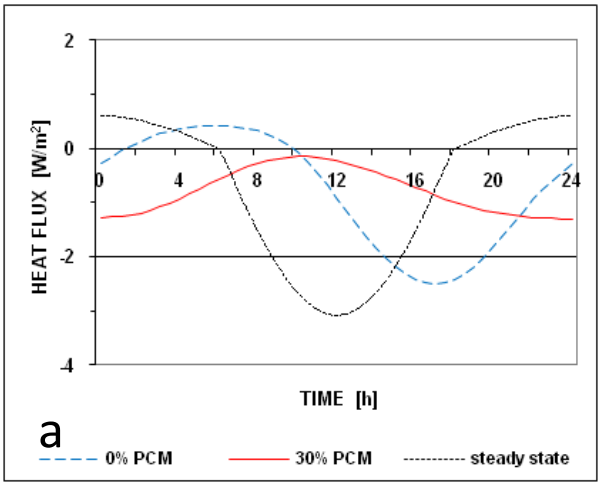

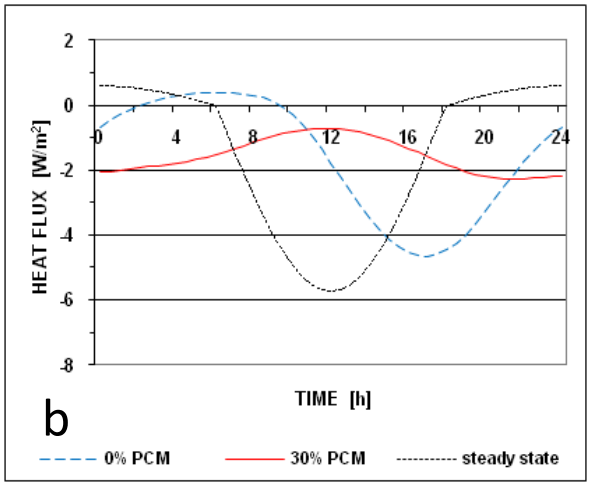

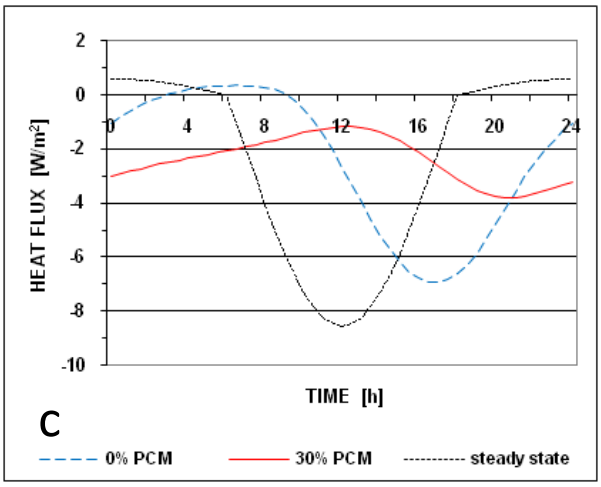

Figure 9. Comparison of the daily heat flux profiles at the internal surface of the attic floor containing 11.8-in. (0.3-m) thick insulation layer with 0% PCM and 30% PCM for internal temperature T_i = 68°F (20°C) and temperature swing schedules with thermal peaks of 113°F (45°C) in schedule "a," 149°F (65°C) in schedule "b," and 185°F (85°C) in schedule "c"

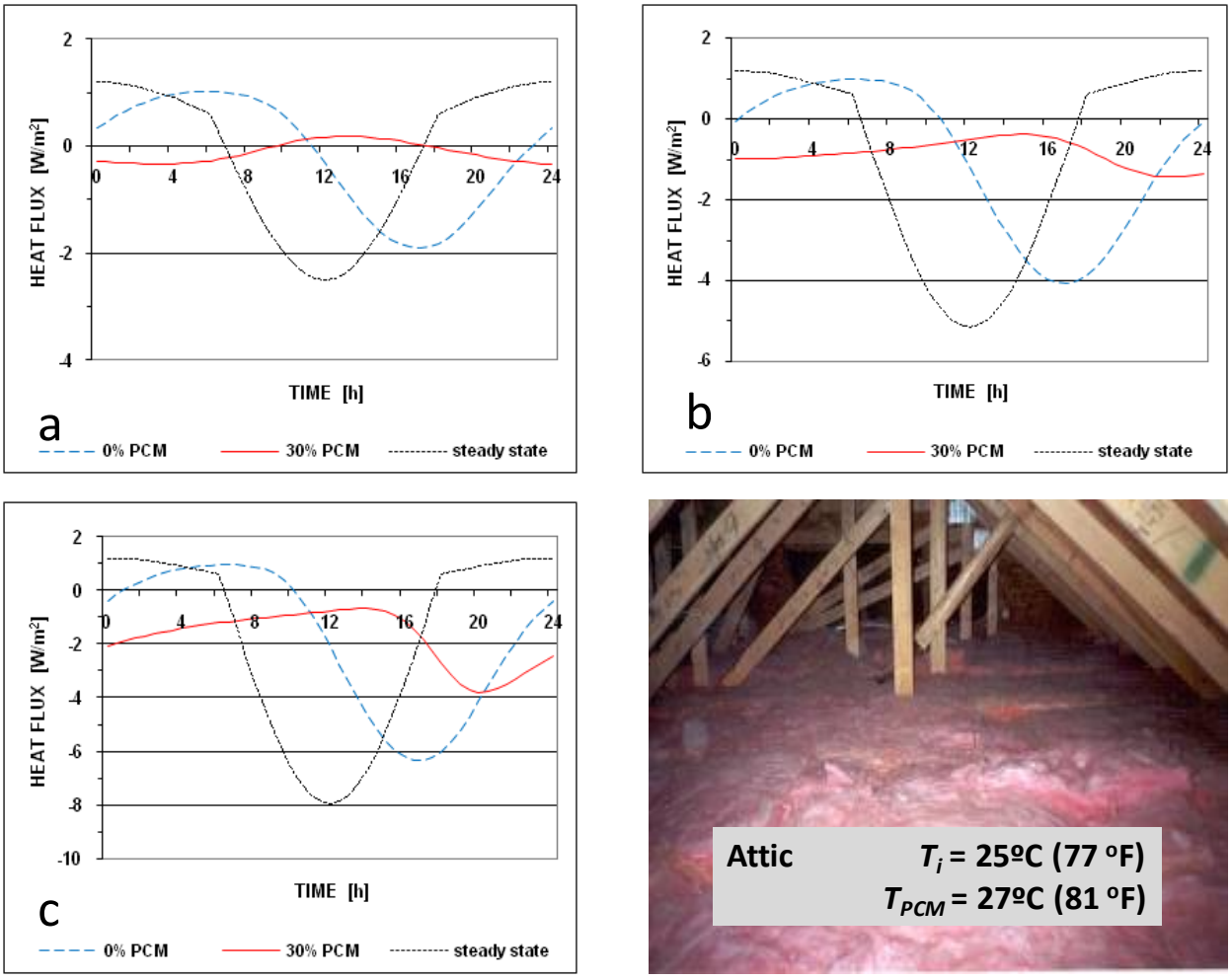

Figure 10. Comparison of the daily heat flux profiles at the internal surface of the attic floor containing 12-in. (30-cm) thick insulation layer with 0% PCM and 30% PCM for internal temperature T_i = 77°F (25°C) and temperature swing schedules with thermal peaks of 113°F (45°C) in schedule "a," 149°F (65°C) in schedule "b," and 185°F (85°C) in schedule "c"

The study team repeated simulations for the assembly containing a PCM content of 30% and having a density of 2.1 lb/ft^3 (33.6 kg/m^3); that is, about 0.62 lb of PCM per square foot of the wall (3 kg/m^2). Similar to the 5.5-in. (0.14-m) thick assemblies, the highest reductions of the total heat flow were observed for temperature swing schedules "a" and "b." For T_i = 68°F (20°C), the heat gain maxima are reduced by 48%, 50%, and 45% for schedules "a," "b," and "c," respectively, as external sol-air temperature maxima increases from 113°F (45°C) to 185°F (85°C). For T_i = 77°F (25°C), the corresponding heat gains (heat fluxes integrated over the time) are reduced by 82%, 65%, and 40%.

Figure 11 summarizes the results of simulations showing percent load reductions for both thicknesses for the building envelope assemblies. The highest energy savings were observed for the exterior temperature schedule "a" with the peak temperature of 113°F (45°C). For insulation thickness of 5.5-in. (0.14 m), percent load reductions were over 20% when compared to the plain thermal insulation. This occurred only when the amplitude of the external temperature T_{es} was not too high (with daily peak of 113°F [45°C]) and savings were notably smaller for higher

external temperature peaks. Note that the potential cooling load savings are significantly higher for thick layers of the PCM-enhanced insulation of 11.8-in. (0.3 m; representing PCM-enhanced attic floor insulations). In this case, the percent reduction in the cooling loads may reach 70%. As shown in Figure 11, the potential cooling load savings can be two to three times lower for thinner insulation assemblies (i.e., vaulted ceilings and walls).

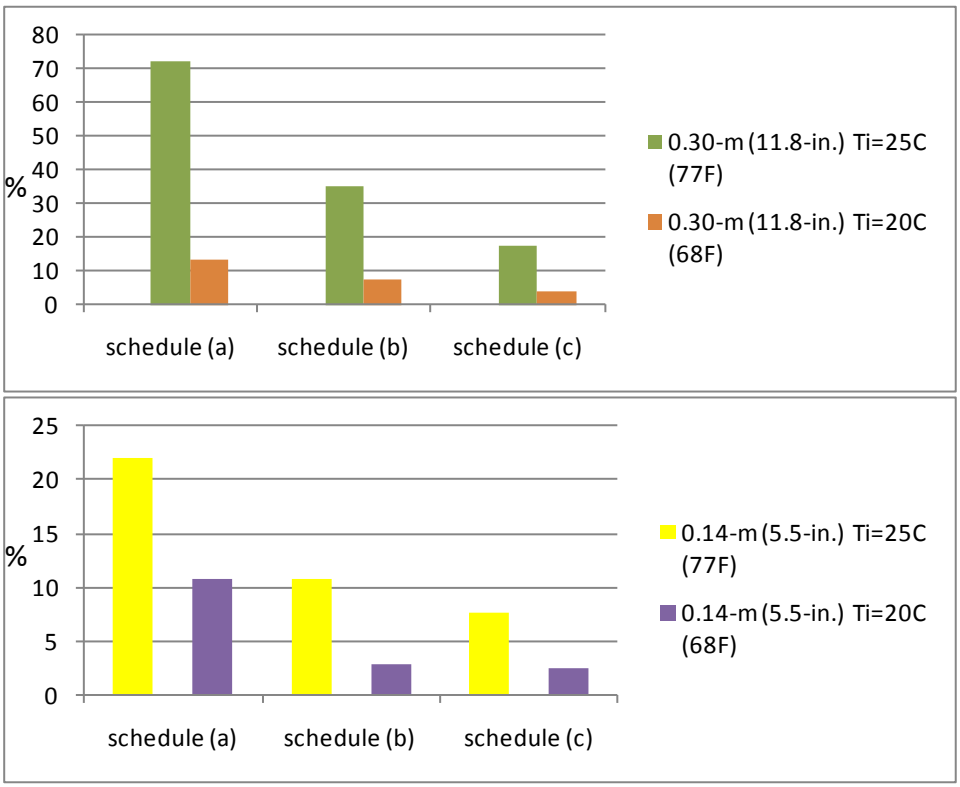

Figure 11. Reductions of heat gains calculated for the two thicknesses of the building envelope assemblies. For each material configuration and at internal temperatures T_i, heat gains represent heat fluxes integrated over the time period.

Proper selection of the PCM phase transition temperature plays a very important role in the overall energy performance. The results of the transient modeling demonstrated that the overall load reductions are significantly higher in situations when the PCM melting temperature is closer to the internal space set-point temperature. In the analysis of the 11.8-in. (0.3-m) thick layer of insulation, the temperature schedules "a" and "b" represented the approximate temperature excitations that are characteristic of the attic floor insulation in southern U.S. applications. For this case, the numerical results presented in Figure 11 indicate that the daily heat gain savings can range between 35% and 70% (considering only a 4°F or 2°C difference between PCM melting temperature and the internal space set-point temperature). Accordingly, for a higher temperature difference of ~13°F (7°C), the attic-generated heat gain savings can vary between 8% and 10%. Similar relationships between the PCM melting temperature and the internal space set-point temperature can be observed for thinner assemblies. This fact confirms the earlier experimental results (Kośny 2008), and indicates that it is beneficial to design the PCM transition temperature as close as possible to the internal space set-point temperature.

3.2 Estimation of the Competitive Price Level for Phase Change Material Attic and Wall Applications

The study team's thermal performance analysis for 11.8-in. (0.3-m) and 5.5-in. (0.14-m) thick layers of PCM-enhanced thermal insulation yielded maximum theoretical energy savings exceeding 72% and 22% , respectively—assuming that PCM enthalpy was 52 Btu/lb (120 kJ/kg). As shown in Figures 7 through 11, the thermal efficiency of PCM-enhanced roof/attic systems depends strongly on the thermal characteristics of PCMs and PCM carriers (thermal insulation in this analysis). The magnitude of the exterior climatic thermal loads is an additional factor that affects the overall thermal efficiency. If the exterior thermal excitations are too large, PCMs can be melted or frozen at a very fast rate and the overall thermal effectiveness of the PCM-enhanced building envelope can be relatively low (as in the case of cathedral-style roof PCM applications; see thermal schedule "c" in Figures 7 and 11).

PCM cost effectiveness was estimated for the PCM systems using dispersed blends with fiber insulations and PCM-enhanced wall boards. For each of the PCM applications considered and for five southern U.S. climates, potential cooling energy savings were estimated using heating and cooling load levels generated by whole-building energy simulations and numerically estimated heat gain reductions for specific building envelope components (see Section 3.1). Table 6 gives residential electricity costs for each location. According to the U.S. Bureau of Labor Statistics,[13] the average price of electricity in the United States in 2011 was $0.125/kWh. In the following analysis, the study team based estimates of the energy saved by employing PCM-enhanced building envelopes based on the unit electricity costs for each selected location.

Table 6. Residential Electric Energy Prices for Five Southern U.S. Climates Used in Whole-Building Energy Analysis

Cities	CDD 74°F (23.3°C)	Electricity price, ($/kWh)	Reference
Atlanta	8,475 (15,255)	0.113	Bureau of Labor Statistics (2012)
Bakersfield	16,641 (29,954)	0.340	*Bakersfield News* (2011)
Fort Worth	20,163 (36,294)	0.094	Direct Energy (2012)
Miami	21,889 (39,401)	0.116	Florida Power and Light (FPL; 2012)
Phoenix On-Peak	30,224 (54,404)	0.216	APS (2012)
Phoenix Off-Peak		0.054	

In the United States, different microencapsulated PCMs are available for building applications with paraffinic products and blends of different fatty oils, of which esters are the most common. For the cost analysis, the study team assumed four typical PCM enthalpies used by the industry—52 Btu/lb (120 kJ/kg), 65 Btu/lb (150 kJ/kg), 82 Btu/lb (190 kJ/kg), and 95 Btu/lb (220 kJ/kg). The amount of PCM was normalized against the heat storage capacity of the basic wall and roof systems assuming a baseline enthalpy of 52 Btu/lb (120 kJ/kg). Finally, the cost of PCM was analyzed for the PCM price range between $1.50/lb and $7.50/lb. For each of the PCM-enhanced envelope configurations, a payback period was computed.

[13] See www.bls.gov/ro4/aepatl.htm for more information

3.3 Payback Period Analysis for Attic Applications of Dispersed Phase Change Materials

Conventional attic designs with soffit and ridge ventilation are good examples of the dynamic building envelopes for cooling-dominated climates. The ventilation air redirects some of the heat emanating from the roof deck away from the insulation on the attic floor. The attic insulation works against an internal attic air temperature instead of the dynamic temperatures observed on the roof surface (for comparison, cathedral-style roofs directly conduct heat into the conditioned space). In general, benefits of the attic thermal system are as follows:

- Effectively reduces roof solar loads
- Reduces nighttime cooling effects
- Provides a conduction break between the attic floor and the roof deck
- Causes stratification of the attic air
- Causes a shifting of the attic thermal loads.

Earlier research showed that adding PCMs to the attic floor insulation can be a very efficient way to reduce the overall cooling loads generated by the attic and to shift the peak-hour cooling loads to the afternoon or nighttime (Kośny et al. 2011; Kośny 2008). As mentioned previously, during the summer in southern U.S. locations, the attic floor insulation is usually facing attic space temperature fluctuations between the range of schedules “a” and “b” (i.e., temperature peaks reaching between 113°F [45°C] and 149°F [65°C]).

In the study team’s energy performance simulations for PCM-enhanced insulations, a 11.8-in. (0.3-m) thick layer of an ideal insulation was assumed. In the following cost analysis, to simplify the calculations and limit the number of insulation configurations, analysts assumed only cellulose insulation. Considering thermal bridging generated by the attic floor structural members, this will yield very conservative thermal performance predictions of PCM-enhanced R-30 cellulose insulation installed on the attic floor. The amount of PCM required was calculated to be approximately 522 lb (237 kg) of PCM necessary for the attic (30% by weight of the insulation). The study team also assumed that the roof pitch was 6 to 12 in. (2.4 to 4.7-cm.), the attic floor framing was 16 in. (0.40 cm) o.c., and the central attic floor beam structure was 11.8-in. (0.305-m) thick.

Table 7 shows the annual costs for attic-generated cooling electrical energy consumed in each of the geographic locations. For Phoenix, the study team assumed that all roof-generated cooling electricity was used during either peak or off-peak hours. The off-peak assumption is based on analysis performed in Section 3.1, which demonstrated that significant time shifting is possible in cases of thicker building envelope applications containing PCM.

Table 7. Annual Costs of Cooling Electric Energy Generated by the Attic Calculated for a Single-Story Ranch House for Five Southern U.S. Climates

Cities	Total Cooling Energy Consumption (kWh)	Attic-Generated Cooling Energy Consumption (kWh)	Annual Cost of Electricity Used for Cooling (Attic-Generated, $)
Atlanta	1,683	269.3	30.43
Bakersfield	2,817	456.4	155.18
Fort Worth	3,082	458.0	43.05
Miami	6,076	911.4	105.72
Phoenix On-Peak	5,805	870.8	188.09
Phoenix Off-Peak			47.02

Anticipated cooling energy cost savings were calculated for the attic for each of the climatic locations. For each location, two levels of savings were calculated considering PCM performance predictions for schedules "a" and "b" (as described in Figure 6) and an internal space temperature of T_i = 77°F (25°C) as shown in Table 8. Next, using the calculated cooling energy cost savings and assuming a PCM price range of $1.50/lb to $7.50/lb, payback periods were computed for four typical PCM enthalpies; 52 Btu/lb (120 kJ/kg), 65 Btu/lb (150 kJ/kg), 82 Btu/lb (190 kJ/kg), and 95 Btu/lb (220 kJ/kg). Amounts of PCM were normalized against the heat storage capacity of the attic system using the PCM of 52 Btu/lb (120 kJ/kg) enthalpy. The study team assumed that PCMs represented 30% by weight of the 11.8-in. (0.3-m) thick attic insulation. Considering that the cellulose density was about 1.6 lb/ft^3 (25.6 kg/m^3) and assuming that the attic framing, the roof structural components, the attic entry hatch, and the air-handler unit reduced nominal volume of the attic insulation by about 27%, the overall PCM load in the attic was close to 522 lb (237 kg). Figures 12 through 16 present the results of these calculations.

Table 8. Calculated Annual Cooling Electricity Cost Savings Generated by the Attic for a Single-Story Ranch House for Five Southern U.S. Climates

Cities	Annual Cost of Electricity Used for Cooling (Attic-Generated, $)	Annual Cooling Electricity Cost Savings – PCM, Schedule "a" (Attic-Generated, $/ft^2-Floor Area)	Annual Cooling Electricity Cost Savings – PCM, Schedule "b" (Attic-Generated, $/ft^2-Floor Area)
Atlanta	30.43	21.91 (0.014)	10.65 (0.007)
Bakersfield	155.18	111.73 (0.073)	54.31 (0.035)
Fort Worth	43.05	31.00 (0.020)	15.07 (0.010)
Miami	105.72	76.12 (0.049)	37.00 (0.025)
Phoenix On-Peak	188.09	135.43 (0.088)	65.83 (0.043)
Phoenix Off-Peak		143.96 (0.093)[a]	85.64 (0.056)[a]

[a] Off-peak savings for Phoenix were calculated as a sum of on-peak savings and savings calculated for price differences between on-peak and off-peak rates, assuming that attic-generated peak cooling loads are shifted after 7:00 p.m.—

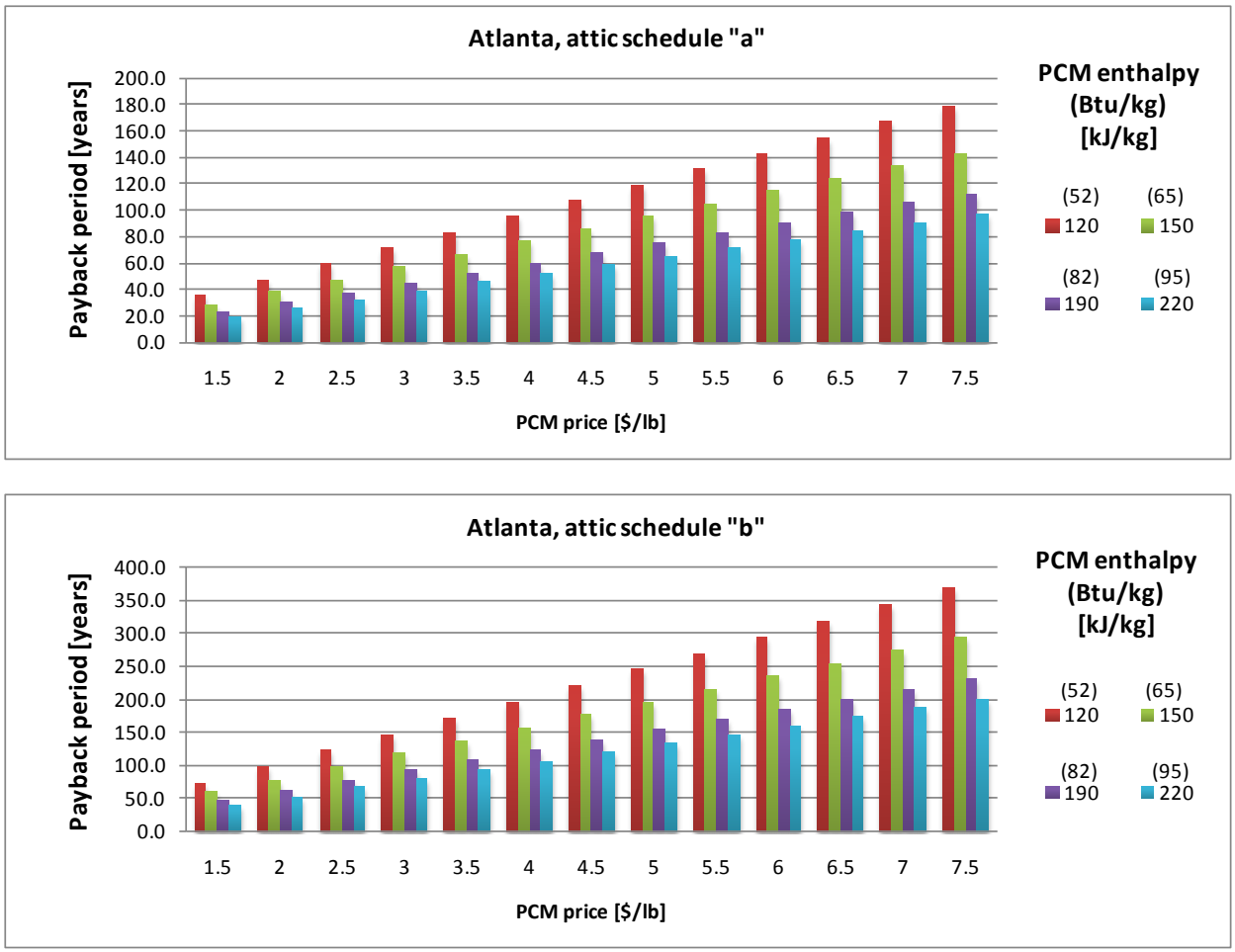

Figure 12. Payback periods for the PCM-enhanced R-30 cellulose insulation configuration installed on the attic floor as a function of the PCM price for a single-story ranch house in Atlanta. The external temperature profiles have been defined as "a" and "b."

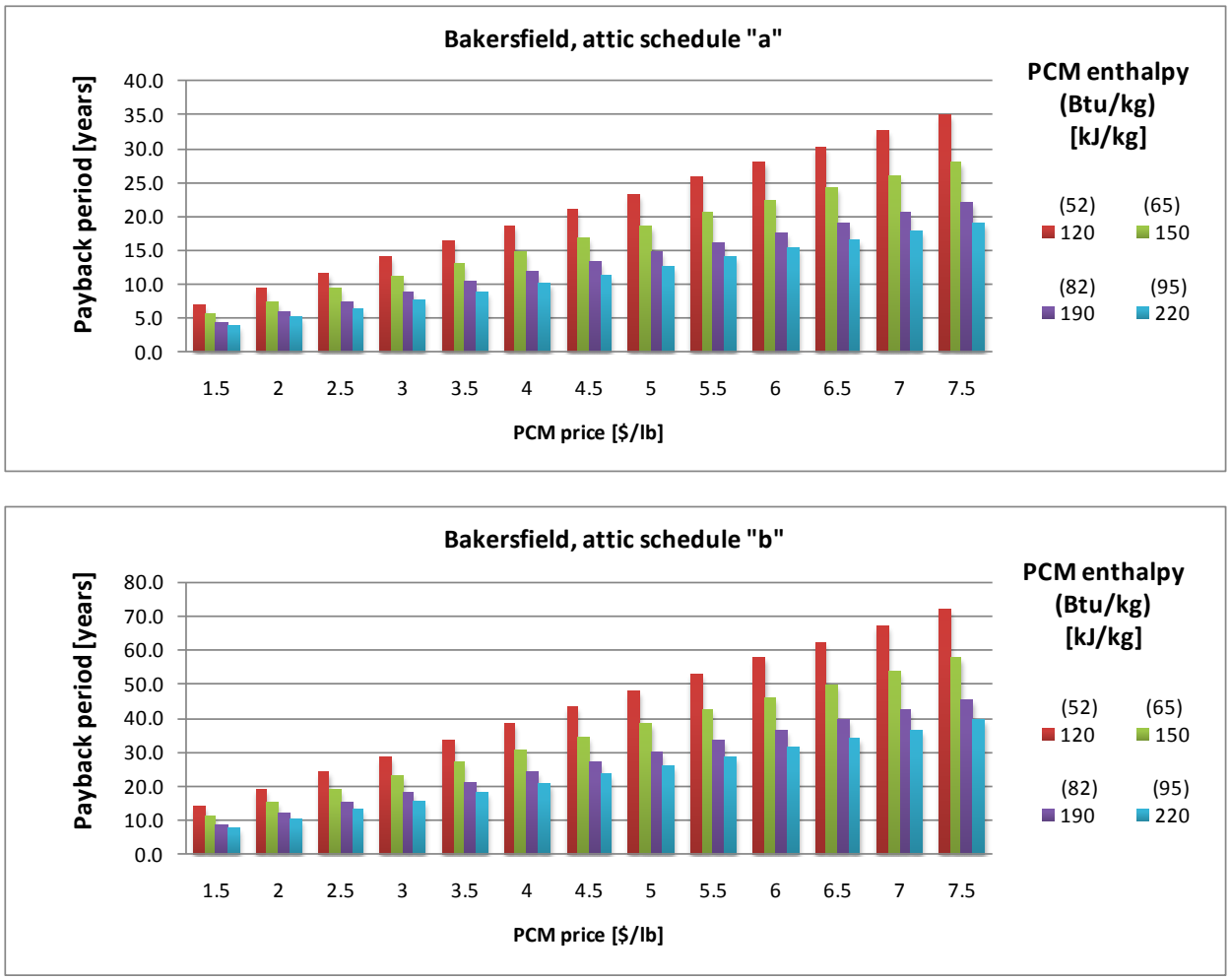

Figure 13. Payback periods for the PCM-enhanced R-30 cellulose insulation configuration installed on the attic floor as a function of the PCM price for a single-story ranch house in Bakersfield. The external temperature profiles have been defined as "a" and "b."

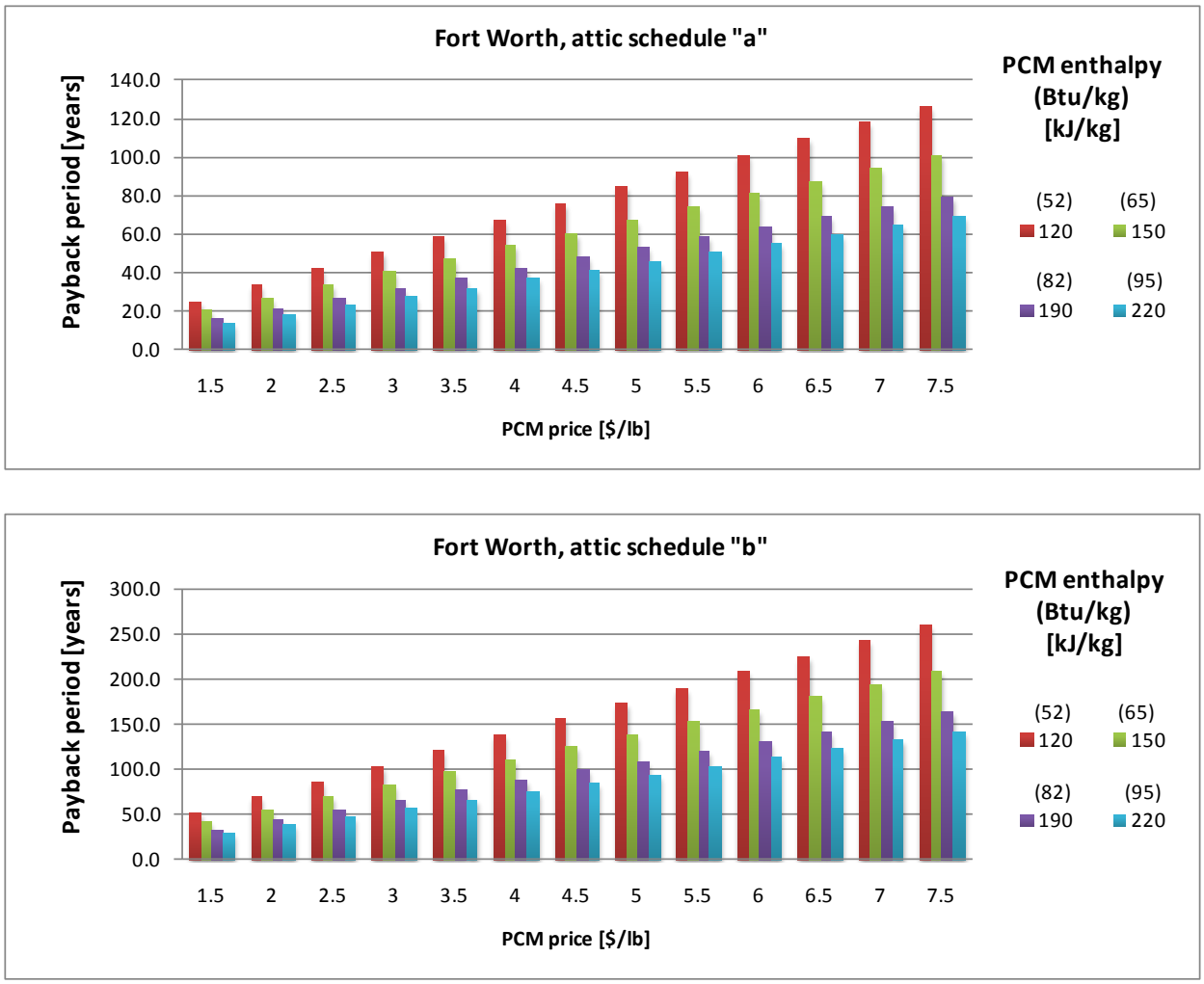

Figure 14. Payback periods for the PCM-enhanced R-30 cellulose insulation configuration installed on the attic floor as a function of the PCM price for a single-story ranch house in Fort Worth. The external temperature profiles have been defined as "a" and "b."

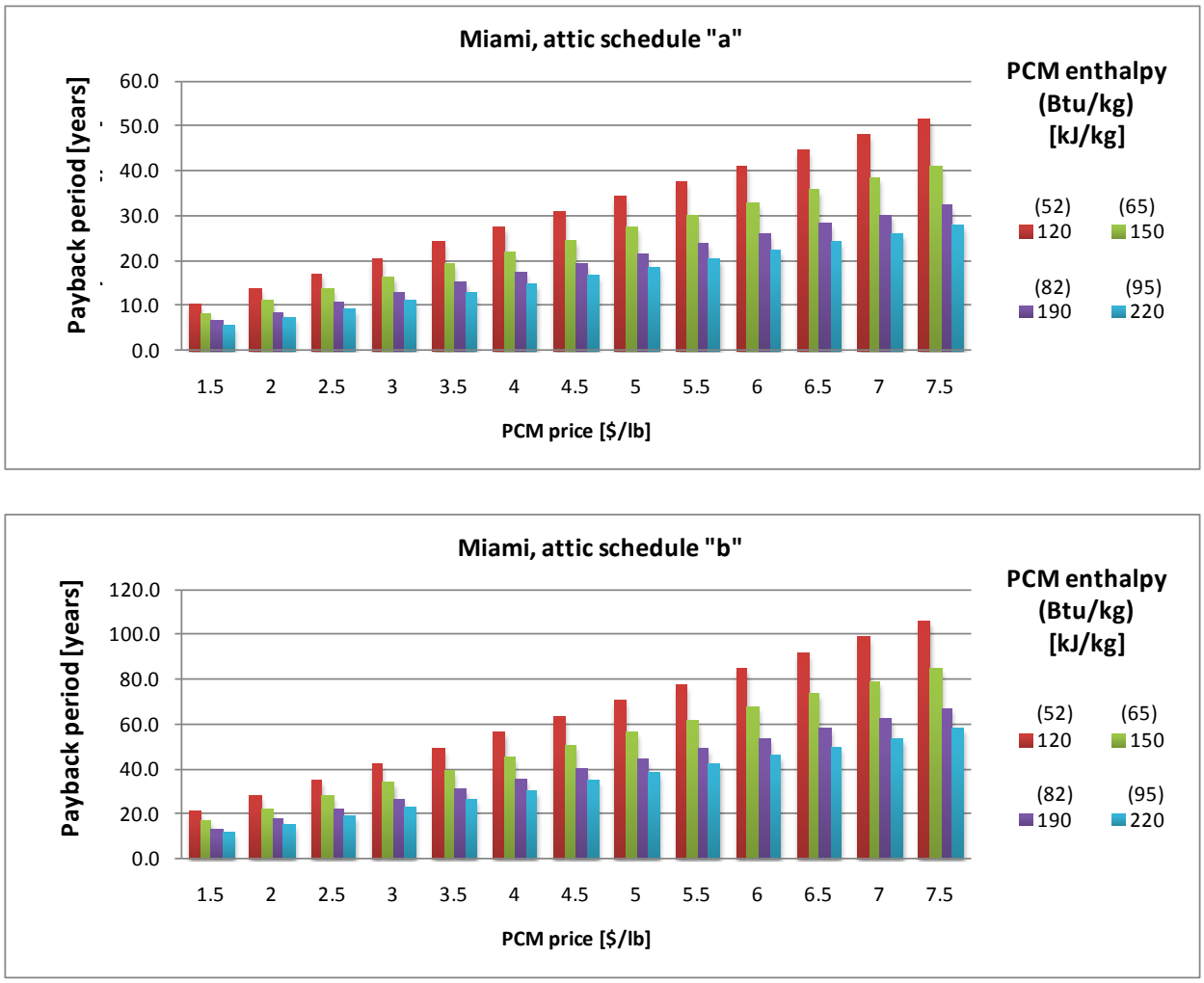

Figure 15. Payback periods for the PCM-enhanced R-30 cellulose insulation configuration installed on the attic floor as a function of the PCM price for a single-story ranch house in Miami. Two external temperature profiles have been defined as "a" and "b."

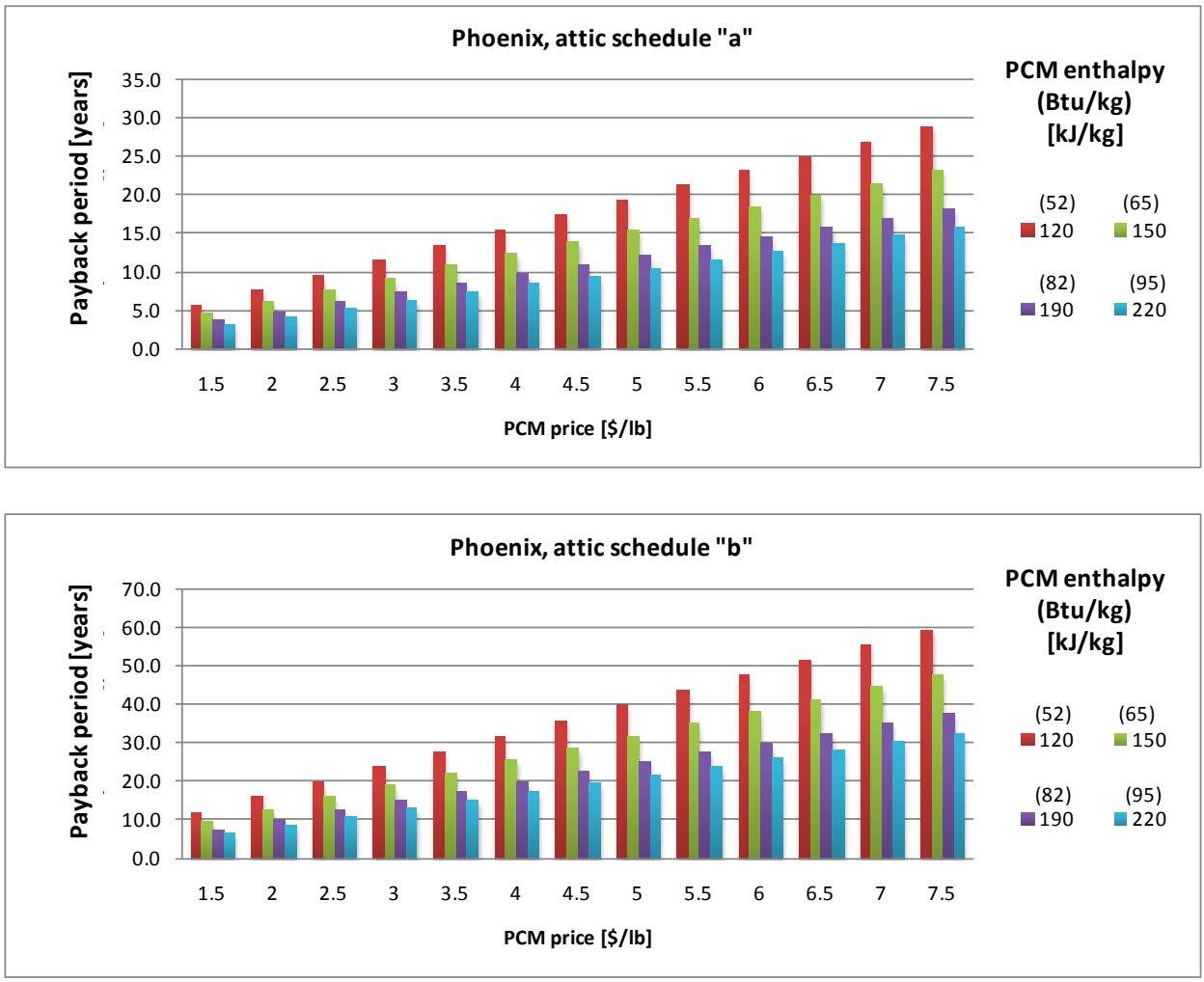

Figure 16. Payback periods for the PCM-enhanced R-30 cellulose insulation configuration installed on the attic floor as a function of the PCM price for a single-story ranch house in Phoenix. The external temperature profiles have been defined as "a" and "b."

As shown in Table 8, installing attic floor insulation that contains dispersed PCM may bring substantial energy and cost savings in several southern U.S. locations. Overall cost effectiveness of the PCM-enhanced attic floor insulation was estimated for two thermal performance levels described previously (see Figure 6, , and 10). To reiterate, detailed thermal modeling of the specific attic configuration will help to develop a better understanding of the thermal processes within the attic space. In addition, this will be useful in obtaining a more precise estimation of the potential energy savings accruing from the PCM application. In this report, the study team assumed that the thermal performance of the PCM-enhanced attic insulation will be between the PCM performance levels described earlier, depending on the attic configuration and climatic conditions. Analysts also expect that the optimized selection of the PCM (better selection of the enthalpy profile in relation to the internal attic air temperature) will bring additional performance improvements.

For the payback period study, the team assumed a PCM price range between $1.50 and 7.50/lb (refer to Figures 12 through 16). If a payback period of 10 years is set as a target and exterior temperature schedule "a" is assumed the following three locations will qualify:

- Phoenix—a maximum PCM price of $4.50/lb for the two enthalpy cases of 82 and 95 Btu/lb (190 and 220 kJ/kg); a maximum price of $2.50/lb for the case of 52 Btu/lb (120 kJ/kg), which is a commonly used PCM price in Europe
- Bakersfield—a maximum PCM price of $3.50/lb for the two enthalpy cases of 82 and 95 Btu/lb (190 and 220 kJ/kg)
- Miami—a maximum PCM price of $2.50/lb for the two enthalpy cases of 82 and 95 Btu/lb (190 and 220 kJ/kg).

If a payback period of 7 years is set as a limit and exterior temperature schedule "a" is assumed, the following three locations would qualify:

- Phoenix—a maximum PCM price of $3.50/lb for the two enthalpy cases of 82 and 95 Btu/lb (190 and 220 kJ/kg)
- Bakersfield—a maximum PCM price of $3.00/lb for the two enthalpy cases of 82 and 95 Btu/lb (190 and 220 kJ/kg)
- Miami—a maximum PCM price of $2.00 /lb for the enthalpy cases of 95 Btu/lb (220 kJ/kg).

3.4 Additional Benefits of Thick Applications of the Phase Change Material-Enhanced Attic Floor Insulation

Two additional important features of the thick PCM-enhanced thermal insulations are reductions of the peak-hour thermal loads and the capability to significantly time-shift thermal loads in place where application is located. As shown in Figures 9 and 10, the peak-hour load reductions generated by PCM-enhanced attic floor insulations can easily be between 50% and 80%. For different climatic locations and for specific PCM configurations, it is also important to consider the number of days (as a percentage) on which phase change processes are allowed to take place. Figure 17 summarizes these findings for load schedules "a" and "b." For geographic locations that have two separate electricity cost rates for on-peak and off-peak hours, the capability to reduce load during peak hours is critical. In these places, peak-hour load reductions combined with significant load time-shifting can be essential sources of energy cost savings.

As depicted in Figure 9, 10, 17, and 18, the peak-hour load-shifting generated by 11.8-in. (0.3-m) thick PCM-enhanced attic floor insulations can be between 4 and 11 hours, depending on the PCM selection and the intensity of the exterior thermal excitations (refer to Figure 6). Remember that in many locations with a double electricity tariff, the off-peak time starts at 7:00 p.m. For such locations, the most useful configuration would be an attic insulation system that provides at least a 5-hour time delay for attic-generated cooling loads. Figure 18 shows that all the configurations considered in this analysis for an 11.8-in. (0.3-m) thick PCM-enhanced attic floor insulation will most likely meet this requirement. Phoenix is the only location that has double electricity rates. Cooling energy cost savings calculated for Phoenix as given in Table 8 show that it is possible to save up to 30% of the attic-generated cooling electricity cost by taking

advantage of the load-shifting capability of the PCM-enhanced attic insulation. Figure 19 presents the results of the payback period calculations for Phoenix with off-peak energy savings taken into account.

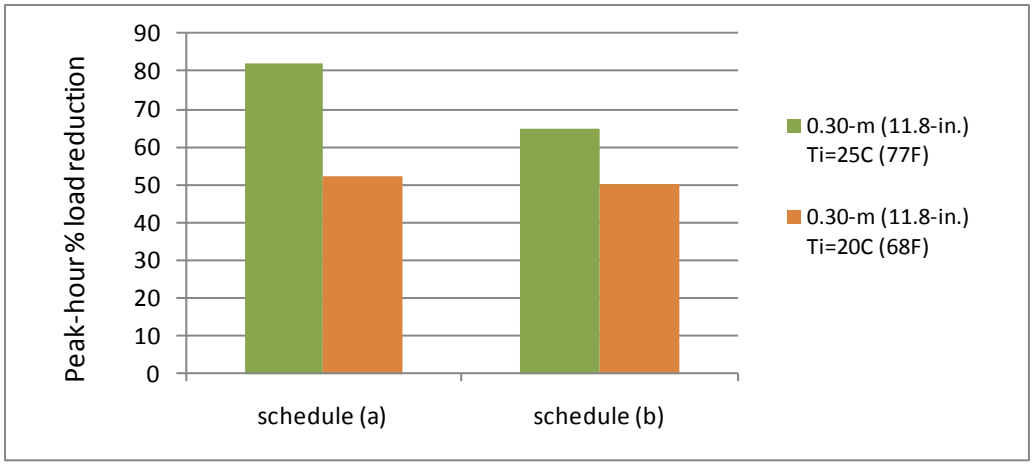

Figure 17. Percent peak-hour cooling load reductions for 11.8-in. (0.3-m) thick PCM-enhanced attic floor insulation

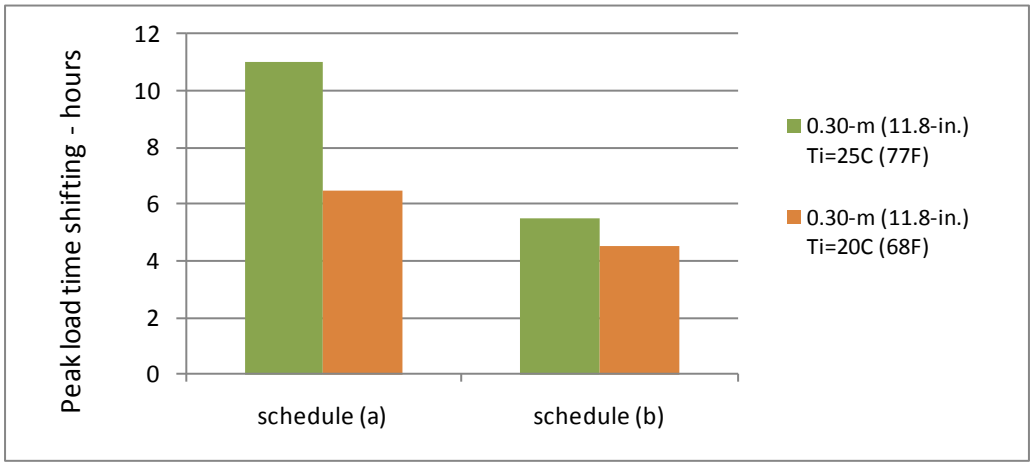

Figure 18. Peak-hour cooling load time-shifting for 11.8 in. (0.3-m) thick PCM-enhanced attic floor insulation

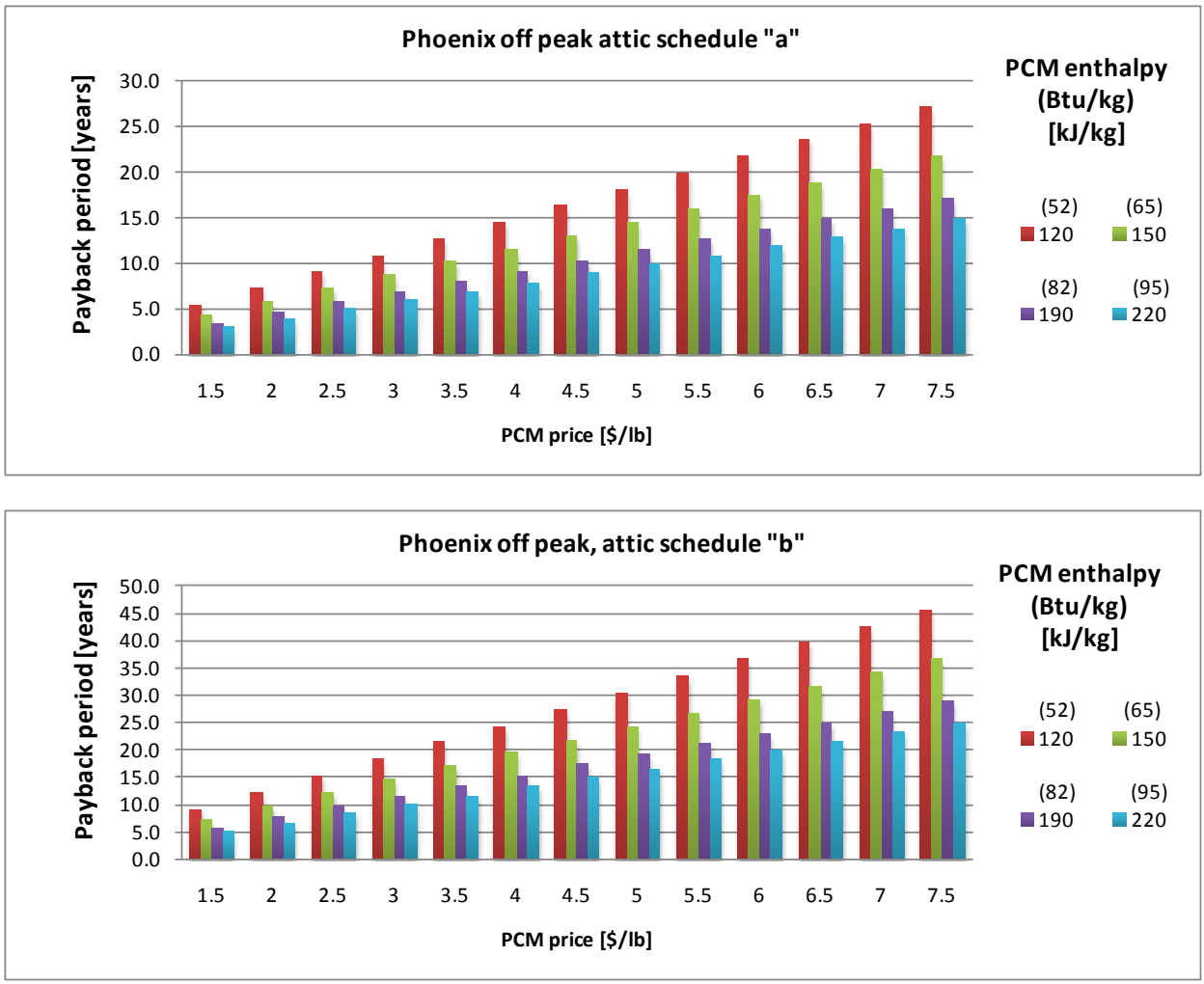

Figure 19. Payback periods calculated using cooling cost reductions for 11.8-in. (0.3-m) thick PCM-enhanced attic floor insulation computed using the off-peak-hour electricity tariff for Phoenix. The external temperature schedules have been defined as "a" and "b."

As shown in Figures 17 through 19, a significantly lower off-peak electricity rate in Phoenix allows PCMs that cost $0.50 more to be applied. For example, for a 10-year payback period (schedule "a"), microencapsulated PCM with an enthalpy of 52 Btu/lb (120 kJ/kg) may cost a maximum of about $3.00/lb as compared to $2.50/lb, estimated previously under a one-tariff schedule.

Simulation results presented in Figure 9, 10, and 18 indicate that including a PCM in an insulation layer can result in a significant time-shifting of the peak-hour loads. The thicker 11.8-in. (0.3-m) assemblies yield larger load-shifting—in most cases at least four times larger than the 5.5-in. (0.14-m) thick assemblies (see Figures 7 through 10). In the 11.8-in. (0.3-m) thick building envelope assembly containing PCM with an internal set-point temperature of T_i = 77°F (25°C), the peak-hour load may be shifted by 11 hours. Figure 20 shows that in this building envelope assembly, the heat flows in the opposite direction 70% of the time (~17 hours a day), compared to a similar assembly without any PCMs. During the day, this PCM-enhanced assembly generates a passive cooling effect. These simulation results have confirmed earlier

field test data, as described by Kośny and coworkers (2010), for walls and attics containing PCM-enhanced insulation.. It is expected that in combination with greater than 70% reduction of the total loads and "free" cooling during the day (see Figure 11), this configuration can be an attractive alternative to conventional building envelope systems in the future.

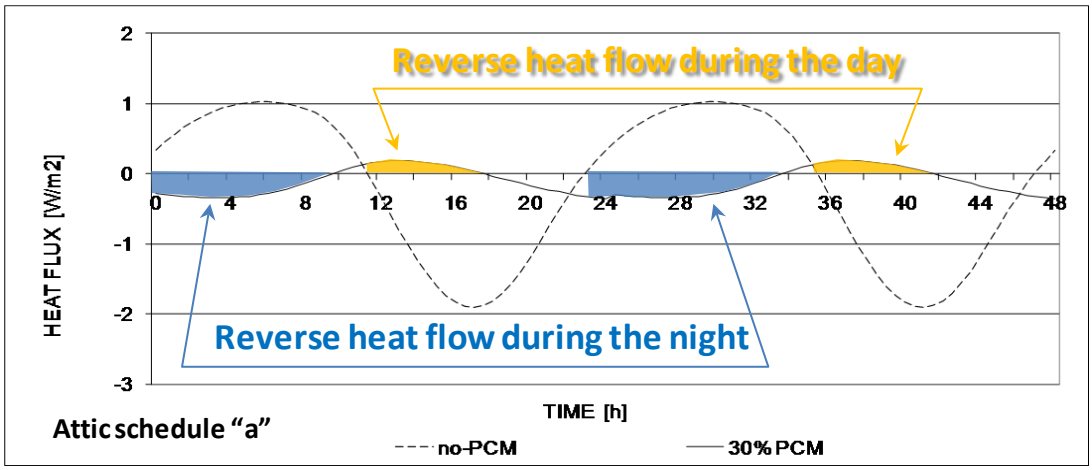

Figure 20. Reverse heat flow effect generated by significant time shifting of thermal loads in 11.8-in. (0.3-m) thick PCM-enhanced attic floor insulation in Phoenix. The external temperature schedule has been defined as "a"

In July 2008, a full-scale experimental attic was constructed and instrumented to field-test blown fiberglass insulation combined with microencapsulated PCMs (Kośny et al. 2010). One purpose of this experiment was to use the collected data to inform future modifications in the attic design, and to eventually optimize the PCM thermal characteristics. A full-scale residential attic was filled with about 10 in. (0.25 m) of blown fiberglass insulation with an approximate density 1.8 lb/ft^3 (29 kg/m^3). Next, on top of this insulation, four 0.5-in. (0.013-m) thick layers of a PCM-adhesive blend were installed with 0.5-in. (0.013-m) thick layers of blown fiberglass installed in between, as shown in Figure 21. The total thickness of the added PCM-fiberglass multilayer "sandwich" was approximately 4 in. (0.10 m). The PCM melting temperature was close to 84°F (29°C), and the nominal phase change enthalpy was about 73 Btu/lb (170 kJ/kg). This experiment demonstrated that it is possible to observe and measure the theoretically predicted reverse heat flow in thick layers of PCM-enhanced insulation under full-scale field conditions.

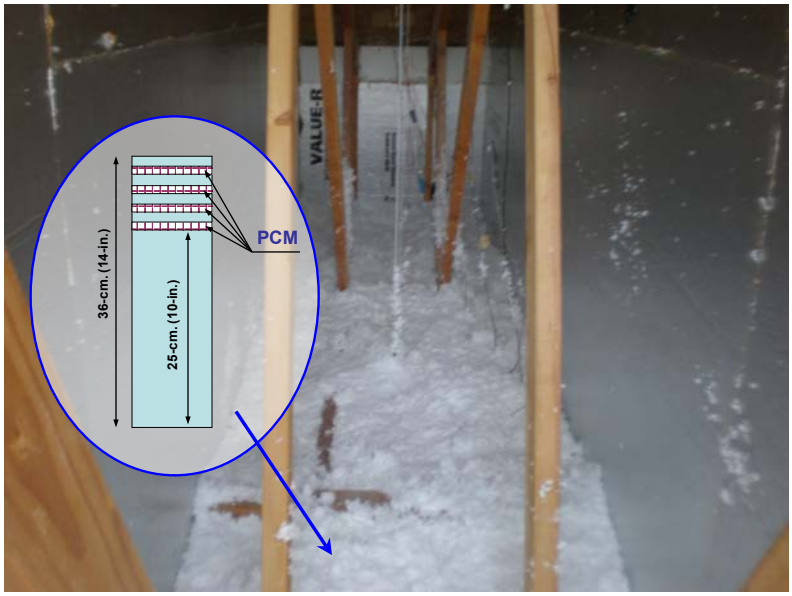

Figure 21. Photograph of the test attic with blown PCM-enhanced fiberglass insulation

To develop a better understanding of the reverse heat flow effect within the attics containing PCM-enhanced insulation, detailed transient modeling of the attic space temperatures and heat fluxes generated on the attic floor is necessary.. Optimization of the insulation thickness and configuration of the PCM heat sink may significantly improve the overall energy effectiveness of residential and small commercial attics beyond the level of savings shown in the parametric analysis.

3.5 Potential Cost Savings Associated With Phase Change Material Load Reductions in Phase Change Material-Enhanced Attic Floor Insulations

Recall that one of the goals of this project was to define the energy performance and cost limits for PCM-enhanced building technologies. For this reason, the study team assumed a near-maximum amount of PCM that can be supported by the fiberglass insulation. A uniform PCM load level of 30% by weight was assumed for all applications of the PCM-enhanced fiberglass insulation. This fact yielded very conservative PCM cost predictions and relatively long payback periods.

Previous research has demonstrated, however, that in building applications PCM loads do not need to be so high. It is worthwhile to mention that initially the PCM-enhanced cellulose insulation was developed with about 22% PCM content (Kośny et al. 2006). At the same time, the study team performed most of the tests and numerical analysis of the cellulose- and fiberglass-based insulations mixed with microencapsulated PCM for load levels between 20% and 25% by weight (Kośny et al. 2010; Kośny 2008). In these studies, performance levels were very close to the thermal performance of the samples containing 30% of PCM. Note that the latest ORNL numerical study confirmed this finding as well (ORNL 2012). In that light, about a 25% reduction in the PCM amount (from the 30% by weight level used in this study) can easily

be allowed , with insignificant reduction of the thermal performance of PCMs. Figure 22 shows the modified levels of payback period for attic PCM applications in Miami and Phoenix. This study found that 25% reduction in the PCM load can reduce the payback period by approximately 1 to 2 years, depending on the location, PCM type, and cost level.

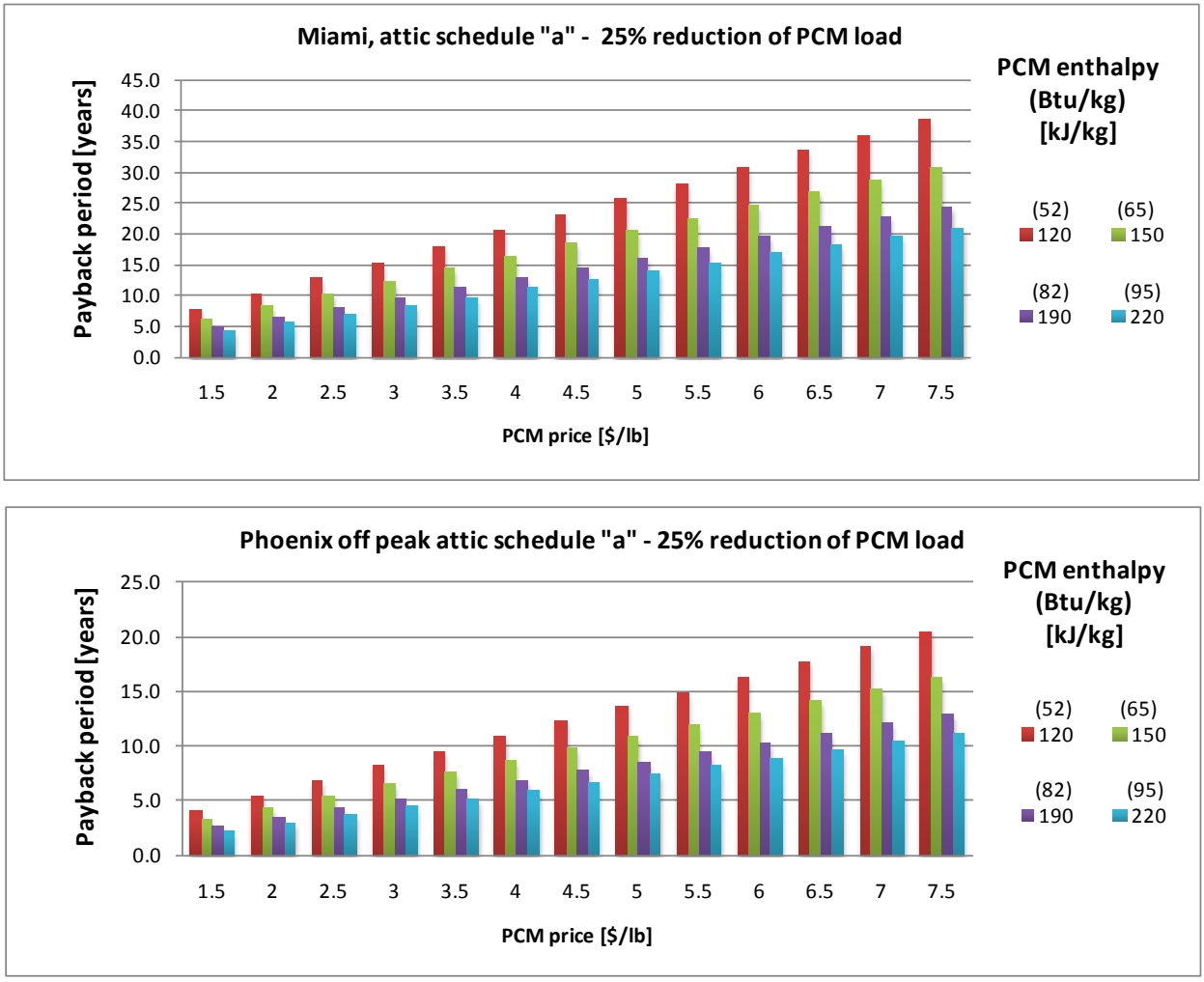

Figure 22. Modified levels of payback periods for attic PCM applications in Miami and Phoenix, considering a 25% reduction in PCM loading

When a payback period of 10 years was assumed as a top cost level for Miami, two PCM-enhanced insulation configurations were found to meet this cost target for a PCM price of $3.00/lb and below (under thermal schedule “a”). These configurations are (1) 82 Btu/lb (190 kJ/kg) and (2) 95 Btu/lb (220 kJ/kg). Similarly, the same payback period target for Phoenix required the PCM price to be $6.00/lb and below. For Phoenix, at an enthalpy of 52 Btu/lb (120 kJ/kg), the maximum price was calculated at $3.50/lb and the payback period would be 10 years.

If a payback period of 7 years is the limit and considering enthalpies of 82 and 95 Btu/lb (190 and 220 kJ/kg), the PCM price (for schedule “a”) would need to be below $3.50/lb and $5.00/lb in Miami and Phoenix, respectively. Also, in Phoenix, microencapsulated PCM with an enthalpy

of 52 Btu/lb (120 kJ/kg) would need to cost less than $3.00/lb to be considered for this application.

In addition, remember that dynamic hot-box testing and transient modeling demonstrated that not all PCMs in the wall cavity or on the attic floor always undergo phase transition (Kośny et al. 2007). Experimental work showed that often up to 50% of the PCM content may not perform phase transition. For precise analysis of this process and optimization of the PCM amount, detailed transient modeling is necessary.

3.6 Payback Period Analysis for Wall Applications of Dispersed Phase Change Materials

Conventional 2 × 6 wood-framed wall assemblies usually use either fiberglass batt cavity insulation or blown cellulose insulation. In this report, the study team considered only PCM-enhanced cellulose cavity insulation. As mentioned previously, during the summer in southern U.S. locations, the wall cavity insulation is usually facing temperature fluctuations close to schedule "a" with temperature peaks reaching 113°F (45°C). To reach the same PCM heat storage density that was assumed in the theoretical analysis, 202 lb (92 kg) of PCM was used in the cost analysis of wall insulation.

Table 9 shows the annual costs for wall-generated electric cooling demands in each of the study's geographic locations. For Phoenix, all wall-generated cooling electricity was used either during the on-peak hours or during the off-peak hours.

Table 9. Annual Costs of Cooling Electric Energy Generated by 2 × 6 Walls, Calculated for a Single-Story Ranch House for Five Southern U.S. climates

Cities	Total Cooling Energy Consumption (kWh)	Wall-Generated Cooling Energy Consumption (kWh)	Annual Cost of Electricity Used for Cooling (Wall-Generated, $)
Atlanta	1,683	236.77	26.75
Bakersfield	2,817	437.70	148.82
Fort Worth	3,082	455.61	42.83
Miami	6,076	856.73	99.38
Phoenix On-Peak			207.52
Phoenix Off-Peak	5805	960.68	51.88[a]

[a] Assuming that the cost of all electric cooling used was calculated using the off-peak tariff for the wall-generated portion of the cooling energy

The study team calculated anticipated cooling energy cost savings for walls for each selected geographic location. As shown in Table 10, for each climate, two levels of savings were calculated based on the efficiency predictions given in Figure 11 for schedule "a" with an internal space temperature T_i = 77°F (25°C). Next, using the calculated cooling energy cost savings and assuming a PCM price range of $1.50–$7.50/lb, payback periods were computed for the following four typical PCM enthalpies: 52 Btu/lb (120 kJ/kg), 65 Btu/lb (150 kJ/kg), 82 Btu/lb (190 kJ/kg), and 95 Btu/lb (220 kJ/kg). Amounts of PCM were normalized against the heat storage capacity of the wall system using a PCM of 52 Btu/lb (120 kJ/kg) enthalpy as a baseline. Results of these calculations are presented in Figures 21 through Figure 26.

The simulation results presented in Figures 7 through 10 indicate that the effect of PCMs in an insulation layer may result in significant time-shifting of the peak-hour loads. The thicker attic insulation assemblies yield larger load shifting—in most cases at least four times larger than the thinner case of 5.5-in. (0.14-m) thick wall assemblies. In the case of the 5.5-in. (0.14-m) thick building envelope assembly containing PCMs, and where the internal set-point temperature is 77°F (25°C), the peak-hour load may shift by 3 hours. Because the 3-hour time shift will not completely move the peak-hour loads to the off-peak time, only 60% of off-peak savings were included in the energy cost savings analysis. More detailed thermal modeling is needed to better approximate the scale of this effect for PCM-enhanced wall insulations. In this study, the team assumed that PCMs represented 30% by weight of insulation installed in the 5.5-in. (0.14-m) thick wall cavity and that the wall framing factor was 25%. Considering that the cellulose density was about 1.6 lb/ft^3 (25.6 kg/m^3), and windows and doors represent 20% of the total wall area, the overall PCM load in all four walls was close to 203 lb (129 kg).

Table 10. Annual Cooling Electricity Cost Savings Generated by the Attic Calculated for a Single-Story Ranch House for Five Southern U.S. Climates

Cities	Annual Cost of Electricity Used for Cooling (Wall-Generated, $)	Annual Cooling Electricity Cost Savings—Schedule "a" (Wall-Generated, $/ft^2-floor area)
Atlanta	26.75	5.89 (0.004)
Bakersfield	148.82	32.74 (0.021)
Fort Worth	42.83	9.42 (0.006)
Miami	99.38	21.86 (0.014)
Phoenix On-Peak	207.52	45.65 (0.030)
Phoenix Off-Peak		61.39 (0.040)[a]

[a] In energy cost savings analysis, the study team included only 60% of off-peak savings.

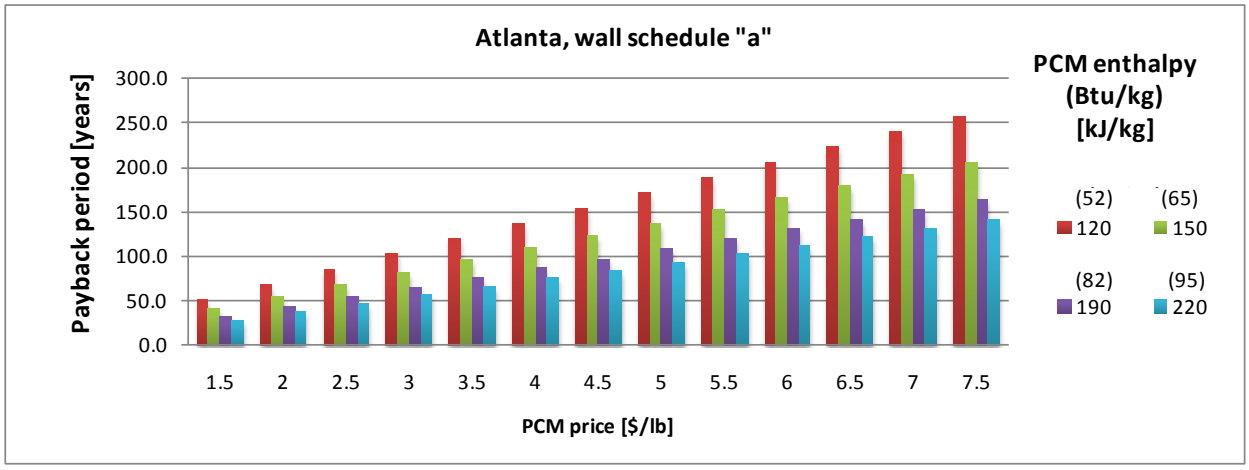

Figure 23. Payback period for PCM-enhanced cavity wall insulation as a function of the PCM price for a single-story ranch house in Atlanta. Wall assemblies are assumed to experience the external temperature schedule defined as "a."

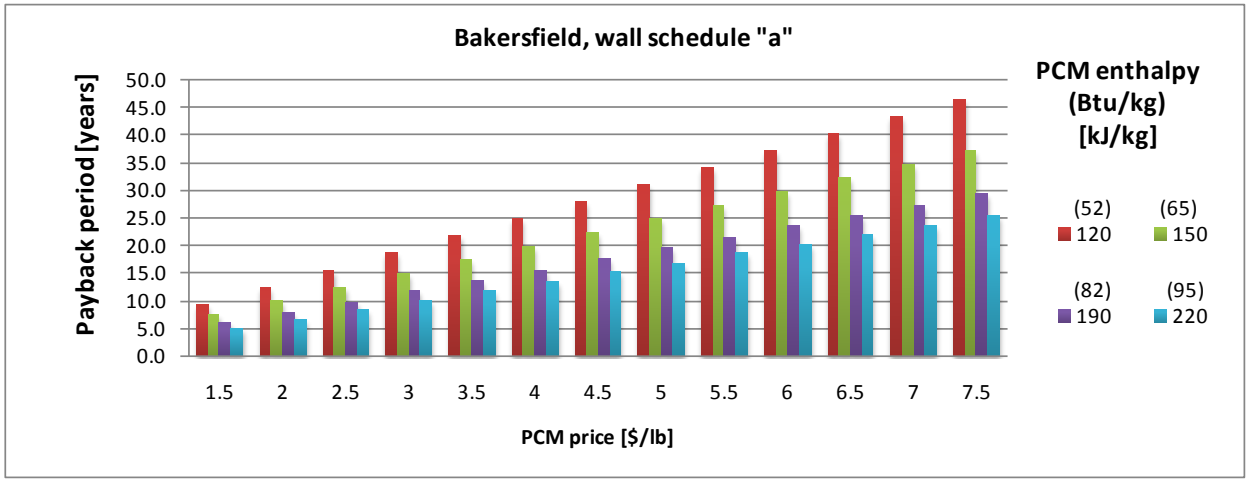

Figure 24. Payback period for PCM-enhanced cavity wall insulation as a function of the PCM price for a single-story ranch house in Bakersfield. Wall assemblies are assumed to experience the external temperature schedule defined as "a."

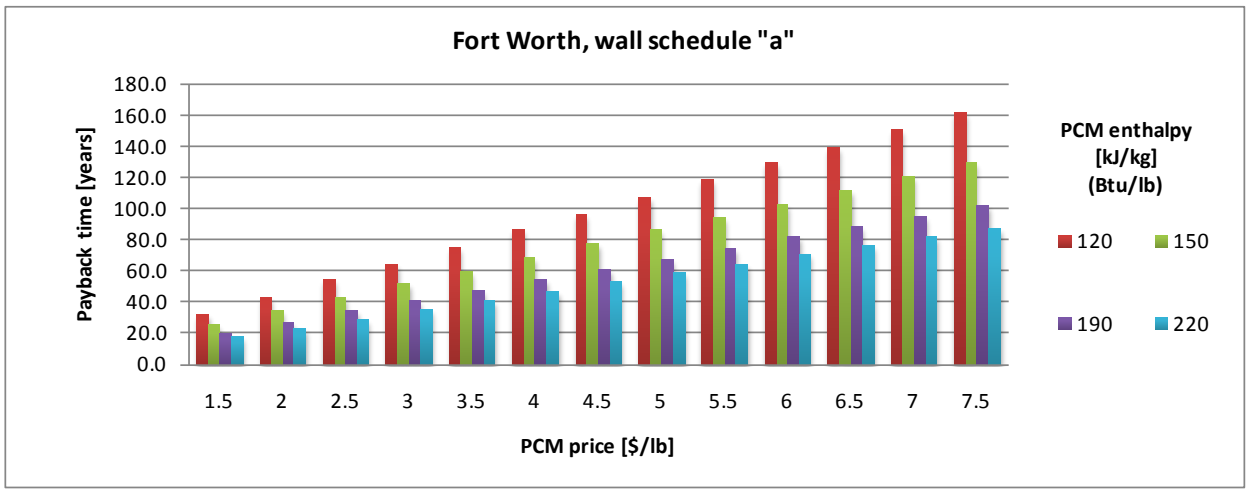

Figure 25. Payback period for PCM-enhanced cavity wall insulation as a function of the PCM price for a single-story ranch house in Fort Worth. Wall assemblies are assumed to experience the external temperature schedule defined as "a."

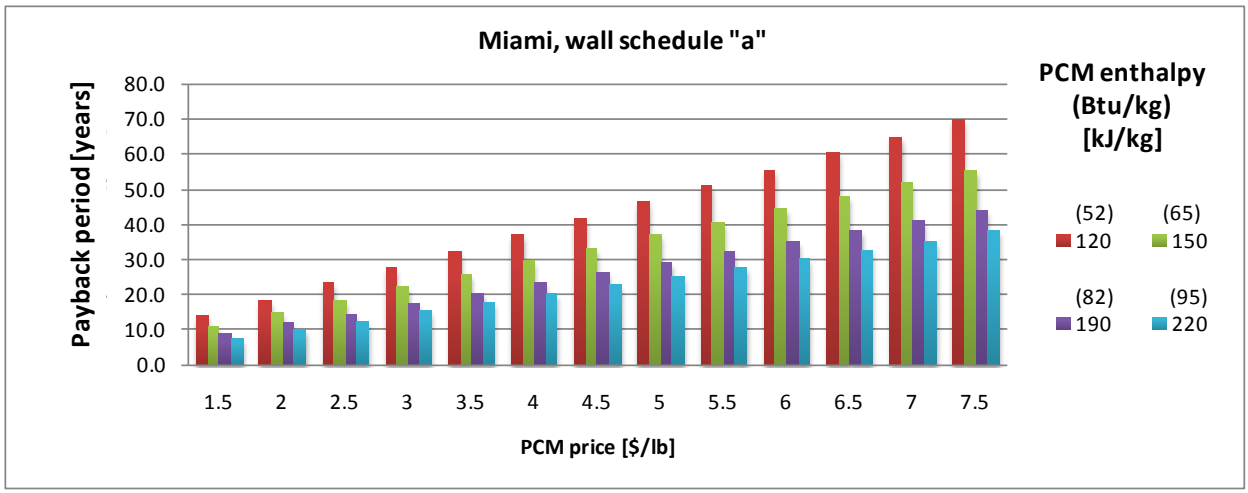

Figure 26. Payback period for PCM-enhanced cavity wall insulation as a function of the PCM price for a single-story ranch house in Miami. Wall assemblies are assumed to experience the external temperature schedule defined as "a."

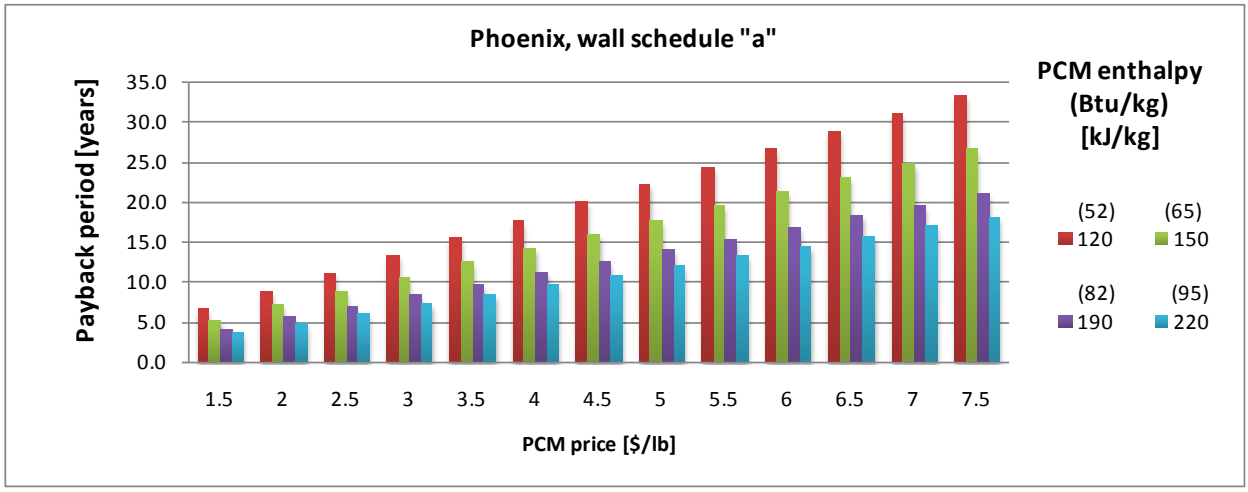

Figure 27. Payback period for PCM-enhanced cavity wall insulation as a function of the PCM price for a single-story ranch house in Phoenix. Wall assemblies are assumed to experience the external temperature schedule defined as "a."

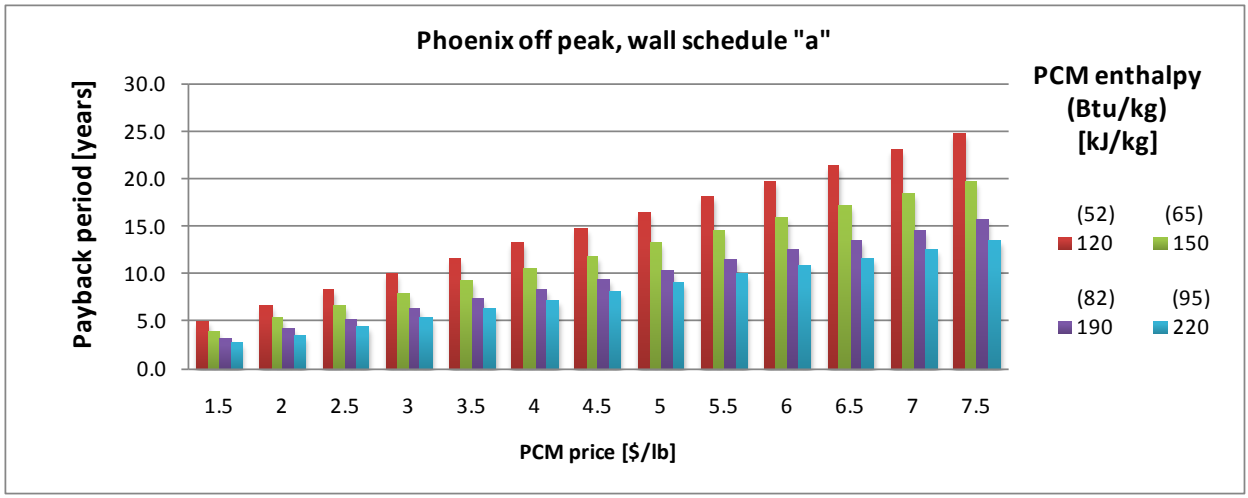

Figure 28. Payback period for PCM-enhanced cavity wall insulation as a function of the PCM price for a single-story ranch house in Phoenix. Wall assemblies are assumed to experience the external temperature schedule defined as "a" and an off-peak tariff is included.

If a payback period of 10 years is set as a target and the exterior temperature schedule "a" is assumed, three locations will qualify:

- Phoenix—a maximum PCM price of $4.00/lb for the two enthalpy cases of 82 and 95 Btu/lb (190 and 220 kJ/kg) and a maximum price of $2.50/lb for the case of 52 Btu/lb (120 kJ/kg)
- Bakersfield—a maximum PCM price of $2.50/lb for the two enthalpy cases of 82 and 95 Btu/lb (190 and 220 kJ/kg)
- Miami—a maximum PCM price of $1.50/lb for the two enthalpy cases of 82 and 95 Btu/lb (190 and 220 kJ/kg) (see Figures 23 through 27).

If a payback time of 7 years is established as a limit and the exterior temperature schedule "a" is assumed, three locations will qualify:

- Phoenix—a maximum PCM price of $3.00/lb for the two enthalpy cases of 82 and 95 Btu/lb (190 and 220 kJ/kg)
- Bakersfield—a maximum PCM price of $2.00/lb for the two enthalpy cases of 82 and 95 Btu/lb (190 and 220 kJ/kg)
- Miami—a maximum PCM price of $1.50 /lb for the enthalpy case of 95 Btu/lb (220 kJ/kg) (see Figures 23 through 27).

Remember that the hot-box testing and numerical analysis showed that in a 2 × 6 wall cavity insulated with fiber insulation containing dispersed PCM, not all PCMs may undergo a phase change. Based on this finding, the analysts believe that there is still a potential for at least a 20% reduction in the amount of PCM without compromising the overall thermal performance.

3.7 Payback Period Analysis for Wall Applications of Phase Change Material-Enhanced Gypsum Boards

Historically, performance investigations focused on impregnating concrete, gypsum, or ceramic masonry with salt hydrates or paraffinic hydrocarbons. PCM-enhanced gypsum board and PCM-impregnated stucco are probably the best-known PCM applications in buildings. Most of the research studies performed on these materials found that PCMs improved building energy performance by reducing the peak-hour cooling loads and shifting the peak-demand time. During early testing in the United States, gypsum boards were impregnated with PCMs. Later, microencapsulated PCMs were used. In these tests paraffinic hydrocarbon PCMs generally performed well, but they compromised the flammability resistance of the building envelope.

In this study, the team assumed that PCM represented 20% by weight of the ½-in. (~0.012-m) thick drywalls that were installed on the internal surfaces of the exterior walls. Considering that the drywall density is about 37 lb/ft^3 (593 kg/m^3) and assuming that windows and doors represent 20% of the total wall area, the overall PCM load in all four walls was close to 284 lb (129 kg) for all building configurations described in Section 3.

In this part of the analysis, the study team used either the experimental performance data or limited numerical predictions yielded by computer programs that were validated with the test data (as described in Table 1). For applications of PCM-enhanced drywall in walls, different research groups reported cooling energy savings ranging between 7% and 20% for different U.S. locations.. Following this historical experimental data, in this work, the study team considered 15% cooling energy savings for the PCM-enhanced gypsum board applications. Figures 29 through 34 present the results of the payback period calculations. About 1 hour of load-shift time was reported for PCM-enhanced gypsum board in earlier research reports (see, for example, Tomlinson et al. 1992).

Remember that the PCM applications represented in this report are exclusively for a steady internal space temperature. In addition, internal walls are finished with PCM-enhanced drywalls in many applications. Given that many successful applications of the PCM-enhanced gypsum boards use different variable internal temperature schedules and different PCM loads, the study team strongly recommends performing additional, more detailed cost analysis for each of individual application scenarios.

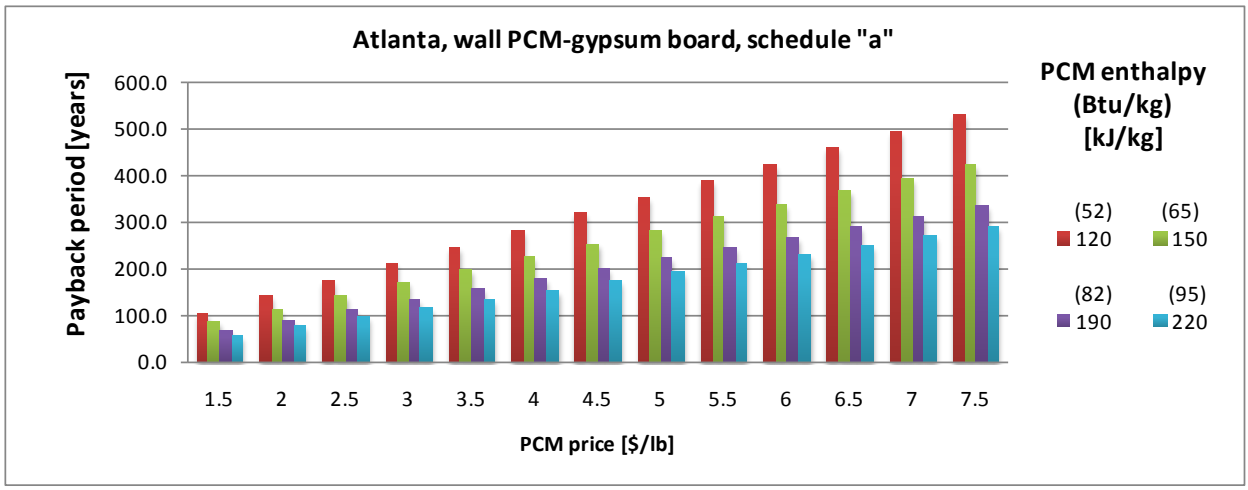

Figure 29. Payback period for PCM-enhanced gypsum boards that are used for wall application as a function of the PCM price for a single-story ranch house in Atlanta. Wall assemblies are assumed to experience the external temperature schedule defined as "a."

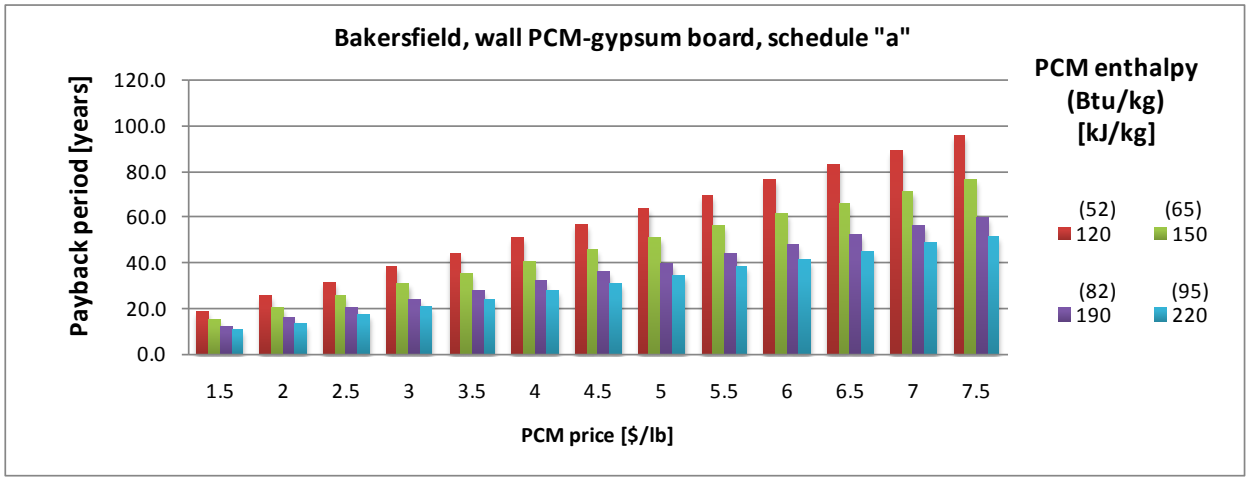

Figure 30. Payback period for PCM-enhanced gypsum boards that are used for wall application as a function of the PCM price for a single-story ranch house in Bakersfield. Wall assemblies are assumed to experience the external temperature schedule defined as "a."

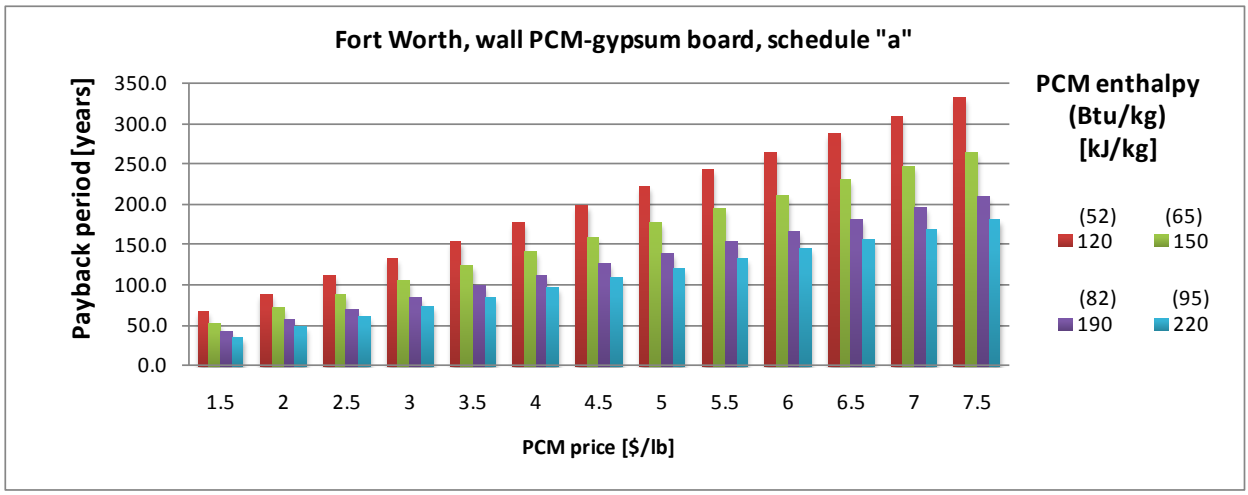

Figure 31. Payback period for PCM-enhanced gypsum boards that are used for wall application as a function of the PCM price for a single-story ranch house in Fort Worth. Wall assemblies are assumed to experience the external temperature schedule defined as "a."

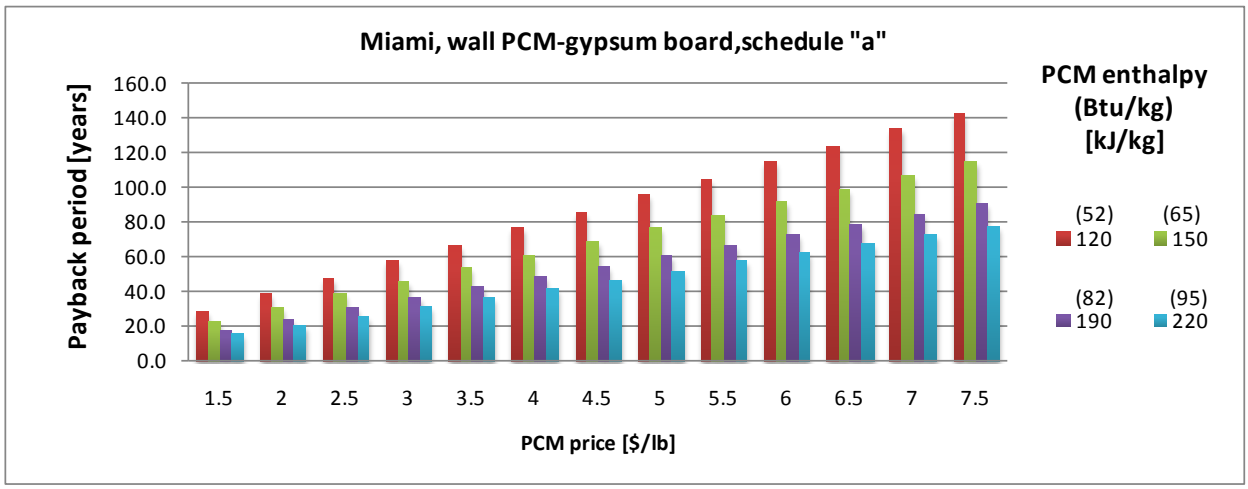

Figure 32. Payback period for PCM-enhanced gypsum boards that are used for wall application as a function of the PCM price for a single-story ranch house in Miami. Wall assemblies are assumed to experience the external temperature schedule defined as "a."

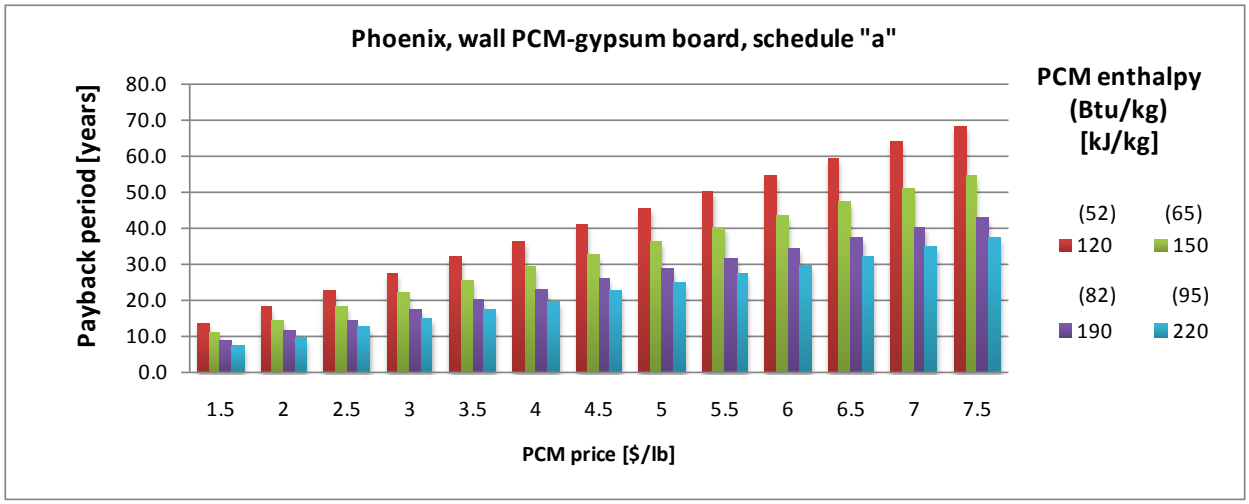

Figure 33: Payback period for PCM-enhanced gypsum boards that are used for wall application as a function of the PCM price for a single-story ranch house in Phoenix. Wall assemblies are assumed to experience the external temperature schedule defined as "a."

The figures (Figure 29 through 34) show that if a payback time of 10 years is assumed as a maximum cost level, PCMs with a price $2.00/lb and lower with enthalpies between 82 and 95 Btu/lb (190 and 220 kJ/kg) can meet this target in Phoenix. Figure 34 shows the approximate payback times computed for Phoenix, considering energy cost savings resulting from applying the off-peak electricity rate. Similar to applications with PCM-enhanced fiber insulation, notable improvements in the cost effectiveness can be observed.

When cost reductions resulting from off-peak electricity rates are included, a payback period of 7 years is calculated for two PCMs of enthalpies between 82 and 95 Btu/lb (190 and 220 kJ/kg) with a price limit $3.00/lb. In addition, Figure 34 shows that for these two PCMs, a 10-year payback period is possible for a PCM price not exceeding $3.50/lb.

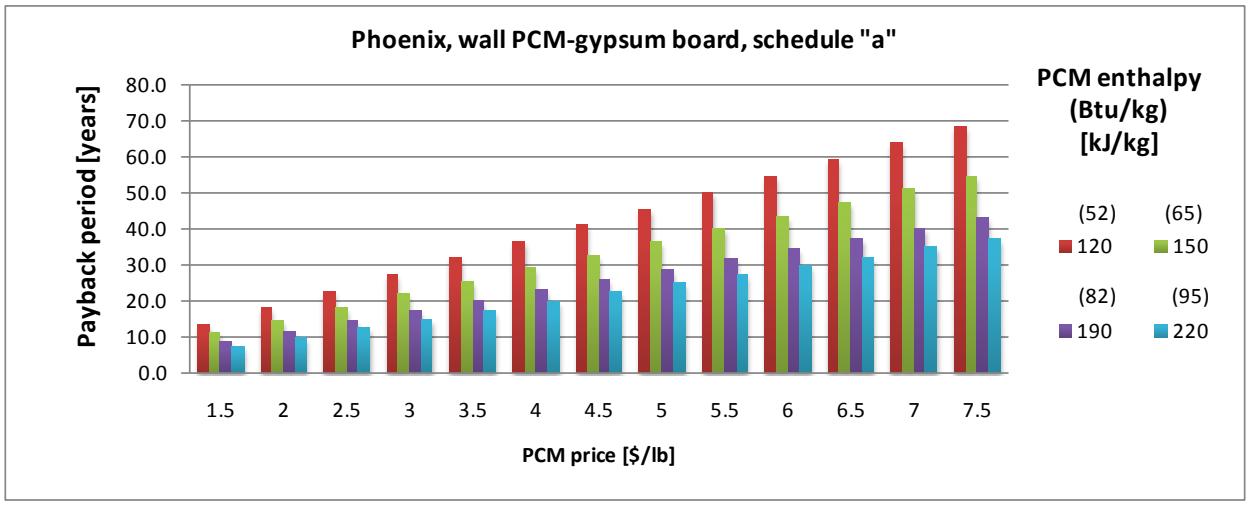

Figure 34. Payback period for PCM-enhanced gypsum boards that are used for wall application as a function of the PCM price for a single-story ranch house in Phoenix. Wall assemblies are assumed to experience the external temperature schedule defined as "a" and an off-peak tariff is used.

Remember that when PCM-enhanced gypsum boards are used in a house, they are often installed on the exterior and interior walls and the ceilings. This significantly changes the whole-house dynamic energy response. In such cases, when overnight pre-cooling is used, the energy performance for these systems can improve considerably. This method is mostly used in Europe. For applications in the United States, detailed whole-building modeling that uses variable internal space temperature schedules will be necessary to assess potential energy savings and enable cost analysis. In addition, full-scale field testing can be helpful in predicting additional energy savings for cases with variable internal space temperature profiles and PCM applications on internal walls and ceilings. This is important to remember because, in practice, for these cases payback periods can be significantly different from the experimental data presented in this report for constant internal temperatures.

An application of thinner ⅜-in. (1-cm) thick boards that contain PCM in conjunction with carbon or graphite fillers (to enhance thermal conductivity) may be considered as an alternative for performance improvement and cost reduction. Figure 35 depicts the payback times computed for a ⅜-in. (1-cm) thick PCM-enhanced drywall in Phoenix. The study team assumed that the board thickness reduction brought about 25% savings in the PCM cost. At the same time, an addition of highly conductive fillers added an extra 5% to the cost, bringing total cost savings to 20%.

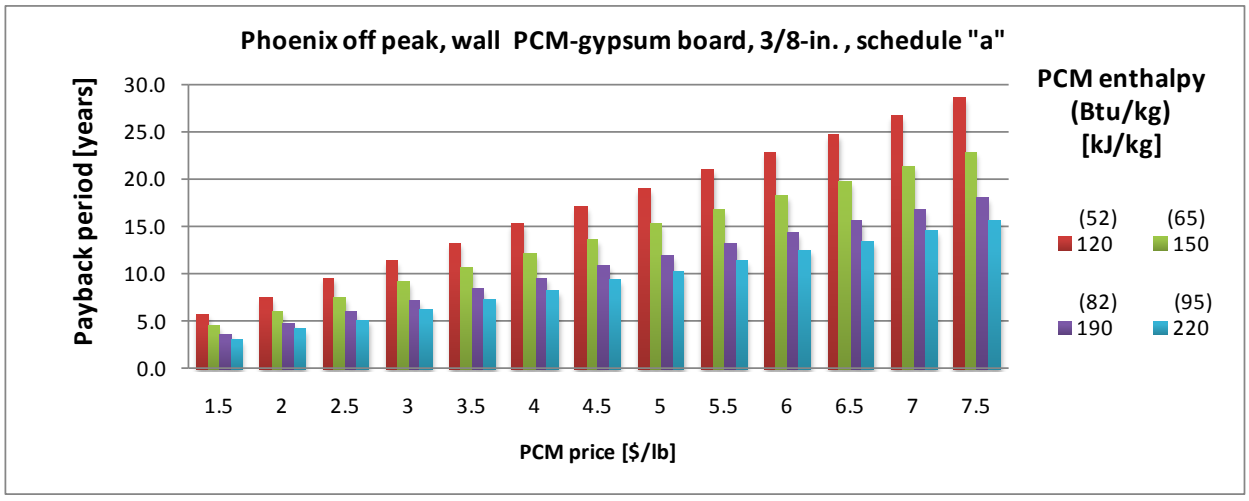

Figure 35: Payback period for 3/8-in. thick PCM-enhanced gypsum boards that are used for wall application as a function of the PCM price for a single-story ranch house in Phoenix. Wall assemblies are assumed to experience the external temperature schedule defined as "a" and an off-peak tariff is used.

3.8 Performance Comparisons Between Conventional Insulations and Phase Change Material-Enhanced Insulations

The whole-building energy analysis results presented in Figures 2 and 3 indicated that in building envelopes with higher R-values, the thermal effectiveness of conventional insulations can be surprisingly low. Analytical data presented in Figures 7 through 10, however, indicate that if these insulations are mixed with microencapsulated PCMs, the overall efficiency of the PCM-insulation composite can be significantly higher.

Based on the study team's whole-building energy performance analysis, Table 11 shows the computed approximate energy savings for the attic used in the analysis. Two applications were analyzed, one with conventional insulation only, and the other with PCM-enhanced insulation added to the conventional insulation. In both analyzed cases, the initial attic floor was insulated with R-30 insulation. In the case of the conventional insulation, additional R-19 was installed on top of the existing R-30. This scenario yielded about 9% to 10% of the attic-generated cooling energy savings in the whole-building energy model. In case of the PCM application, the R-30 conventional insulation was replaced by a 30% by weight blend of PCM and conventional insulation of the same thickness. To enable performance comparisons, PCM enthalpy of 82 Btu/lb (190 kJ/kg) was assumed. As in earlier analysis, an equivalent amount of PCM was calculated using a PCM of enthalpy of 52 Btu/lb (120 kJ/kg) as a baseline.

Next, energy savings were calculated for schedules "a" and "b." The results showed that by using PCM-enhanced insulation and assuming schedule "a," the cost of saved cooling energy is up to eight times higher compared to case in which conventional R-19 insulation was added. Correspondingly, under schedule "b," the cost of saved cooling energy is about four times higher.

Table 12 shows comparisons of energy cost savings and material costs calculated for a single-story ranch house in five southern U.S. climates. The table shows that adding microencapsulated PCM would be about 1.3 times more expensive than applying the R-19 blown fiberglass and about 1.9 times more expensive than installing the cellulose. Notice that, as described in previous sections, the amount of PCM can still be significantly reduced without compromising the overall energy efficiency of the PCM-enhanced insulation. In that light, PCM-enhanced insulations in cooling-dominated climates can be considered as cost-effective alternatives for future thermal improvements of moderately insulated attics, or for new constructions with higher energy efficiency targets.

Table 11. Potential Savings in Annual Costs of Cooling Electric Energy Generated by the Attic Calculated for a Single-Story Ranch House and for Five Southern U.S. Climates

Cities	Attic-Generated Cooling Energy Consumption (kWh)	Annual Cost of Electricity Used for Cooling (Attic-Generated, $)	Annual Cost Savings of Electricity Used for Cooling (Attic-Generated, $)		
			R-19 Insulation Over Existing R-30 (Level of Savings for Each Location)	30% by Weight Blend of Microencapsulated PCM and R-30 Conventional Insulation (Savings Level for Schedule "a")	30% by Weight Blend Of Microencapsulated PCM and R-30 Conventional Insulation (Savings Level for Schedule "b")
Atlanta	269.3	30.43	2.74 (9%)	21.91	10.65
Bakersfield	456.4	155.18	15.52 (10%)	111.73	54.31
Fort Worth	458.0	43.05	3.87 (9%)	31.00	15.07
Miami	911.4	105.72	9.52 (9%)	76.12	37.00
Phoenix	870.8	188.09	16.93 (9%)	135.43	65.83

Table 12. Comparisons of Energy Cost Savings and Material Costs Calculated for a Single-Story Ranch House for Five Southern U.S. Climates

Cities	Annual Cost Savings of Electricity Used for Cooling (Attic-Generated, $)		Approximate Cost of Materials (Assuming Net Attic Floor Area of 1,108 ft^2, $)	
	R-19 Insulation Over Existing R-30 (Level of Savings for Each Location)	30% by Weight Blend of Microencapsulated PCM and R-30 Conventional Insulation, Savings Levels for Schedules "a" and "b"	R-19 Insulation—Based on U.S. RSMeans Fiberglass, $0.77/ft^2 (Cellulose, $0.55/ft^2)	Addition of Microencapsulated PCM at $3.50/lb (Assuming Enthalpy of 82 Btu/lb [190 kJ/kg])
Atlanta	2.74 (9%)	21.91 (10.65)	853.16 (609.40)	1151
Bakersfield	15.52 (10%)	111.73 (54.31)	853.16 (609.40)	1151
Fort Worth	3.87 (9%)	31.00 (15.07)	853.16 (609.40)	1151
Miami	9.52 (9%)	76.12 (37.00)	853.16 (609.40)	1151
Phoenix	16.93 (9%)	135.43 (65.83)	853.16 (609.40)	1151

4 Discussion of Results

4.1 Selection of Climatic Locations

Energy and cost performance analysis presented in this work indicate that successful applications of PCM-enhanced building envelope insulations and PCM-enhanced drywall are most likely possible in southern U.S. locations that fall in ASHRAE climatic zones 1, 2, and 3 with CDDs (74°F [23.3°C]) preferably greater than 16,667 (30,000).

The local electrical energy cost is equally important. Preferably, on-peak and off-peak electricity tariffs should be available in these locations, or the overall electricity price should be higher than $0.20/kWh. For other locations, detailed energy modeling would be necessary to establish a relationship between energy savings and energy costs.

4.2 Phase Change Material Load Levels in Blends With Thermal Insulations

Remember that initially, PCM-enhanced cellulose insulation was developed with about 22% PCM content. In this study, the study team assumed a uniform PCM load level of 30% by weight for all applications of the PCM-enhanced fiber insulation investigated. Most of the this study's tests and numerical analyses of the cellulose and fiberglass-based blends mixed with microencapsulated PCM, however, were performed for load levels between 20% and 25% by weight. As a result, the analysts believe that this study yielded very conservative PCM cost predictions and relatively high payback periods.

Another important fact is the experimental work performed by ORNL, which demonstrated that not all PCM in the wall cavity or on the attic floor may undergo a phase transition. Hot-box tests have shown that often up to 50% of the PCM content may not be cycling. For precise analysis of this process and optimization of the amount of PCM, detailed transient modeling is necessary. These computer simulations would need to take into account specific thermal characteristics of the PCMs and boundary conditions on both sides of the building assembly containing PCM.

In summary, the nominal 30% PCM content evaluated in this report was relatively higher than the configurations tested and analyzed during the last decade. In both situations, it is possible to reduce amount of PCM by 25%–50% without significantly compromising the nominal thermal performance. For precise optimization of the amount of PCM for each specific building application, , the study team recommends detailed transient modeling.

4.3 Phase Change Material Cost Limits

The cost analysis presented in this report indicates that the effective enthalpy of the PCM-enhanced building envelope components plays an important role in determining the overall cost effectiveness and payback period. Historically, microencapsulated paraffin PCMs with enthalpies between 43 and 52 Btu/lb (100 and 120 kJ/kg) have been the most popular around the world. This team's research data presented show that in most of the applications studied, the PCM price needs to be below $2.00/lb to achieve a 10-year payback period. At this point, an imposing question is whether the PCM industry can achieve this price level.

Higher PCM enthalpies result in improved energy performance and cost effectiveness. For the locations where PCM-enhanced building envelopes can be paid back within a maximum of 10 years, the highest acceptable PCM price with enthalpies between 82 and 95 Btu/lb (190 and 220

kJ/kg) should be between $3.50 and $4.00/lb for the microencapsulated product. The best-known PCM candidates for these cost levels are biobased PCMs (mixtures of fatty acids and fatty esters) and low-cost salt hydrates.

The most promising developments to reduce the cost of PCM products are the reduction of microencapsulation cost for organic PCMs, and the development of microencapsulation technology for inorganic PCMs. Inorganic PCMs are nonflammable and have significantly higher enthalpies. The European Union has already recognized the potential for significant cost reductions of PCM heat storage. An international program involving most of the European research centers working in the area of PCMs—with a focus on encapsulation of inorganic PCMs—has been already initiated (see Fraunhofer ISC 2007).

This study's thermal performance and cost analysis showed that for most locations with a single electric tariff, the most critical factor would be the development of PCM-insulation blends that would have the highest potential for dynamic load reductions in a desired temperature range. Earlier research found that it is very important to optimize a PCM's concentration, overall heat storage capacity, and enthalpy profile to maximize the performance of PCM-enhanced building envelope assemblies.

A second important characteristic affecting energy performance and cost effectiveness is peak-hour load shifting. This feature is especially important for locations with time-of-use pricing. Cost analysis presented in this report demonstrated that it is possible to reduce the cooling energy costs by up to 30% with PCM applications of significant peak-hour load shifting capability and by taking advantage of the off-peak electricity tariff. In most locations, off-peak time starts at 7 p.m. Because of this, developing PCM building envelope products with at least a 5-hour load shifting potential is critical.

The thermal modeling presented in this work showed that high R-value blends of PCM and thermal insulation yield significant time-shifting of thermal loads. It is possible during 70% of the time (~17 hours a day) to have heat flowing in the opposite direction as a similar assembly without PCMs. As a result, a passive cooling effect is caused by this kind of PCM-enhanced assemblies during the day. These simulation results have already been confirmed by the field-test-generated attic heat flow profiles recorded for the experimental attic containing PCM-fiberglass insulation, as described by Kośny and coworkers (2010). It is expected that this passive cooling phenomena may significantly enhance the overall cost effectiveness of the dispersed PCM applications—well above the cost saving levels described previously. The study team strongly recommends more research in this area.

4.4 Payback Periods

One of the goals of this work was to investigate the possibility of finding a dispersed PCM configuration in a southern U.S. location that would allow 7- to 10-year payback periods for building envelopes containing PCMs. In general, the results were encouraging. For the five southern U.S. locations analyzed in this work, two locations showed potential to pay back in 7 years with a PCM price range between $3.00/lb and $4.50/lb. If a 10-year payback period was considered, three locations qualified with a PCM price range between $2.00/lb and $4.50/lb.

Earlier research, though, demonstrated that it is possible to reduce the amount of PCM from the nominal 30% content used in this analysis, without significant reduction in the PCM thermal performance. On the other hand, because of the passive cooling effect, or other positive effects of integration with other building envelope components, the overall performance can be notably higher than the theoretical predictions in this report. The study team also found that a 25% reduction in PCM load can lower the payback period by approximately 1 to 2 years, depending on the location, PCM type, and cost level.

From the other perspective, remember that in most building envelope applications, PCMs are not always deployed in thermal conditions that a full phase change process. Too-high nighttime air temperatures, which keep the PCM melted all night during the summer, are the most common reason for the lack of the phase transition. Historical field test data generated in eastern Tennessee climatic conditions showed that PCMs were cycling about 60%–70% of the total number of days. For different locations, additional field testing or detailed dynamic thermal simulations of a specific PCM application would be necessary to assess the potential of climate-related performance reductions.

For the PCM-enhanced gypsum board application in Phoenix, when cost reductions resulting from off-peak electricity rates are included, a payback period of 7 years can be expected for PCMs with enthalpies between 82 and 95 Btu/lb (190 and 220 kJ/kg) with a price limit of $3.00/lb. A 10-year payback period, then, would be possible for a PCM price level that does not exceed $3.50/lb.

5 Conclusions

The main purpose of this report was to evaluate the cost levels for simple PCM systems at which they can be cost competitive with conventional building thermal insulations. Two basic PCM applications were examined in this analysis: dispersed PCM applications and simple building systems using concentrated PCMs. The study team reports the following list of findings:

1. Dispersed PCMs in attic and wall applications are an effective means of cooling load reductions:
    a. Through overall reductions of the attic or wall heat flow rates
    b. Through the significant time-shifting of thermal loads.
2. Dispersed PCMs in attic and wall applications can be cost effective and payback periods for their building applications can be less than 10 years.
3. Southern U.S. locations with CDDs (74.0°F [23.3°C]) preferably higher than 16,667 (30,000) and an electricity cost higher than $0.20/kWh, or locations with on-peak and off-peak electricity tariffs are the best candidates for these applications.
4. Off-peak electricity tariffs significantly improve the overall cost effectiveness of the PCM-enhanced building applications
5. Future PCM cost reductions can be achieved through:
    a. Applying PCMs of higher enthalpies (around 86 Btu/lb or 200 kJ/kg); the best-known PCM candidates are biobased PCMs (mixtures of fatty acids and fatty asters) and low-cost salt hydrates
    b. Reducing the cost of basic raw PCM; for example, by using inorganic PCMs
    c. Reducing microencapsulation costs or finding less costly methods of micropackaging
    d. Developing low-cost methods for microencapsulation of inorganic PCMs
    e. Optimizing PCM loads in building envelope products
    f. Considering the PCM price; for the southern U.S. locations with a maximum expected payback period of 10 years, the highest acceptable PCM price should be between $3.50 and $4.00/lb for the microencapsulated products with enthalpies between 82 and 95 Btu/lb (190 and 220 kJ/kg).

More theoretical and experimental work is necessary to select a proper PCM type for specific applications and climatic conditions.

References

APS – 2012 – Residential Service Rate Plans & Tariffs
www.aps.com/aps_services/residential/rateplans/ResRatePlans_1.html

ASHRAE -62 – ASHRAE 62-2001, Ventilation for Acceptable Indoor Air Quality (IAQ) – ASHRAE – Atlanta, 2001

ASTM International (2006a). *ASTM Standard C518, Test Method for Steady-State Heat Flux Measurements and Thermal Transmission Properties by Means of the Heat Flow Meter Apparatus.* West Conshohocken, PA: ASTM International.

Bakersfield News (2011). "PG&E Rates Said To Decrease." www.turnto23.com/news/28307841/detail.html

Balcomb, J.D.; Jones, R.W.; Kosiewicz, C.E.; Lazarus, G.S.; McFarland, R.D.; Wray W,O. (1982). *Passive Solar Design Handbook.* Boulder, CO: American Solar Energy Society.

Biswas, K.; Kośny, J.; Kriner, S. (September 2011). "Performance Evaluation of a Sustainable and Energy Efficient Re-Roofing Technology Using Field-Test Data." Presented at the NRCA International Roofing Symposium, September 7–9, Washington, DC.

Boh, B.; Sumiga, B. (2008). "Microencapsulation Technology and its Applications in Building Construction Materials." *RMZ- Material and Geoenvironment* (55:3); pp. 329–344.

Brandt, R.; Meier, C.; Reichenauer, G.; Ebert, H-P. (2006). *Small and Wide Angle X-Ray Scattering Investigation of SiOx Micro-Encapsulated Na_2CO_3 Hydrates.* Erlangen, Germany: Bavarian Center for Applied Energy Research (ZAE Bayern).

Bureau of Labor Statistics (2012). Average Energy Prices in Atlanta–July 2012. http://www.bls.gov/ro4/aepatl.htm.

Chai, H.; Zeng, L.K.; Liu, P.A.; Wang, H.; Cheng, X.S.; Shui A.Z. (2007). "Preparation and Thermal Properties of SiO_2 Coated Stearic Acid as Phase Change Materials by Low Temperature One-Step Solid-State Chemical Reaction." *Bulletin of Chinese Ceramic Society* (35:11); pp. 1430–1433.

Christian, J.; Kośny, J. (March 1996). "Thermal Performance and Wall Rating." *ASHRAE Journal.*

Dincer, I.; Rosen, M. (2011). *Thermal Energy Storage: Systems and Applications.* West Sussex, United Kingdom: John Wiley & Sons.

Direct Energy (2012). "Energy Plans for the Oncor (Dallas/Fort Worth/North Texas) Service Territory." http://residential.directenergy.com/EN/Energy/Texas/Pages/ELE/Plans-For-Dallas.aspx.

Farid, M.M.; Khudhair, A.M.; Razack, S.A.K.; Al-Hallaj, S. (2004). "A Review on Phase Change Energy Storage: Materials and Applications." *Energy Conversion and Management* (45:9-10); pp. 1597–1615.

Feustel, H.E. (1995). *Simplified Numerical Description of Latent Storage Characteristics for Phase Change Wallboard.* Berkley, CA: Lawrence Berkeley National Laboratory, Indoor Environmental Program, Energy and Environment Division, University of California.

Feustel, H.E.; Steti, C. (1997). *Thermal Performance of Phase Change Wallboard for Residential Cooling Application.* Berkeley, CA: Lawrence Berkeley National Laboratory, Indoor Environmental Program, Energy and Environment Division, University of California.

FPL (2012). Residential Rate Schedule, Effective May 2012 and July 2012. http://www.fpl.com/rates/pdf/Residential.pdf

Fraunhofer ISC – "Annual Report" – Fraunhofer-Institut für Silicatforschung ISC,- Würzburg, Germany, 2007.

Garg, H.P.; Mullick, S.C.; Bhargava, A.K. (1985). *Solar Thermal Energy Storage.* Springer.

Günther, E.; Hiebler, S., Mehling, H.; Redlich, R. (August 2009). "Enthalpy of Phase Change Materials as a Function of Temperature: Required Accuracy and Suitable Measurement Methods." *International Journal of Thermophysics* (30:4).

Hessbrugge, B.J.; Vaidya, A.M. (1997). "Preparation and Characterization of Salt Hydrates Encapsulated in Polyamide Membranes." *Journal of Membrane Science* (128:2); 175–182.
Huang, Y.J.; Ritschard, R.; Bull, J. (1987). *Technical Documentation for a Residential Energy Use Data Base Developed in Support of ASHRAE Special Project 53.* Berkeley, CA: Lawrence Berkeley National Laboratory.
Huang, J.; Hanford, J.; Yang, F. (1999). *Residential Heating and Cooling Loads Component Analysis.* Berkeley, CA: Lawrence Berkeley National Laboratory, Building Technologies Department, Environmental Energy Technologies Division, University of California.
Inaba, H.; Tu, P. (1997). "Evaluation of Thermophysical Characteristics of Shape Stabilized Paraffin as a Solid-Liquid Phase-Change Material." *Heat and Mass Transfer* (32:4); 307–312.
Jing, H.; Min, C.; Limin, W. (2011). "Organic-Inorganic Nanocomposites Synthesized via Miniemulsion Polymerization." *Polymer Chemistry* (2:4); 760–772.
Kissock, J.; Kelly, J.; Hannig, M.; Thomas, I. (1998). "Testing and Simulation of Phase Change Wallboard for Thermal Storage in Buildings." *Proceedings of 1998 International Solar Energy Conference*; June 14–17, Albuquerque, New Mexico. Edited by J.M. Morehouse and R.E. Hogan. New York: American Society of Mechanical Engineers.
Kissock, K,; Limas, S. (2006). "Diurnal Load Reduction through Phase-Change Building Components." *ASHRAE Transactions* (112:1); 509–517.
Kośny, J. (September 2008). *2006/07 Field Testing of Cellulose Fiber Insulation Enhanced with Phase Change Material.* Oak Ridge, TN: Oak Ridge National Laboratory.
Kośny, J.; Yarbrough, D.; Miller, W. (2008). "Use of PCM-Enhanced Insulations in the Building Envelope." *Journal of Building Enclosure Design* (Summer/Fall)., pp 55-59.
Kośny, J.; Biswas, K.; Miller, W.; Kriner, S. (2012). *Field Thermal Performance of Naturaly Vented Solar Roof with PCM Heat Sink.* ORNL/Metal Construction Association /Fraunhofer project draft report, January.
Kośny, J.; Biswas, K.; Miller, W.; Childs, P.; Kriner, S. (2011). "Sustainable Retrofit of Residential Roofs Using Metal Roofing Panels, Thin-Film Photovoltaic Laminates and PCM Heat Sink Technology." National Institute of Building Sciences, Building Enclosure Technology and Environment Council, *Journal of Building Enclosure Design* (Winter), pp 11-13.
Kośny, J.; Yarbrough, D.; Miller, W.; Childs, P.; Mohiuddin, S.A. (2007). "Thermal Performance of PCM-Enhanced Building Envelope Systems." Presented at the Thermal Performance of the Exterior Envelopes of Whole Buildings X International Conference, December 2–7, Clearwater Beach, Florida.
Kośny, J.; Yarbrough, D.; Wilkes, K.; Leuthold, D.; Syad, A. (June 2006). "PCM-Enhanced Cellulose Insulation–Thermal Mass in Lightweight Natural Fibers." Presented at the ECOSTOCK Conference, May 31–June 2, Galloway, New Jersey.
Kośny, J.; Yarbrough, D.; Miller, W.; Shrestha, S.; Kossecka, E.; Lee, E. (2010). "Numerical and Experimental Analysis of Building Envelopes Containing Blown Fiberglass Insulation Thermally Enhanced with Phase Change Material (PCM)." *Proceedings of the 1st Central European Symposium on Building Physics;* September 13–15, Cracow, Poland.
Kossecka, E. (1999). "Method of Averages to Determine Insulation Conductivity under Transient Conditions." *Journal of Thermal Insulation and Building Science* (23); 145–158.
Kossecka, E.; Kośny, J. (2001). "Influence of Insulation Configuration on Heating and Cooling Loads in a Continuously Used Building." Presented at the Thermal Envelopes VIII Conference, December 2–7, Clearwater, Florida.
Lane, G.A. (1992). "Phase Change Materials for Energy Storage Nucleation to Prevent Supercooling." *Solar Energy Materials and Solar Cells* (27:2); 135–160.
Li, J.; Xue, P.; Ding, W.; Han, J.; Sun, G. (2009). "Micro-Encapsulated Paraffin/High-Density Polyethylene/Wood Flour Composite as Form-Stable Phase Change Material for Thermal Energy Storage." *Solar Energy Materials and Solar Cells* (93:10); 1761–1767.
Mehling, H.; Cabeza, L.F. (2008). *Heat and Cold Storage with PCM: An Up to Date Introduction Into Basics and Applications.* Springer, p. 95.

Miller, W.A.; Kośny, J. (2008). "Next Generation Roofs and Attics for Residential Homes." Presented at the American Council for an Energy-Efficient Economy (ACEEE) Summer Study on Energy Efficiency in Buildings, August 17–22, Pacific Grove, California.

Miller, W.A.; Keyhani, M.; Stovall, T.; Youngquist, A. (2007). "Natural Convection Heat Transfer in Roofs with Above-Sheathing Ventilation." Presented at the Thermal Performance of the Exterior Envelopes of Whole Buildings X International Conference, December 2–7, Clearwater Beach, Florida.

Mulligan, J.C.; Gould, R.D. (2002). *Use of MicroPCM Fluids as Enhanced Liquid Coolants in Automotive and HEV Vehicles−Final Report.* Department of Energy Cooperative Agreement DE−FC02−00EE50631.

Murugananthama, K.; Phelanb, P.; Horwath, P.; Ludlam, D.; McDonald, T. (2010). "Experimental Investigation of a Bio-Based Phase-Change Material to Improve Building Energy Performance." *Proceedings of ASME 2010 4th International Conference on Energy Sustainability*; May 17–22, Phoenix, Arizona.

Özonur, Y.; Mazman, M.; Paksoy, H.Ö.; Evliya, H. (2006). "Microencapsulation of Coco Fatty Acid Mixture for Thermal Energy Storage with Phase Change Material." *International Journal of Energy Research* (30:10); 741–749.

ORNL. (2012). *Use of Phase Change Material in a Building Envelope: A Case Study.* Oak Ridge, TN: ORNL, draft, January.

Petrie, T.W.; Wilkes, K.E.; Desjarlais, A.O. (2004). "Effect of Solar Radiation Control on Electricity Demand Costs− An Addition to the DOE Cool Roof Calculator." *Performance of Exterior Envelopes of Whole Buildings IX International Conference: Conference Proceedings.* Atlanta, GA: ASHRAE.

Rößner, F. Deutsche Patentanmeldung, Offenlegungsschrift DE 19954 771 A1. Bsp. 1 (1999)

Ryu, H.W.; Woo, S.W.; Shin, B.C.; Kim, S.D. (1992). "Prevention of Supercooling and Stabilization of Inorganic Salt Hydrates as Latent Heat-Storage Materials." *Solar Energy Materials and Solar Cells* (27:2); 161–172.

Salyer, I.; Sircar, A. (1989). Development of PCM Wallboard for Heating and Cooling of Residential Buildings. Presented at the U.S. Department of Energy Thermal Energy Storage Research Activities Review, March 15–17, New Orleans, Louisiana.

Sari, A. (2005). "Eutectic Mixtures of Some Fatty Acids for Low Temperature Solar Heating Applications: Thermal Properties and Thermal Reliability." *Applied Thermal Engineering* (25:14-15); 2100–2107.

Sari, A. (2003). "Thermal Reliability Test of Some Fatty Acids as PCMs Used for Solar Thermal Latent Heat Storage Applications." *Energy Conversion and Management* (44:14); 2277–2287.

Sari, A.; Sari, H.; Onal, A. (2004). "Thermal Properties and Thermal Reliability of Eutectic Mixtures of Some Fatty Acids as Latent Heat Storage Materials." Energy Conversion and Management (45:3); 365–376.

Sari, A, Alkan, C.; Karaipekli, A.; Uzun, O. (2009). "Microencapsulated n-Octacosane as Phase Change Material for Thermal Energy Storage." *Solar Energy* (83:10); 1757–1763.

Sherman, M.; Grimsrud, D.T. (1980). *Measurement of Infiltration Using Fan Pressurization and Weather Data.* Berkeley, CA: Lawrence Berkeley National Laboratory.

Su, J.F.; Wang, L.X.; Ren, L. (2006). "Fabrication and Thermal Properties of MicroPCMs: Used Melamine-Formaldehyde Resin as Shell Material." *Journal of Applied Polymer Science* (101:3); 1522–1528.

Telkes, M. (1952). "Nucleation of Supersaturated Inorganic Salt Solutions." *Industrial and Engineering Chemistry* (44: 6); 1308–1310.

Tomlinson, J; Jotshi, C.; Goswami, D. (1992). "Solar Thermal Energy Storage in Phase Change Materials." *Proceedings of Solar '92: The American Solar Energy Society Annual Conference*; June 15–18, Cocoa Beach, Florida.

Wilson A. – " Storing Heat in Walls with Phase-Change Materials" -Green Building Advisor - Nov 24 2009

Bao, Y., Pan, W., Wang, T., Wang, Z., Wei, F., and Xiao, F. (2011). ”Microencapsulation of Fatty Acid as Phase Change Material for Latent Heat Storage.” *J. Energy Eng.*, 137(4), 214–219.

Yinping, Z.; Guobing, Z.; Kunpinga.(2006). “Our Research on Shape-Stabilized PCM in Energy-Efficient Buildings.” *Proceedings of ECOSTOCK, 10th International Conference on Thermal Energy Storage*; Stockton, USA.

Zhang, M.; Medina, M.A.; King, J. (2005). “Development of a Thermally Enhanced Frame Wall with Phase-Change Materials for On-Peak Air Conditioning Demand Reduction and Energy Savings in Residential Buildings.” *International Journal of Energy Research* (29:9); 795–809.

buildingamerica.gov

U.S. DEPARTMENT OF ENERGY | Energy Efficiency & Renewable Energy

DOE/GO-102013-3692 ▪ January 2013

Printed with a renewable-source ink on paper containing at least 50% wastepaper, including 10% post-consumer waste.